***The Role of Piccolo and Bassoon in the Regulation of Voltage-Gated Calcium Channels at Presynaptic Neurotransmitter Release Sites***

Thesis

for the degree of

**doctor rerum naturalium (Dr. rer. nat.)**

approved by the Faculty of Natural Sciences of Otto von Guericke University Magdeburg

by M.Sc. Eneko Pina Fernández,

born on 04. Oktober 1987 in Bilbao (Spain)

Examiner: apl Prof. Dr. Constanze Seidenbecher

Prof. Dr. Carolin Wichmann

submitted on: 26. January 2021

defended on: 13. July 2021

# Summary

The active zone is the region of the presynaptic membrane where neurotransmitter release takes place. This region is characterized by a dense meshwork of proteins called the cytomatrix at the active zone (CAZ). Proteins of the CAZ define the release sites, localize to voltage-gated calcium channels (VGCC) within the presynaptic membrane, and coordinate the exo-endocytotic events during the synaptic vesicle cycle. These processes enable fast and reliable neurotransmission. Bassoon and Piccolo are large components of the CAZ, highly homologous, implicated in these processes. Both have been reported to be important for correct neurotransmission. The lack of one or both scaffolding proteins results in a failure of the presynaptic function. However, their implication in the processes governing the neurotransmitter release is not fully understood. Rim-binding proteins (RBPs), other components of the CAZ, have been shown to be important for the neurotransmission in multiple ways. Despite the reported interaction between Piccolo and Bassoon with RBPs, the functional consequences are not well known. In this study, using whole-cell voltage clamp recordings and imaging techniques of mature hippocampal wild-type and Piccolo-mutant neurons, I observed that Piccolo is important for a correct presynaptic function in these neurons. Based on imaging techniques, I determined that Piccolo mutant synapses have lower synaptic strength, although the synaptogenesis is not impaired. I reported RBP2 as a binding partner of Piccolo, which has been shown to functionally and structurally link presynaptic proteins to VGCC. Functional analysis of presynaptic calcium income showed that the VGCC recruitment and contribution to synaptic transmission are not affected in Piccolo-mutant neurons. Nevertheless, the synaptic vesicle (SV) recycling is impaired. Whereas the size readily releasable SV pool is not significantly changed, the recycling pool is decreased, most likely, due to an impairment in the Rab3-mediated SV replenishment, but not to a defect in the SV endocytosis. On the other hand, I found some unique and some overlapping functions of Bassoon compared to Piccolo. Surprisingly the absence of Bassoon increases presynaptic calcium influx. Aside from the fact that the mechanisms are not clear yet, my data suggest that Bassoon modulates the contribution of VGCC subtypes. Furthermore, I showed that SV recycling is decreased in Bassoon-lacking neurons.

Changes in the global network activity induce homeostatic adaptations of synapses, which involve pre- and postsynaptic adaptations. While the molecular players contributing to postsynaptic homeostasis are well understood, less is known about the effectors maintaining presynaptic homeostasis. In the second part of the thesis, the role of Bassoon and Piccolo after prolonged silencing in hippocampal neurons was studied. Using imaging techniques, I observed that Bassoon, but not Piccolo, impairs evoked presynaptic calcium income after prolonged silencing, while both seem to regulate SV recycling. Furthermore, since no significant changes were observed in the surface population of AMPA receptors of Bassoon-lacking neurons, I hypothesized that the functional consequences of Bassoon are, most likely, restricted to the presynaptic compartment. The data suggest that despite Bassoon has a more active role in homeostasis than Piccolo, both scaffolds are crucial for homeostatic plasticity mechanisms in the mammalian hippocampus.

Overall, these findings provide new insights into the mechanisms contributing to neurotransmission and synaptic plasticity.

# Zusammenfassung

Bei der aktiven Zone (AZ) von Nervenzellen handelt es sich um eine Region der Präsynapsemembran, an der die Ausschüttung von Neurotransmittern stattfindet. Diese Region ist durch ein dichtes Netzwerk von Proteinen, die sogenannte Cytomatrix an der aktiven Zone (CAZ), charakterisiert. Proteine in dieser Zone definieren die Areale der Neurotransmitterausschüttung, sind mit spannungsgesteuerten Kalzium-Kanälen (VGCC) innerhalb der präsynaptischen Membran kolokalisiert und koordinieren exo-endozytotische Prozesse während des synaptischen Vesikel-Kreislaufs. Diese Prozesse ermöglichen eine schnelle und zuverlässige Übertragung von Neurotransmitter-Signalen. Wichtige Proteine für diese Prozesse sind Bassoon und Piccolo, strukturell verwandte große Komponenten der CAZ. Es konnte gezeigt werden, dass diese beiden Proteine wichtig für eine korrekte Ausschüttung der Neurotransmitter aus der Präsynapse sind. So führt bereits der Verlust eines der beiden Gerüstproteine zur Fehlfunktion der Präsynapse. Dennoch ist ihre Bedeutung für die Prozesse, die die Neurotransmitterausschüttung steuern, noch nicht vollkommen verstanden. Für Rim-bindende Proteine (RBPs), weitere Komponenten der CAZ, konnte bereits gezeigt werden, dass sie für die Übertragung von Neurotransmittern eine wichtige Bedeutung haben. Obwohl bereits bekannt ist, dass Piccolo und Bassoon mit RBPs interagieren, sind die funktionellen Auswirkungen dieser Interaktion nicht völlig aufgeklärt. In dieser Studie habe ich unter Verwendung von elektrophysiologischen und mikroskopischer Methoden an neuronalen Primärkulturen zeigen können, dass Piccolo-Mutanten im Vergleich zum Wildtyp (WT) präsynaptische Dysfunktionen aufweisen. Die Analyse von mikroskopischen Imagingdaten zeigt, dass Piccolo-Mutanten eine verringerte synaptische Stärke haben, während die Synaptogenese unverändert ist. Ich konnte zeigen, dass RBP2 an Piccolo bindet und dass diese Interaktion entscheidend für die strukturelle und funktionelle Kopplung der präsynaptischen Proteine mit den VGCC ist. Funktionelle Analysen von präsynaptischen Kalziumströmen zeigen, dass die Rekrutierung von VGCC und die synaptische Signalweiterleitung in Neuronen von Piccolo-Mutanten nicht beeinträchtigt sind, jedoch das Recycling von synaptischen Vesikeln (SV) beeinflusst wird. Die Größe des sofort freisetzbaren SV-Pools ist unverändert, allerdings ist der sogenannte Recycling-Pool aufgrund einer Störung der Rab3-Protein-vermittelten Wiederauffüllung, aber nicht wegen eines Defekts in der SV-Endozytose, verringert. Ich konnte zeigen, dass Bassoon teilweise ähnliche Funktionen wie Piccolo, teilweise aber auch verschiedene hat. Überraschenderweise weisen Bassoon-Mutanten einen erhöhten präsynaptischen Kalziumeinstrom auf. Obwohl der genaue Mechanismus noch nicht klar ist, weisen die Daten dieser Dissertation darauf hin, dass Bassoon die Funktion verschiedener VGCC-Subtypen moduliert. Des Weiteren zeigt die Arbeit, dass das Recycling von SV in Neuronen von Bassoon-Mutanten verringert ist.

Veränderungen in der globalen Netzwerkaktivität führen zu homöostatischen Anpassungen in Synapsen, welche prä- und postsynaptisch sein können. Während die molekularen Faktoren, welche die postsynaptische homöostatischen Verstärkung regulieren, bereits gut untersucht sind, sind die der präsynaptischen Prozesse weniger gut bekannt. Im zweiten Teil der Dissertation habe ich deshalb die Rolle von Piccolo und Bassoon in hippocampalen Neuronen nach längerer Inkubation mit dem Natriumkanalblocker Tetrodotoxin (TTX) untersucht. Mithilfe mikroskopischer Bildgebung habe ich beobachten können, dass Bassoon, nicht jedoch Piccolo, nach längerer Stilllegung der Netzwerkaktivität die präsynaptischen Kalziumströme

verringert. Jedoch scheinen beide Proteine das Recycling der SV in stillgelegten Synapsen zu regulieren. Da wir in Neuronen von Bassoon-Mutanten keine Verringerung der AMPA-Rezeptoren an der Zelloberfläche feststellen konnten, vermuten wir, dass die homöostatische Anpassung präsynaptisch erfolgt. Unsere Daten lassen vermuten, dass - obwohl Bassoon eine aktivere Rolle bei der homöostatischen Anpassung spielt - beide Proteine wichtig für die homöostatischen Plastizität im Hippocampus von Säugetieren sind.

Zusammenfassend geben die vorgelegten Daten neue Einblicke in die Mechanismen der neuronalen Signalübertragung und homöostatischen Plastizität.

# Table of contents

# Figures and Tables

- **Figures**

- **Tables**

# 1 Introduction

## 1.1 Chemical synapses: molecular composition

The brain, the center of the nervous system, contains billions of neurons. Signal transmission between neurons, that are assembled into complex networks, is a fundamental principle of brain function. Neurons are excitable cells that receive, process and transmit information via electrical or chemical signals. These signals are transmitted through highly specialized intercellular junctions called synapses. Most synapses are chemical; these synapses communicate using chemical messengers. These asymmetric structures are composed of a presynapse (also known as the nerve terminal or bouton), which includes neurotransmitter-containing synaptic vesicles (SVs), a space of approximately 20nm width between the two synaptic membranes, called synaptic cleft, and a postsynapse harboring the neurotransmitter reception apparatus. The signals between neurons are transduced by a temporally and spatially regulated release of neurotransmitters. At presynapses, an incoming action potential arrives causing membrane depolarization, which triggers the influx of calcium ($Ca^{2+}$) ions through voltage-gated calcium channels (VGCCs) into the presynaptic terminal. The increase of intracellular $Ca^{2+}$ levels elicits SV fusion with the presynaptic membrane, and in turn, the release of neurotransmitters into the synaptic cleft.

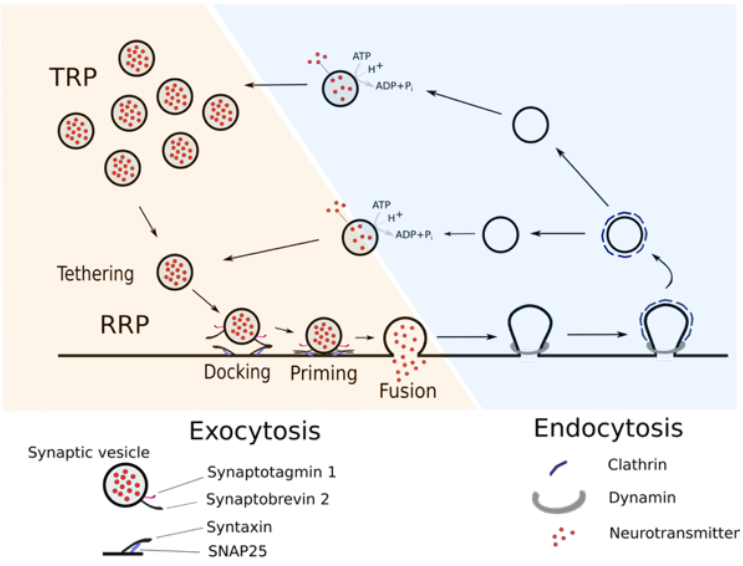


**Figure 1: Synaptic vesicle cycle scheme.** The SVs are loaded with neurotransmitter, and then tethered to the AZ, docked and primed. Enhanced intracellular Ca2+ triggers SV exocytosis. Afterwards, the SV membrane is endocytosed. Abbreviations: TRP, Total recycling pool; RRP, Ready releasable pool; ATP, Adenosine triphosphate; ADP, Adenosine diphosphate; H+, Proton; Pi, Inorganic phosphate.

Within the presynaptic terminal, regulated SV exocytosis occurs at a specialized membrane region called the active zone (AZ) (Couteaux and Pecot-Dechavassine, 1970; Heuser and Reese, 1973). The AZ is characterized by an electron-dense meshwork of proteins facing the presynaptic membrane: the cytomatrix at the AZ (CAZ) (Landis, 1988). These proteins are components of the release apparatus, including Rab3-interacting molecules (RIMs), RIM-

binding proteins (RBPs), Bassoon, Piccolo, cytomatrix at the active zone-associated structural protein (CAST)/ELKS, Liprin-α, and Munc13 proteins (for review see Schoch and Gundelfinger, 2006; Fejtova and Gundelfinger, 2012; Ackermann et al., 2015). These proteins act in spatial and functional manner to mediate membrane trafficking events, called the SV cycle. It includes steps, through which the SVs are tethered to the presynaptic membrane, primed to become fusion-competent, exocytosed in response to $Ca^{2+}$ influx and recycled by endocytosis and refilling (Figure 1).

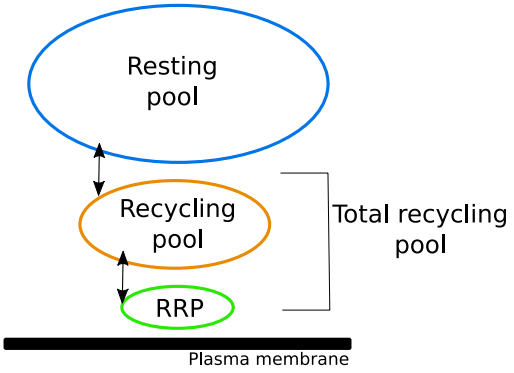


**Figure 2: SV pools.** Scheme depicting the unifying synaptic vesicle pool terminology proposed. Arrows illustrate the interconnectivity between the SVs pools. Abbreviations: RRP, Readily releasable pool.

SVs are organized inside the presynapse in three functionally different pools. These are distinguished by their availability for release and mobilization in response to stimuli: the readily releasable pool (RRP), the recycling pool (RP) and the resting pool ($R_tP$) (review in Rizzoli and Betz, 2005; Alabi and Tsien, 2012) (Figure 2). The RRP includes all vesicles that are immediately available for release upon stimulation (Dobrunz and Stevens 1997; Waters and Smith 2002). After the RRP is depleted, prolonged release occurs from the RP. It is the group of vesicles that maintain the release on physiological stimulation. It consists of 5-20% of the total SVs within the presynaptic bouton. All vesicles able to be released upon physiological stimulation, the RRP and the RP, are enclosed under the term total recycling pool (TRP). However, another pool of vesicles exists in the presynaptic terminal, the $R_tP$, which corresponds to the vesicles that are refractory to release, even in response to prolonged stimulation (Alabi and Tsien, 2012) and comprises about 80-90% of all vesicles (Fernandez-Alfonso and Ryan 2008; Ikeda and Bekkers 2009). The RRP and RP are constantly being replenished by newly endocytosed vesicles, during release upon physiological patterns of stimulation; $R_tP$ is only released and restored during intense stimulation, normally upon unphysiological patterns of stimulation (Rizzoli and Betz, 2005).

The sizes of the SV pools are crucial to define the synaptic strength and plasticity of the neurons (Kim and Ryan, 2010). Synapsins are a family of vesicle-related proteins, located on the surface of the SV. They contribute to the synapse formation, maturation and plasticity. Synapsins regulate the SV dynamics via actin-dependent interaction, having an

impact on vesicular release (Bykhovskaia, 2011). Synapsin phosphorylation has been proposed as one of the mechanisms contributing to SV exocytosis (Benfenati et al., 1992; Torri Tarelli et al., 1992; Hosaka et al., 1999; Menegon et al., 2006). The most abundant member of the Synapsin family, Synapsin I, is phosphorylated by several enzymes including protein kinase A (PKA), $Ca^{2+}$/calmodulin-dependent protein kinases (CaMK), and cyclin-dependent kinases (CDK) 1/5 (Matsubara et al., 1996; Jovanovic et al., 2001), what in turn modulates the binding to SVs and/or F-actin (Hosaka et al., 1999; Menegon et al., 2006; Kim and Ryan, 2010; Verstegen et al., 2014). While PKA regulates the size of the RP positively (Hosaka et al., 1999; Menegon et al., 2006), CDK5 does the opposite, retaining more vesicles in the RtP (Kim and Ryan, 2010; Verstegen et al., 2014). In addition to Synapsin I, other molecules might regulate the SV pool dynamics, such as SNAP25 (Nagy et al., 2004) or Tomosyn I (Cazares et al, 2016).

Presynaptic nerve terminals release neurotransmitters by SV exocytosis. Before vesicles fuse with the plasma membrane of the presynaptic bouton, neurotransmitter-filled SV are tethered, docked and primed. These membrane trafficking events at the AZ occur via a synaptic set of fusion mediators, including conserved proteins involved in universal fusion processes elsewhere in cells, such as soluble NSF attachment protein receptor (SNAREs), SM proteins (Sec1/Munc18-like), and Munc13.

Tethering and docking is defined as the recruitment of the SVs to the vicinity of the AZ. RIM1, a CAZ protein, tethers vesicles via the small GTPase Rab3 into the vicinity of the AZ (Rosenmund et al., 2003). The knockout of RIM1 α-isoform results in an impairment of the quantity and distribution of SVs at the AZ (Fernández-Busnadiego et al., 2013). $Ca_V2.2$ has also been shown to bring SV to the proximity of the AZ through its distal C-terminal in dorsal root ganglion neurons (Wong et al., 2014; Chai et al., 2017). Additionally, SNARE proteins, i.e. the synaptic vesicle protein synaptobrevin (VAMP-vesicle-associated membrane protein), the presynaptic plasma membrane proteins Syntaxin1 and synaptosomal-associated protein 25 (SNAP25) are also involved in the SV docking step. Moreover, Munc18 has been shown to be involved in this process. It interacts with the closed conformation of syntaxin1, preventing it from completing the SNARE complex, suggesting that Munc18 prevents the fusion step (Dulubova et al., 1999; Wu et al., 2001; Südhof and Rothman, 2009). Upon release from Munc18 control, Syntaxin1 binds to SNAP25 and synaptobrevin, proteins located on the vesicle membrane. These proteins

associate to form the SNARE complex, which links vesicular and plasma membranes (Tooner and Verhagen, 2007; Südhof and Rothman, 2009).

After docking, the priming makes vesicles fuse-competent (Rosenmund et al., 2002). Munc18 together with Munc13, RIM and ELKS have been proposed to be important for vesicle priming (Hammarlund et al., 2007; Ma et al., 2011Deng et al., 2011; Kawabe et al., 2017).

The fusion step starts with the conformational changes of the SNARE complex from cis- to trans- (Südhof and Rizo, 2011), promoting the zippering of the trans-SNARE complex, and therefore, the complete pore opening (Toonen and Verhage, 2007). Synaptotagmins are integral membrane proteins of SVs (Tucker et al., 2004) thought to control completion of SNARE complex formation. They function as $Ca^{2+}$ sensors and are crucial for the $Ca^{2+}$-evoked SV exocytosis (Radhkrishnan et al., 2009). Complexins, instead, stabilize and promote the zippering of the SNARE complex (Chen et al., 2002) but impede the complete zippering of it (Huntwork and Littleton, 2007).

After SVs fuse and collapse into the presynaptic lipid bilayer, their membrane and protein constituents must be recovered in the process of SVs compensatory endocytosis (Südhof, 2004). There are three different systems of endocytosis: clathrin-mediated endocytosis, 'kiss and run' and bulk endocytosis (Saheki and De Camilli, 2012). The best-characterized process is the clathrin-mediated endocytosis, which ultimately produces functional SV directly from the plasma membrane (Saheki and de Camili, 2012). It is achieved through four distinct steps (Brodin et al., 2000): a) The triskelion of clathrin is assembled around the area that will be endocytosed. It is recruited by heterotetrameric adaptor complexes (AP2 and AP180) which initiate the process; b) The assembling of the clathrin coat on the surface of the plasma membrane induces a deformation of it and forms the coated pit; c) The fission step requires the activity of the large GTPase dynamin, which leads to scission and detachment of the vesicle from the membrane; d) The last step requires specialized proteins such as amphiphysin, endophylin, auxilin and synaptojanin to dissociate the vesicle from the plasma membrane, and the consecutive disassembly of the clathrin coat.

While the majority of SV pass through a clathrin-mediated process (Maycox et al., 1992), a high demand of SVs activates other processes encompassed under the term clathrin-independent endocytosis. Bulk endocytosis, a type of clathrin-independent endocytosis,

is a process that allows the continuous retrieval of SVs by the formation of large endosome-like structures sprouting vesicles and usually connected to the plasma membrane for long time (Clayton et al., 2007). The machinery involved in this type of endocytosis is not well-known. However, it is believed that clathrin mediates the budding of the vesicles from the endosome-like structure and it depends on the actin cytoskeleton dynamics (Richards et al., 2004). Besides bulk endocytosis, two studies reported a new and fast way to retrieve SV in C. elegans and mouse, the ultrafast endocytosis (Watanabe et al., 2013a; Watanabe et al., 2013b; for review see Watanabe and Boucrot, 2017). This endocytic pathway occurs within 50ms-1s after the stimulation, it takes around 10-20s and recuperates on average equal number of vesicles exocytosed (Balaji et al., 2008; Granseth and Lagnado et al., 2008; Watanabe et al., 2013b).

The alternative pathway 'kiss and run' does not involve full collapse of the vesicles into the plasma membrane. Neurotransmitters are thought to be discharged through the transient fusion pore (He and Wu., 2007). After liberation of the vesicle content, the pore closes and the same vesicle is recycled. Although it is not clear whether this pathway is a dominant mechanism (He and Wu, 2007), it is one of the fastest described (Gandhi and Stevens, 2003).

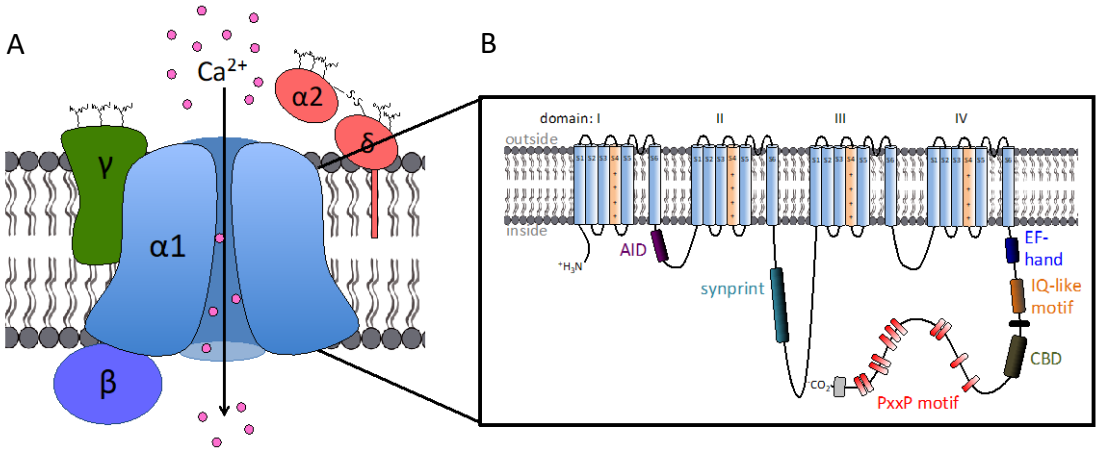


**Figure 3: Structure of a voltage-gated $Ca^{2+}$ channels.** (A) VGCC structure formed by a pore-forming α1-subunit, an intracellular β-subunit, an α2δ and the auxiliary γ subunit. (B) The α1-subunit is built from four homologous domains (I-IV), composed by six transmembrane α-helices (S1-S6). The 4 homologous domains are connected by intracellular loops, which harbour protein interaction sites such as α interaction domain (AID; purple) and synaptic protein interaction site (synprint; cyan). The C-terminal contains several interaction motifs including EF hand-like domain (dark blue), IQ-like motif (orange), calmodulin binding domain (CBD; olive green) and PxxP motifs (red; i.e. RQLPGTP for $Ca_V2.1$ and 2.2) (modified from Catterall, 2011).

Furthermore, recent studies suggested that $Ca^{2+}$ influx facilitates SV recycling in calyx of Held, hippocampal neurons and in inner hair cells (Moser and Beutner, 2000; Sankaranayanan and Ryan, 2001; Zefirov et al., 2006; Dittman and Ryan, 2009; Hosoi et al.,

2009; Wu et al., 2014). Proteins like calmodulin, calcineurin, some members of the synaptotagmin family or SNAP-25 have been suggested to be involved in the regulation of $Ca^{2+}$-mediated SV recycling (see review Igarashi and Watanabe, 2007; Xu et al., 2013; Wu et al., 2014).

## 1.2 Presynaptic voltage-gated calcium channels: structure, function and modulation

VGCC mediate the $Ca^{2+}$ ion influx in response to a depolarization of the membrane in neurons (Dunlap et al., 1995; Catterall and Few, 2008). $Ca^{2+}$ entry can be measured by electrophysiology as calcium income. The influxes have distinct physiological roles and pharmacological properties in different cell types. The pharmacological and physiological diversity of VDCC arises from the existence of multiple α1 subunits. $Ca_v$α1 subunits are encoded by 10 genes in mammals, which give rise to three sub-families with sequence similarities, termed as the $Ca_v$ 1, $Ca_v$ 2 and $Ca_v$ 3 families (Catterall, 2000: Ertel et al., 2000). Synaptic transmission in the central nervous system is mainly operated through the $Ca_v$ 2 family ($Ca_v$2.1, $Ca_v$2.2 and $Ca_v$2.3) (Ricoy and Frerking, 2014). VGCC are multi-subunit proteins composed of a large alpha (α), and three other smaller auxiliary subunits: α2δ, β and γ (Catterall, 2000; Takahashi et al., 1987) (Figure 3A). The transmembrane pore-forming α1 subunit contains four homologous domains, I-IV (Tanabe et al., 1987), containing six transmembrane α-helix segments (S1-S6) (Catterall, 2011). Through the S4, which acts as voltage sensor, the VDCC regulate the opening and closing of the calcium-conducting pore (Lacinová, 2005) (Figure 3B). The smaller auxiliary subunits in association with the α1 subunits, modulate the $Ca^{2+}$ channel's electrophysiological properties and expression in excitable cells types (Cantí et al., 2005; Bernstein and Jones, 2007; Buraei and Yang 2010, Dolphin 2012). $Ca^{2+}$ entering the presynaptic terminal through $Ca_v$2.1 and $Ca_v$2.2 is one of the first events responsible for initiating the synaptic transmission, and thus for the neurotransmitter release at fast conventional synapses (Dunlap et al., 1995; Olivera et al., 1994). In the early stages of development, preceding synaptogenesis, the $Ca_v$2.2, conducting N-type currents, are predominant in neurotransmission (Scholz and Miller, 1995). It seems that $Ca_v$2.2 is important for developmental periods in neurons. However, later at 13-14 DIV, when the neurons form synaptic contacts, a developmental switch occurs that substitutes $Ca_v$2.2 with $Ca_v$2.1 in hippocampus (Scholz and Miller, 1995; Pravettoni et al., 2000).

### 1.2.1 Splice variants

Alternative pre-messenger RNA splicing is an important mechanism for protein diversity and gene regulation. This process allows different proteins to be produced from one original gene, and therefore, thousands of proteins from a small number of genes. Alternative splicing of VGCC produces channels expressed at specialized locations or developmental stages that modulates neurotransmission (Liao and Soong, 2010; Lipscombe, 2015; Thalhammer et al., 2017). The mechanisms of splicing are extremely variable regarding tissue-specific expression and/or activity. In the case of $Ca_v2.2$, the mutually exclusive alternative splicing of exon 37 generates two isoforms, each with different properties. While $Ca_v2.2$e37a correlates with larger N-type currents, more sensitive to certain G protein-coupled inhibition and is mainly expressed in nociceptors, the e37b is found throughout the nervous system and is less sensitive (Bell et al., 2004; Castiglioni et al., 2006). Moreover, Thalhammer et al., (2017) recently showed that the alternative splicing in exon 37 of $Ca_v2.1$ generates two mutually exclusive isoforms. While the 37a promotes synaptic depression, the 37b contributes to synaptic facilitation. However, splicing of exon 47 generates a shortening of the $Ca_v2.1$ α-subunit C-terminus (Krovetz et al., 2000; Soong et al., 2002), which leads to channel modulation (Adams et al., 2012). This process could potentially influence the localization of VGCC due to missing protein interaction sites contained at the C-terminus, including the binding motifs for RBPs (Hibbino et al., 2002) or RIM (Kaeser et al., 2011).

### 1.2.2 Presynaptic interaction partners of voltage-gated calcium channels

Neurotransmitter release is proportional to the power of $Ca^{2+}$ current (Augustine et al., 1987; Zucker & Regehr, 2002). Action potentials (AP) induce a local rise of intracellular $Ca^{2+}$ concentration in close proximity to the VGCC, promoting the formation of microdomains (or nanodomains) (Llinás et al., 1992; Stanley, 1993). The size of microdomains varies from 100nm to 1µm generated from a few channels (Naraghi and Neher, 1997). The regulation mechanism via VGCC density has been reported to be crucial for the synaptic strength and plasticity at the active zone (Sheng et al., 2012). The involvement of the VGCC in synaptic transmission requires interplay with the release apparatus via protein-protein interaction.

Proteins of the release machinery contribute to the positional priming, i.e. a proper localization of VGCC relative to the release site. The synaptic protein interaction (synprint) domain of the $Ca_v\alpha$-subunit is an important motif for these interactions. It has been associated with syntaxin-1, SNAP-25 and synaptotagmin-1 (Sheng et al., 1994; Wiser et al., 1996: Sheng et al., 1997). However, many other protein-protein interactions have been described to be involved in VGCC trafficking. CASKs and Mint1, through their respective motifs, bind to the $Ca_v2.2$ α-subunit C-termini (Maximov et al., 1999; Maximov and Bezprozvanny, 2002). Indeed, a recent study demonstrated that the loss of CASK/ELKS impairs $Ca^{2+}$ influx and channel abundancy (Liu et al., 2014; Dong et al., 2018). Munc13, an AZ molecule essential for exocytosis, has been proven to have a role in the VGCC positional priming (Calloway et al., 2015).

RBPs, large multi-domain proteins located at the AZ, are important molecules with respect to this thesis. They were discovered via their interaction with RIMs (Wang et al., 1997, 2000) and are encoded by three different genes (Mittelstaedt and Shoch, 2007). RBP1 and RBP2 are mainly expressed in the brain, whereas RBP3 occurs primarily in non-neuronal cells (Mittelstaedt and Schoch, 2007). All RBPs have a similar structure, composed of an N-terminal and two C-terminal SH3 domains separated by multiple central fibronectin-like-3 domains. The three SH3 domains can interact with various proteins, that are classified into two major categories depending on their binding motifs: Class I ligands contain a +XφPXφP, whereas class II ligands display the sequence φPXφPX+. The + usually refers to arginine (basic residue), the X to any amino acid, and φ to a hydrophobic residue. In inner ear hair cells, RBPs interact with $Ca_v1.3$ (PxxP motif: RLLPPTP Kaeser et al., 2011) via the three SH3 domains. Furthermore, precipitation assays confirmed the interaction between $Ca_v2.2$ and RBP2 (Hibino et al., 2002). Since the RBP2 interacting motifs do not differ notably, RBP2 can bind likely to various $Ca^{+2}$ channel subtypes, most likely through the PxxP motif (RQLPGTP) contained in the c-terminal of the channels. In line with these results, Drosophila RBP-deficient larval neuromuscular junctions exhibit severe structural and functional impairments (Liu et al., 2011; Müller at al., 2012, 2015), whereas in mammals this does not have strong impact (Acuna et al., 2015). RBP-deficient synapses display slower and unstable neurotransmitter release during high-frequency bursts. Mechanistically, RBPs tether calcium channels, most probably in collaboration with RIMs. RIM1 was first identified as a protein capable to interact with

RBP1 and RBP2 via RQLPQL/VP motif, contained between the two C2 domains (Wang et al., 2000; Hibino et al., 2002). Simultaneously, RIMs interact directly with the pore-forming subunit of presynaptic $Ca_v2.1$ and $Ca_v2.2$ via the PDZ-domain (Kaeser et al., 2011). Both interactions are indispensable for proper coupling of VGCC to RIMs at the release sites (Kaeser et al., 2011: Han et al., 2011; Graf et al., 2012). RIM also interacts with the β subunits of VDCC, what seems to be important, not only for the anchoring of the $Ca_vs$, but also for the regulation of VGCC inactivation (Kiyonaka et al., 2007).

Bassoon (see 1.3), another important protein of the CAZ, including the synaptic ribbon, can create a large number of release sites at hair cells ribbon synapses, organizing $Ca^{2+}$ channels disposition (Frank et al., 2010). Moreover, Bassoon interacts with the β subunit of the VGCC (Chen et al., 2011; Nishimune et al., 2012). Davydova et al., (2014) reported on the importance of the scaffold protein Bassoon in the localization of $Ca_v2.1$ channel to the AZ. The significant reduction of synaptic localization of $Ca_v2.1$ in Bassoon-deficient boutons is comparable with the reduction seen in a full RIM1/2 knockout (Kaeser et al., 2011), or in Drosophila RBP-deficient larval neuromuscular junctions (Liu et al., 2011).

## 1.3 Bassoon and Piccolo

Two integral components of the CAZ are Bassoon and Piccolo. Both were identified as structural components in rat synaptic junctions (Cases-Langhoff et al., 1996; Langnaese et al., 1996). Their structural characterization reported 10 shared regions of homology, covering two zinc fingers and three coiled-coil domains. Piccolo has an additional PDZ (post synaptic density protein (PSD95), Drosophila disc large tumor suppressor (Dlg1) and zonula occludens-1 protein (ZO-1)) domain and two C2 domains (Wang et al., 1999; Fenster et al., 2000) (Figure 4). Bassoon and Piccolo are present in

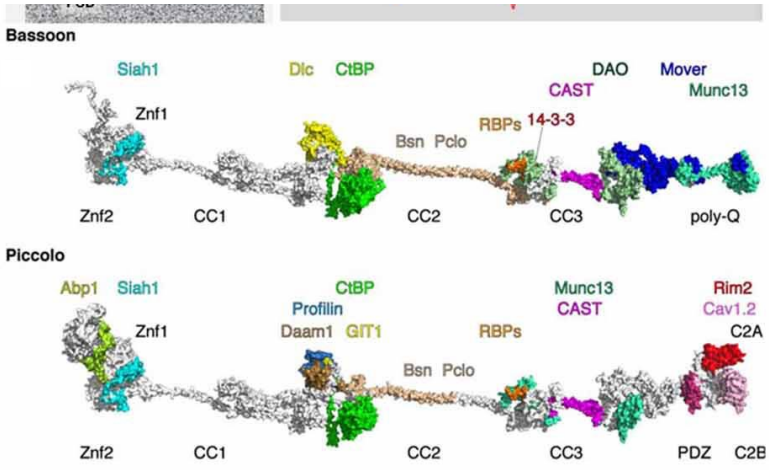


**Figure 4: Piccolo and Bassoon structure.** Bassoon and Piccolo structure scheme including composition domains and docking sites for binding partners color coded (modified from Gundelfinger et al., 2016).

both excitatory and inhibitory central nervous system synapses. They are expressed early during postmitotic neuronal differentiation (Cases-Langhoff et al, 1996; Zhai et al, 2000). They are among the first proteins appearing at the nascent synapse (Friedman et al, 2000; Zhai et al, 2000; Shapira et al, 2003) and have therefore been implicated in synapse formation (Ziv and Garner, 2004; Waites et al, 2005). Bassoon knockout mice show generalized epileptic seizures (Altrock et al., 2003), progressive brain overgrowth (Heyden et al., 2011) and aberrant cortical activity (Angenstein et al., 2007). The attachment of synaptic ribbons, a specialized structure of the CAZ at particular synapses, is affected in retina and inner ear cells ribbon synapses in these mice (Dick et al., 2003; Khimich et al., 2005). However, conventional synapses show no morphological phenotype (Altrock et al., 2003).

Instead, Piccolo mutant mice are smaller with no major impairment in synaptic function (Mukherjee et al, 2010). Nevertheless, recent work suggested a role for Piccolo in endosome-sorting mechanisms, which might contribute to developmental and psychiatric disorders (Ackermann et al., 2019). The absence of both scaffolding proteins in neurons results in defective organization of the SV cluster and a reduction of the readily releasable pool of SV (Mukherjee et al, 2010; Waites et al., 2013; Butola et al., 2017). Leal-Ortiz et al., (2008) showed that Piccolo negatively regulates SV exocytosis by modulating the synapsin-1a dynamics, mobilizing SVs from the reserve pool to the AZ. This phenotype was also attributed to the connection with F-actin, CaMKII and actin modulatory proteins such as Profilin2 (Waites et al., 2011). Moreover, Piccolo has recently been identified as a key effector in the mobilization of subpools within the RRP, sustaining high-frequency synaptic transmission (Parthier et al., 2018). This data indicates that Bassoon and Piccolo seem to be involved in multiple steps of NT release. Furthermore, Piccolo interacts with the prenylated Rab acceptor protein 1 (PRA1) a rab3-VAMP2/SynaptobrevinII-interacting protein (Fenster et al., 2000) and Actin-binding protein 1, which in turn binds to both F-actin and the GTPase dynamin (Fenster et al., 2002). Piccolo´s central part (aa 2197-2350) undergoes a direct interaction with the Spa2-homology domain of GIT1 (Kim et al., 2003), implicated in membrane trafficking events (Kim et al., 2003).

Bassoon localizes VGCC at the release sites (Davydova et al., 2014). This occurs through its RTLPSPP motif (PxxP motif located in the 7$^{th}$ Piccolo-Bassoon homology region (PBH)), which binds to the first SH3 domain of the RBPs, most likely, and subsequently to the VGCC. In this way, the presynaptic protein contributes to the $Ca_v2.1$ recruitment

at the presynaptic release sites (Davydova et al., 2014). Moreover, at inner ear hair cell ribbon synapses, Bassoon contributes to the correct positioning of $Ca_v1.3$ (Khimich et al 2005; Frank et al., 2010). Piccolo contains a similar PxxP motif to Bassoon (RTLPNPP), which only differs in the amino acid at position 5 (Ser→Asn), however, the function of Piccolo regarding positional priming of presynaptic VGCC has been less explored.

Next to the C-terminus, Piccolo contains a region of five-conserved aspartate residues ($C_2$A-domain) (Fenster et al., 2000), which confers to the scaffolding protein the capacity to function as a low-affinity $Ca^{2+}$ sensor (Gerber et al., 2001). Piccolo interacts with cAMP- guanidine nucleotide exchange factor II (cAMP-GEFII) and it serves as a $Ca^{2+}$ sensor in pancreatic β-cells (Fujimoto et al., 2002). Furthermore, in this type of cells the interaction between L-type $Ca^{2+}$ channels and Piccolo has been reported (Shibasaki et al., 2004). A recent study performed in the endbulb of Held showed that Bassoon and RIM levels are disrupted in Piccolo-mutant neurons (Butola et al., 2017), implying possible changes in the $Ca^{2+}$ channel populations.

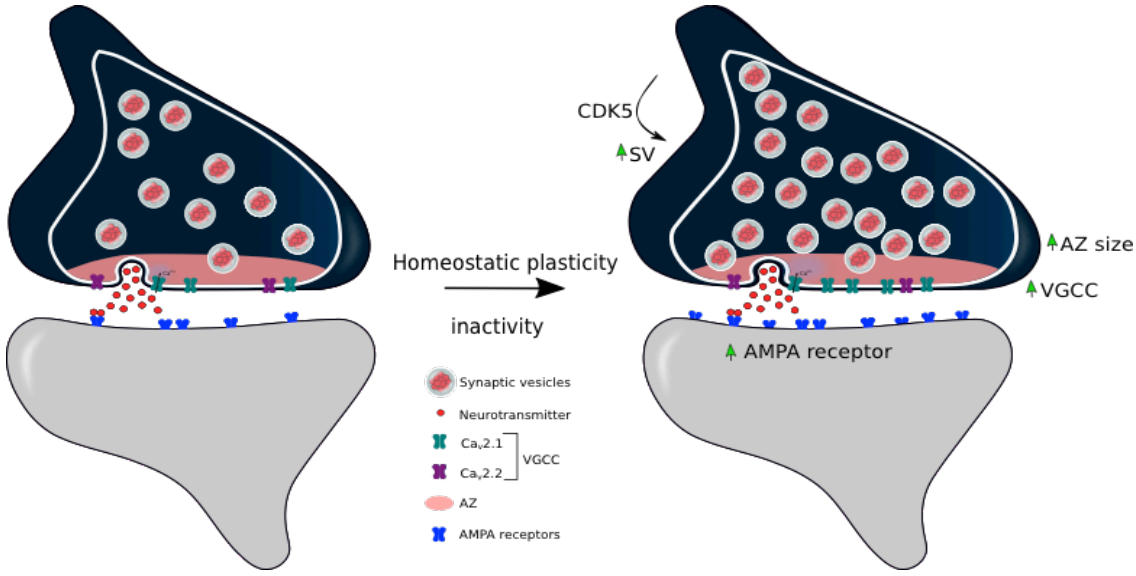


**Figure 5: Homeostatic plasticity changes after a prolonged period of inactivity.** Scheme depicting the major homeostatic adaptations in synapses after overall network inactivation. The mechanisms comprise enlargement of the active zone, enhanced numbers and function of voltage-gated calcium channels, and CDK5-mediated increase in synaptic vesicles, and rise in the AMPA receptor expression. Abbreviations: VGCC, voltage-gated calcium channel; SV, synaptic vesicle; AZ, active zone; CDK5, cyclin-dependent kinase 5; AMPA, α-amino-3-hydroxy-5-methyl-4-isoxazolepropionic acid.

## 1.4 Neuroplasticity

Neuronal plasticity refers to the ability of neurons to adapt their morphology and their function to changes in physiological processes with the consequence to reorganize entire neuronal networks. Neurons constantly adjust their synaptic strength and/or morphology

to external or internal stimuli (Duman, 2004). Two kinds of neuronal plasticity can be distinguished: associative (or Hebbian) plasticity and homeostatic synaptic plasticity. The former is a basic mechanism underlying learning and memory processes. The strengthening or weakening of the synaptic function arises from the persistence of a common stimulation pattern between cell A and cell B (Brown & Milner, 2003). It is illustrated by the phrase "Cells that fire together wire together" (Hebb, 1949). This type of plasticity can last from hours to months. On the other hand, homeostatic synaptic plasticity acts as compensatory mechanism in order to keep neuronal excitability in a physiological range while stabilizing changes in the overall network activity. These changes can occur at the synaptic level where they affect synaptic efficacy and target both pre- and postsynaptic compartments (Wierenga et al., 2006). Upon high network activity, neurons decrease the efficacy of neurotransmission. Contrary, when the activity is suppressed, the synaptic transmission and intrinsic neuronal excitability increases. At the synapse level, homeostatic plasticity is expressed as changes either in the presynaptic release probability (Pr; Murthy et al., 2001) or in the sensitivity of the postsynaptic apparatus (O´Brien et al., 1998; Lindskog et al., 2010).

### 1.4.1 Homeostatic synaptic plasticity

To date postsynaptic mechanisms have been studied in more detail during homeostatic plasticity. Murthy and colleagues, (2001) were among the first to show the importance of presynaptic mechanisms contributing to homeostasis. Suppression of the overall network activity, either by treatment with the sodium channel blocker tetrodotoxin (TTX) or with glutamate receptor antagonists, leads to a rise of the Pr (Murthy et al., 2001). It correlates with increased frequency of miniature excitatory postsynaptic currents (mEPSCs), enlargement of the AZ, an increased number of docked SVs and enhanced SV recycling (Murthy et al., 2001; Bacci et al., 2001; Thiagarajan et al., 2005; Moulder et al., 2006; Han and Stevens, 2009) (Figure 5). However, the over-excitation of a network leads to a decrease of the Pr of excitatory neurons and diminishes SV pool sizes (Moulder et al., 2004; Branco et al., 2008). Cyclin-dependent kinase 5 (CDK5) plays a key role during homeostatic plasticity in balance with calcineurin B (Kim and Ryan, 2013). It modulates the SV pool sizes, in particular the RtP and the RP, facilitating the number of SV available to be released, according to changes in the network activity (Kim and Ryan, 2010). Pre-

synaptic homeostatic plasticity adaptations are not restricted to modulation of the SV cycle, but can also affect presynaptic $Ca^{2+}$ entry. Changes in evoked $Ca^{2+}$ income was registered upon network activity manipulation (Zhao et al., 2011). Jeans et al., (2017) demonstrated that changes in AP-triggered $Ca^{2+}$ influx upon silencing or chronic activation occur through $Ca_v2.1$. Furthermore, the balance between $Ca_v2.1$ splice variant seems to be a key factor in the regulation of the homeostasis (Talhammer et al., 2017), an observation relevant also for the present study.

Several studies have highlighted the importance of the molecular effectors underlying compensatory mechanisms in response to global network activity changes (Thiagarajan et al., 2005; Cohen et al., 2011; Lazarevic et al., 2011). In the presynapse, network inactivation induces modulation of SV proteins, and components of the release machinery, such as Bassoon, Piccolo, RIM or Munc13 (Lazarevic et al., 2011). RIM levels correlate with the activity at single synapses, being redistributed on the demands of neurotransmission. However, the role of Bassoon or Piccolo during homeostatic plasticity is still unclear. In mammals, to date, only RIM has been reported to contribute to the regulation of the Pr during homeostasis (reviewed in Lazarevic et al., 2013).

Homeostatic plasticity in the postsynapse is expressed as changes in the sensitivity and responsiveness of the postsynaptic receptor apparatus (O´Brien et al., 1998; Thiagarajan et al., 2005). Global forms of homeostasis are bidirectional. While chronic stimulation in vitro with Bicuculline, a drug that blocks inhibitory $GABA_A$ receptors, and thus, increases network activity, reduces α-amino-5-hydroxy-3-methyl-4-isoxazole propionic acid (AMPA) receptor transmission and expression (Turrigiano et al., 1998; Shepherd et al., 2006; Stellwagen and Malenka, 2006), chronic silencing with either TTX or APV and CNQX was shown to induce synaptic scaling by increasing AMPAR levels and transmission (Turrigiano et al., 1998; Shi et al., 2001; Matsuzaki et al., 2004; Harms et al., 2005; Plant et al., 2006; Ehlers et al., 2007).

## 1.5 Aims of the study

Several groups have shown the importance of Piccolo in the processes governing neurotransmitter release. Piccolo, an organizational component of the presynaptic active zone,

has been linked to major health disorders such as Pontocerebellar hypoplasia type3 or bipolar disorder (Sullivan et al., 2009; Choi et al., 2011; Minelli et al., 2012; Woudstra et al., 2013; Giniatullina et al., 2015; Ahmed et al., 2015). Nevertheless, how the scaffolding protein is involved in the development of these diseases, and its function, is not yet well understood.

Some clues from cellular, biochemical and molecular analyses indicate that Piccolo is important in mechanisms such as organization of the release machinery, linkage of actin dynamics, SV exocytosis and vesicle replenishment. However, a possible link between Piccolo and VGCC has not been yet explored. Based on these data, it was the aim of my thesis to study the role of Piccolo in the regulation of neurotransmitter release and during synaptic plasticity. In this context, I have studied 1) the functional link between Piccolo and VGCC and 2) the role of Piccolo during presynaptic homeostatic plasticity. As Bassoon is a closely related protein to Piccolo, it was further of interest to study the functions of its paralogous scaffolding protein Bassoon, e.g. in the regulation of presynaptic $Ca^{2+}$ influx and during presynaptic homeostasis.

1) As described above, the interaction of Bassoon with VGCC through RBPs has implications in the distribution of the channels within the AZ, and therefore in the neurotransmitter release. Since Piccolo contains a similar RBP-interacting motif, I was keen to know the effect of Piccolo absence for the presynaptic VGCC $Ca^{2+}$ income. Therefore, it is of high importance to study the interaction of Piccolo and RBPs, and the functional consequences derived from it. In the frame of this project the following aspects were addressed:

- Electrophysiological consequences of Piccolo absence in primary hippocampal cultures of Piccolo-mutant mice.
- Piccolo binding to VGCC via the RBP2 was characterized. I explored the consequences of the Piccolo mutation in the recruitment and contribution of VGCC to synaptic transmission in hippocampus.
- Another goal was to investigate the implications of Piccolo in the SV cycle in terms of Pr: the size of the SV pools and SV replenishment were assessed in Piccolo-mutated hippocampal cultures.

2) Homeostatic plasticity contributes to maintain synapses in a functional state while preserving the specificity of synaptic changes that encode information. Lazarevic et al.

(2011) reported a profound reorganization of the release apparatus upon overall network silencing, highlighting the importance of RIM and $Ca_v2.1$. RIM is redistributed upon activity suppression. The number of RIM-positive puncta was reduced, nevertheless, the remaining ones were larger. Contrary to RIM, the Cav2.1 level was enhanced. Extensive evidence has been reported about the importance of the $Ca^{2+}$ influx during homeostatic plasticity (reviewed in Frank et al., 2014; Zhao et al., 2011; Jeans et al., 2017; Talhammer et al., 2018). Given this, and considering the interplay between Bassoon, and presumably Piccolo, with VGCC, the hypothesis was that synapses lacking Bassoon or Piccolo were not able to adjust their synaptic strength properly during homeostatic plasticity. More specifically, I addressed the following points:

- The consequences of Bassoon deletion were explored in the pre- and postsynaptic compartment during homeostatic plasticity adaptations after chronic silencing. I studied whether the presynaptic scaffold controls presynaptic functions through interaction with VGCC, and if its deletion modifies the AMPA receptor levels on the surface of the postsynaptic membrane.
- Based on the potential link between VGCC and Piccolo, I studied the role of Piccolo in homeostasis within the presynapse, and how it might modulate the presynaptic $Ca^{2+}$ entry.

# 2 Material and Methods

## 2.1 Materials

### 2.1.1 Antibodies

| Antibody | Species | Dilution | Company |
|---|---|---|---|
| Alexa Fluor® 488 | Goat or Donkey | 1:2000 | Jackson ImmunoResearch |
| AMPA2 (panGluA) | Mouse | 1:500 | Synaptic Systems |
| Bassoon (sap7f) | Mouse | 1:1000 | ENZO |
| $Ca_V2.1$ (P/Q-type) | Rabbit | 1:1000 | Alomone labs |
| $Ca_V2.2$ (N-type) | Rabbit | 1:1000 | Synaptic Systems |
| Cy3 | Goat or Donkey | 1:2000 | Jackson ImmunoResearch |
| Cy5 | Goat or Donkey | 1:1000 | Jackson ImmunoResearch |
| Gephyrin | Guinea Pig | 1:1000 | Synaptic Systems |
| Homer1 | Rabbit | 1:1000 | Synaptic Systems |
| Munc13-1 | Mouse | 1:1000 | Synaptic Systems |
| RIM1/2 (against Zn-finger domain) | Rabbit | 1:1000 | Synaptic Systems |
| SV2B | Rabbit | 1:1000 | Synaptic Systems |
| Synapsin 1,2 | Rabbit | 1:1000 | Synaptic Systems |
| Synapsin 1,2 | Guinea Pig | 1:1000 | Synaptic Systems |
| Synaptophysin 1 | Guinea Pig | 1:1000 | Synaptic Systems |
| Synaptotagmin1 lumenal domain labeled with Oyster®550 | Rabbit | 1:70 | Synaptic Systems |
| VGAT | Rabbit | 1:1000 | Synaptic Systems |
| VGluT1 | Rabbit | 1:1000 | Synaptic Systems |

Table 1: Antibodies

### 2.1.2 Animals

Rodent lines used in this thesis to obtain tissue and cells were: Bassoon knockout mouse strain ($Bsn^{gt}$) (Hallermann et al., 2010; Davidova et al., 2014), Bassoon conditional Knockout (B2E) (which lacks Bassoon in excitatory synapses, Annamneedi et al., 2018) and Piccolo (Pclo3) mouse strain (Mukherjee et al, 2010). Using a gene trap strategy Bassoon knockout strain was obtained from Omnibank ES cell line OST486029 by Lexicon Pharmaceuticals, Inc. (The Woodlands, TX, USA). Pclo3 constitutive mutant line was obtained crossing the $Pclo^{tm2Sud}$ (Jackson Laboratory), which possess the exon 14 flankered with loxP sites, with the ubiquitously expressing Cre line Tg(CMV-Cre)1Nagy (Nagy et al., 1998). They were bred in the animal facility of the Leibniz Institute for

Neurobiology, Magdeburg. Homozygous mutant mice were obtained from heterozygous breedings.

### 2.1.3 Pharmacological reagents

| Compound | Biological activity | Working Concentration | Company |
|---|---|---|---|
| ω-Conotoxin GVIA (ConoTx) | Specific blocker of $Ca_v2.2$ VGCC | 1 µM | Alomone Labs |
| ω-Agatoxin IVA (AgaTx) | Specific blocker of $Ca_v2.1$ VGCC | 0.4 µM | Alomone Labs |
| Tetrodotoxin (TTX) | Selective inhibitor of sodium channels conductance | 1 µM | Tocris |
| 6-Cyano-7-nitro-quinoxaline-2,3 dione di-sodium (CNQX) | Competitive AMPA/keinate receptor antagonist | 10 µM | Tocris |
| D-(-)-2-Amino-5- phosphonopentanoic acid (D-APV5) | Competitive NMDA receptor antagonist | 50 µM | Tocris |
| Ionomycin | $Ca^{2+}$ ionophore | 5 µM | Sigma-Aldrich |
| Bafilomycin A1 (BafA) | Specific inhibitor of vacuolar type $H^+$-ATPase | 0.1 µM | Calbiochem/Merck Millipore |

Table 2: Pharmacological reagents

### 2.1.4 Molecular biology reagents

| Reagent | Purchased from |
|---|---|
| Restriction enzymes/ Endonucleases | Thermo scientific |
| Taq DNA polymerase | Quiagen |
| Deoxynucleoside triphosphate set (dNTPs) | Thermo scientific |
| Oligonucleotides (Primer) | Invitrogen |
| Phusion® DNA polymerase | Thermo scientific |
| Proteinase K | Thermo scientific |

Table 3: Molecular biology reagents

### 2.1.5 Culture media for bacteria

| Type of medium | Composition |
|---|---|
| SOC-medium | 20 g/l peptone 140 (Gibco); 5 g/l yeast extract (Gibco); 10 mM NaCl; 2.5 mM KCl; 10 mM $MgSO_4$; 20 mM |
| LB-medium | 20 g LB Broth Base (Invitrogen) / 1000 mL LB-medium |
| LB-agar | 15g Select Agar (Invitrogen) / 1000 mL LB-medium |

Table 4: Culture media for bacteria

### 2.1.6 Mammalian cell lines

| Mammalian cell line | Company |
|---|---|
| Human Embryonic Kidney cells (HEK293-T) | ATTC, Manassas, VA |

Table 5: Mammalian cell lines

### 2.1.7 Culture media and reagents for culture of mammalian cell lines

| Media and Reagents | Composition |
|---|---|
| Hanks Balanced Salt solution (HBSS) -/- (Without $Mg^{2+}$ and $Ca^{2+}$) | Gibco |
| DMEM (10% FCS) | 10% FCS (Gibco); 1% Penicillin /Streptomycin 100x (Gibco); 2 mM L-Glutamine (Gibco) in DMEM (Gibco) |
| Trypsin | 0.5% stock solution diluted 1:10 in HBSS (invitrogen) |
| Poly-D-lysin (D-PLL) | 100 mg/l D-PLL in 100 mM boric acid, pH 8.4 |

Table 6: Media and reagents

### 2.1.8 Culture media and reagents for primary neuronal and glial cultures

| Media and reagents | Composition/ Company |
|---|---|
| HBSS -/- | Gibco |
| 10x Trypsin | Gibco |
| DNase | Roche |

| | |
|---|---|
| Neurobasal A complete | Neurobasal A media (Gibco) supplemented with 1xB27 (Gibco), 4 mM Glutamax (Gibco), 1 mM Sodium Pyruvate (Gibco) and 100 U/mL penicillin and streptomycin (Gibco) |
| Neurobasal complete | Neurobasal A media (Gibco) supplemented with 1 x B27 (Gibco), 4 mM Glutamax (Gibco), 1 mM Sodium Pyruvate (Gibco) and 100 U/mL penicillin and streptomycin (Gibco) |
| Plating media | DMEM (Gibco) supplemented with 1% Glutamine and 1% mL penicillin and streptomycin (Gibco) |
| Glial growing media | DMEM (Gibco) supplemented with 10% FCS, 1% Glutamine (Gibco) and 1% penicillin and streptomycin (Gibco) |
| Poly-L-Lysine (L-PLL)/D-PLL | 100 mg/l L-PLL or D-PLL in 100mM boric acid, pH 8.4 |
| Paraffin | Paraplast embedding medium (Fisher) |
| Cytosine β-D-Arabinofuranoside (Ara C) | 1.5 mM (Sigma-Aldrich) |

Table 7: Media and reagents for primary neuronal cultures

### 2.1.9 Commonly used buffers and reagents for live imaging and live staining experiments

| Buffer type | Composition |
|---|---|
| HEK293T cells lysis buffer (Double-Co-immunoprecipitation) | 10 mM Hepes 7.2pH, 0.5% Triton 100-X, 150 mM NaCl, 10% Glycin and 0.1 % Deoxycholate |
| HEK293T cells lysis buffer (Triple-Coim-munoprecipitation) | 40 mM Tris HCl 7.4, 0. % Triton 100-X, 150 mM NaCl |
| PBS | 2.7 mM KCl; 1.5 mM $KH_2PO_4$; 8 mM $Na_2HPO_4$, pH 7.4 |
| PBS-T | 2.7 mM KCl; 1.5 mM $KH_2PO_4$; 8 mM $Na_2HPO_4$, pH 7.4; 0.1% Tween20 |
| Sucrose buffer A | 5 mM Tris-HCl pH 7.4; 5 mM $MgCl_2$; 0.32 M sucrose; 1 mM DTT; 2 mM ATP |
| Sucrose buffer B | 5 mM Tris-HCl, pH 8.1; 5 mM $MgCl_2$; 0.32 M sucrose; 1 mM DTT; 2 mM ATP |
| Extracellular imaging solution (Tyroides buffer) | 119 mM NaCl, 2.5 mM KCl, 25 mM HEPES pH 7.4, 30 mM glucose, 2 mM $MgCl_2$ and 2 mM $CaCl_2$ |

| | |
|---|---|
| High tyrodes buffer) | 119 mM NaCl, 2.5 mM KCl, 25 mM HEPES pH 7.4, 30 mM glucose, 2 mM $MgCl_2$ and 2 mM $CaCl_2$, 1 mM KCl |
| Blocking solution | 10% FCS; 0.1% glycin; 0.3% Triton X-100 in PBS |
| **Solutions used for Western Blot** | |
| 5xSDS loading buffer | 250 mM Tris-HCl pH 6.8; 30% Glycerol; 7.5% SDS; 0.25% Bromophenol blue |
| Electrophoresis buffer | 192 mM glycine, 1% (w/v) SDS, 25 mM Tris-base, pH 8.3 |
| 4x separating buffer | 1.5 M Tris-HCl, pH 8.8 |
| 4x stacking buffer | 0.5 M Tris-HCl, pH 6.8 |
| Separation gel (20 %) | 8.25 ml separation buffer; 7.5 ml 87% Glycerol; 16.5 ml 40% Acrylamyde; 330 µl EDTA (0.2 M); 330 µl SDS; 22 µl TEMED; 120 µl 0.5% Bromophenol blue and 85 µl 10% APS |
| Separation gel (5 %) | 8.25 ml separation buffer; 17.94 ml $dH_2O$; 1.89 ml 87% Glycerol; 4.12 ml 40% Acrylamide; 330 µl EDTA (0.2 M); 330µl SDS; 22 µl TEMED and 128 µl APS |
| Stacking gel (5 %) | 6 ml stacking buffer; 7.84 ml $dH_2O$; 5.52 ml 87% Glycerol,<br>3.90 ml 30% Acrylamyde; 240 µl EDTA (0.2 M); 240 µl 10% SDS, 17.2 µl TEMED; 140 µl Phenol red and 137 µl 10% APS |
| Blotting buffer | 192 mM glycine, 0.2% (w/v) SDS, 25 mM Tris-base |
| Lysis buffer double coimmunoprecipitation | 10 mM HEPES ph7.2, 0.5% triton100-X, 150 mM NaCl, 10% Glycin, 0.1% Sodium Deoxicolate |
| Lysis buffer triple coimmunoprecipitation | 40 mM Tris HCl ph7.4, 0.1 Triton100-X, 150 mM NaCl |

Table 8: Used buffers and reagents for live imaging experiments and Western blotting

## 2.2 Methods

### 2.2.1 Biochemical methods

#### 2.2.1.1 Immunoprecipitation from HEK293T cell extracts

Calcium phosphate was the method used for HEK293T cell transfection. The solution A (250 µl for 25 $cm^2$ flask) was mixed with DNA, while solution B was added (250 µl) after 30 sec. The mixture was incubated for 1 min in total and applied on top of the cells. From 4 to 6hrs later, the medium was exchanged for fresh pre-warmed medium. After 48h of expression, the transfected cells were lysed for 5 to 10 min on ice with two different buffers depending on the type of immunoprecipitation (Double or Triple; Table 7) supplemented with complete protease inhibitors and PhosStop. Following a clearance by centrifugation the co-immunoprecipitation (Co-IP) was performed using MicroMACS anti-GFP Microbeads and Micro Columns (Miltenyi Biotec). The protocols provided by the company were followed, except for the washing steps that were done with lysis buffer. The proteins co-immunopreciptated were eluted with SDS-loading buffer, and collected for immunoblotting.

#### 2.2.1.2 Protein concentration determination: Bicinchoninic acid assay

Protein concentration was determined by the colorimetric Bicinchoninic acid (BC) assay (Uptima). To prepare the calibration curve (0 – 2 mg/ml), 25 µl of each step of the standard curve was put into a 96 well microplate (in triplicates). 200 µl of reaction buffer (reaction buffer A + Reaction buffer B, 50:1) was added to both, the standard and sample (in parallel to the standard curve) solutions. All samples were incubated for 30 min at 37ºC. The absorption was measured at 562 nm by the Molecular Devices/ Versa max microplate reader.

#### 2.2.1.3 SDS-PAGE

Proteins were separated using one-dimensional sodium dodecyl sulphate polyacrylamide gel electrophoresis (SDS-PAGE) under fully denaturing and reducing conditions (Laemmli, 1970), as it was described previously in Lazarevic et al., (2011). Due to its large size, the VGCC samples required special treatment. These proteins tend to form aggregates after boiling, being necessary no boiling. SDS-PAGE was performed in a gradient gel. The samples were first incubated with sample buffer at 95ºC for 5 min and then

loaded onto the gel. Gels were run at a constant current strength of 12 mA in an electrophoresis chamber (Hoefer Mighty Small System SE 250 from Amersham Biosciences) filed with 1x electrophoresis buffer. Subsequently, the gels were used for immunoblotting at 4ºC, 200 mA for 1 h and 30 min (TG) and 2 h (TA) with blotting buffer (Table 7). Blots were then incubated with primary antibodies (in PBS containing 5% BSA, 0.1% Tween and 0.025 % sodium azide) at 4°C overnight, followed by 3 washes with PBS-T and incubation at RT for 1h with HRP-conjugated secondary antibody (diluted in 5% non-fat dry milk/PBS-T). For quantitative westernblotting with secondary antibodies (in PBS containing 1% BSA, 0.1% Tween) for 1 h at RT. Immunodetections were performed using Pierce ECL WB Substrate (Thermo Scientific) and ChemoCam Imager (Intas). In addition, quantitative immunoblots were read using Odyssey Infrared Scanner (LI-COR). Identical rectangular ROIs (regions of interest) were set around the bands to measure the ID values. Values were normalized the mean value of the wild-type group for each individual membrane.

## 2.2.2 Molecular biological methods

### 2.2.2.1 Genotyping of mutant mice

Newborn pups (p0-p1) were labeled and tail cut samples were taken for DNA extraction. The tail cut samples were incubated together with 200µl lysis buffer (10 mM Tris-HCl pH 8.0, 100 mM NaCl supplemented with 0.4 mg/ml Proteinase K) at 1000 rpm for 35 min (55ºC) in a thermoshaker (Eppendorf). Thereafter, the enzyme was inactivated by incubation for 10 min at 95°C, the sample was ready for PCR. One tube without tail cut sample was used as a negative control. The PCR master mix contained 4 µl of DNA extract, 1 pM of both forward and reverse primer (Table 10), 2.5 mM $MgCl_2$, 0.1 U/µl Taq-polymerase, 0.2 mM dNTPs and 1x PCR buffer (Qiagen). The tables describe temperature profile used for the PCR reactions:

| **Process** | **Time and temperature** | **Cycles** |
|---|---|---|
| Initial denaturation | 95°C for 5 min | 1 |
| Denaturation<br>Annealing<br>Extension | 95°C for 30 sec<br>65°C for 30 sec<br>78°C for 45 sec | 35 |
| Final extension | 68°C for 5 sec | 1 |

Table 9: PCR program used for genotyping of $Bsn^{gt}$ mice pups

| Process | Time and temperature | Cycles |
|---|---|---|
| Initial denaturation | 95°C for 5 min | 1 |
| Denaturation<br>Annealing<br>Extension | 95°C for 30 sec<br>65°C for 30 sec<br>78°C for 45 sec | 35 |
| Final extension | 68°C for 5 sec | 1 |

Table 10: PCR program used for genotyping of Pclo3 pups

| Process | Time and temperature | Cycles |
|---|---|---|
| Initial denaturation | 94°C for 5 min | 1 |
| Denaturation<br>Annealing<br>Extension | 94°C for 30 sec<br>60°C for 60 sec<br>78°C for 45 sec | 35 |
| Final extension | 72°C for 7 min | 1 |

Table 11: PCR program used for genotyping of Emx-1 for B2E mice pups

| Process | Time and temperature | Cycles |
|---|---|---|
| Initial denaturation | 94°C for 3 min | 1 |
| Denaturation<br>Annealing<br>Extension | 94°C for 30 sec<br>66°C for 45 sec<br>78°C for 45 sec | 35 |
| Final extension | 72°C for 7 min | 1 |

Table 12: PCR program used for genotyping of Bsn2 for B2E mice pups

| Genotype | Forward primer | Reverse primer |
|---|---|---|
| $Bsn^{gt}$ WT<br>$Bsn^{gt}$ KO | 5'-ctaagctattgcttcctcctcac-3'<br>5'-ctaagctattgcttcctcctcac-3' | 5'-ctgaggctcttgagttcctacga-3'<br>5'-ataaaccctcttgcagttgcatc-3' |
| Pclo3 WT<br>Pclo3 KO | 5'-gctctggtacagaggtaaagcttgc-3'<br>5'-ccttgaggtcaatgtgatcagc-3' | 5'-ttgtgtcacgtagtcagactg-3'<br>5'-ccaagttctaattccatcagaagc-3' |
| Bsn2 | 5´-gcagattctagtcggtgatctagc-3´ | 5´-gttgcctaatgtatgcagagtcc-3´ |
| Emx-1 | 5´-gcggtctggcagtaaaaactatc-3´<br>5´-gtgaaacagcattgctgtcactt-3´ | 5´-aaggtgtggttccagaatcg-3´<br>5´-ctctccaccagaaggctgag-3´ |

Table 13: Primer sequences used for genotyping of Bsngt, Pclo3, B2E and wild-type alleles

After PCR, reaction mixtures were run on 1.5% agarose gels (Biozym LE agarose, dissolved in TAE buffer (Biorad)) for 1h, and then bands visualized via illuminating with UV light (Science Imaging, Intas).

### 2.2.2.2 Lentiviral particle production

For transfection of single flasks of HEK293T cells the calcium phosphate method was used. 500 µl of solution A (0.5 M CaCl2) was mixed with a total of 20 µg of DNA (FUGW: psPAX2: pVSVG = 5,5:9:5,5 µg (Lois et al., 2002)). 500 µl of solution B (140 mM NaCl, 50 mM HEPES, 1.5 mM $Na_2HPO_4$, pH 7.05) was added to the previous mix after 30 seconds, the mixture was applied on top of the cultured cells. They were kept in the incubator at 37ºC, 5% $CO_2$ for 6-8h before exchanging the media for Neurobasal A complete media. 48h later, the supernatant containing the virus produced by the cells was collected, and centrifuged at 2000 g for 10 min at RT. The virus was kept aliquoted at -80ºC and ready for further use.

Neurons were infected at 4 DIV by adding 80-100 µl of the virus solution on top of the coverslips for 7-9 h prior returning them to their astrocyte-containing plates.

### 2.2.2.3 Cell culture techniques

Primary hippocampal cultures from mice were prepared following well-established protocols (Kaech and Banker, 2006; Davydova et al., 2014).

P0-P1 newborn mice were selected according to their genotype and decapitated to obtain their brains, from where the hippocampi were extracted. Meninges were removed and the cleaned hippocampi were incubated for 15 min at 37ºC with 0.025% of Trypsin and followed by mechanical trituration with a glass Pasteur pipette. The suspension was washed two times with HBSS -/- (Table 6), then plated in plating media (Table 6) on L-PLL-precoated glass coverslips (18 mm) in a concentration of 25.000-30.000 cells/per coverslip. After one hour, the coverslips were transferred into dishes containing a confluent monolayer of mouse astroglial embedded in Neurobasal A complete. The cultures were kept in the incubator at 37ºC and 5 % CO2. AraC was added to hippocampal cultures in a concentration of 0.6 µM after 20-24 h. A second AraC application was done at 3 DIV (days in vitro) to reach a final concentration of 1.2 µM.

The neurons were always infected at 4-5 DIV. ~100 µl of media containing virus was applied for 7-8 h onto the coverslips. Afterwards, the covers were returned to the original

dishes with conditioned media, and kept in the incubator till at least 17 DIV, before experiments were performed. Reagents used in these procedures are summarized in Table 6.

### 2.2.2.4 Calcium imaging

$Ca^{2+}$ imaging was performed in 18-22 DIV primary hippocampal cultures infected with lentivirus containing the genetically encoded calcium sensor Sy-GCaMP5G at 4 DIV. This tool is the result of fusing the calcium sensor GCaMP with the exclusive neuronal hSyn1 promoter. Coverslips were placed into an imaging chamber (RC-49MFSH; Warner instruments) with two platinum wire electrodes placed 10 mm apart in order to apply electric stimulation to the neurons at RT in extracellular imaging solution (tyroides buffer) supplemented with 50 µM APV and 10µM CNQX. Inverted microscope (Zeiss Axio Observer.A1) was used, equipped with an EMCCD camera (Evolve delta; Photometrics) controlled by VisiView (Visitron Systems GmbH) using a 63x oil immersion objective NA 1.4, and an EGFP ET filter set (ET470/40x; ET525/50m; T495LPXR). Lentiviral infection efficacy was 93-98 %. Cells were electrically stimulated using different train of pulses delivered at 20 Hz (5, 10 and 20 AP). Pulses were evoked by delivering currents of 50 mA for 1 ms using an isolator unit (World Precision Instruments) connected to a pulse generator (Master-8). Average of the responses were considered in order to obtain more robust data. Image acquisition was made at a frequency of 50 Hz. From each coverslip, at least one visual field was imaged and analyzed, keeping three minutes of recovery time between stimulations in case more than one was taken, and applying a pulse of ionomycin at the end of each imaged coverslip to reveal total expression levels of the sensor. AgaTX (ω-Agatoxin IVA) and ConoTX (ω-Conotoxin GVIA) were applied for 8 and 10 mins, respectively, in order to dissect the subtype contribution of VGCC to the $Ca^{2+}$ responses. Image acquisition was done, before and after toxin bath, to compare the effect in the region of interest.

Analysis was performed using ImageJ (NIH, http://rsb.info.nih.gov/ij/). Responding boutons were identified by subtracting 5 frames prior to the stimulation (baseline) from the 5 frames following it. ROIs of 3x3 pixel size were placed in the responding boutons by using “Find Maxima” from ImageJ. Mean grey values from ~100 ROIs/region of interest

were analyzed and mean response ± standard error of the mean (s.e.m) of each visual field was considered for statistical purposes.

The $\Delta F/F_0$ was calculated from the mean gray values, and then, analyzed in Excel. 10 frames prior fluorescence response onset was considered as the $F_0$. Signal-to-noise (SNR) ratio was calculated for each ROI as the maximum value within 10 frames after the average response onset divided by the standard deviation of $F_0$ and only responses with, at least, the double of the SNR (Dreosti et al., 2009) were considered. The analysis was performed using Graph Pad Prism (GraphPad Software Inc., Calif., USA).

The experiments of the double KO were performed in 19-20 DIV primary hippocampal cultures infected with Sy-GCaMP5G-contained virus. The Fluorescence was excited with a polychrome 3000 lamp (Adgiland technologies/TILL Photonics) through a 60 x 1.4 NA oil immersion objective (Olympus). Images were captured by an EMCCD camera (iXon+ 897, Andor Technology) controlled by MetaMorph imaging software (Universal Imaging) at a frame rate of 50 Hz. Field stimulation was carried out using two platinum electrodes placed on the coverslip in a distance of 15 mm. The triggering of extracellular stimulus (50 mA for 1 ms) was controlled by an isolated pulse generator (A&M Systems) and delivered via a stimulus isolator unit A385 (World Precision Instruments). The responses were analyzed as described above.

### 2.2.2.5 Synapto-pHluorin imaging

The original mRFP-synaptophysin-pHlourin (sypHy) construct was obtained from Professor Dr. Thomas Oertner (Rose et al., 2013). The SV pools sizes and endocytosis measurement was performed using sypHy in mature hippocampal neurons (18 DIV) infected at 4DIV with a lentivirial vector containing the sypHy. Neurons expressing sypHy were placed in a field stimulation chamber on an inverted microscope equipped with an EMCCD camera controlled by VisiView (Visitron Systems GmbH). The 63x immersion oil objective and an ET GFP/mCherry filter set (ET470/40x; ET572/35x) were used to perform the experiments. The camber, containing the neurons, was filled with extracellular imaging solution (tyroides buffer) supplemented with 50µM APV and 25µM CNQX, but also Bafilomycin A1 (BafA) (blocks the vesicular V-type ATPase and prevents vesicular reacidification). Neurons expressing the sypHy construct were identified by their red signal (mRFP).

To study the SV pool sizes, the SV were released and measured following an established protocol (Burrone et al., 2006): RRP was released by delivery 40 pulses at 20 Hz and the TRP was released, two minutes later, by delivery of 900 pulses at 20 Hz, all in the presence of BafA (1 μM) in order to prevent the fluorescence quenching after endocytosis. Relative sizes of RRP and TRP were then calculated as the fraction of the total sypHy-containing vesicle pool visualized upon application of 60 mM $NH_4Cl$. Subtracting 10 frames before the stimulation to the 20 frames recorded after the onset of the response the responding boutons were selected. 3x3 pixel ROIs were placed in the resulting imaging and mean grey intensity was measured using ImageJ. Calculation of $\Delta F/F_0$ was done as for the $Ca^{2+}$ imaging analysis (explained above). Data were normalized to the values obtained for the application of NH4Cl pulse. Boutons responding with differences between the TRP fluorescence and the NH4Cl-evoked fluorescence lower than 20% were discarded (Burrone et al., 2006).

Endocytosis experiments were performed at room temperature (at 25ºC) in extracellular solution previously described, without BafA (to measure the fluorescence decay) on inverted microscope (Observer, D1; Zeiss) using EGFP ET filter st (excited 470/40, emitter 525/50, dichroic 495 LP) and Cy3 ET filter set (excited 545/25, emitter 605/70, dichroic 565 LP). The action potentials were applied by delivering of 1ms constant voltage pulses (70V) at 20 Hz using a S48 stimulator (GRASS Technologies). A stream of 5-sec images was acquired before the stimulation of 200 stimuli at 20 Hz and imaging recovery of additional 60 sec. The analysis was perform as described above.

### 2.2.2.6 Immunostaining of cell cultures, image acquisition and analysis

For immunostaning well-established protocols were followed (Lazarevic et al., 2011; Altmüller et al., 2017). Neurons were fixed with a solution containing 4 % paraformaldehyde (PFA) and 4% sucrose in PBS at RT for 3-5 min. After 30 min of blocking solution, to reduce the background and permeabilize the cells, the primary antibodies were incubated overnight at 4ºC. Three times PBS washings were done to wash off the excess of antibody. The secondary antibodies were incubated for one hour at RT. After 3 washes, the cover slips were mounted using Mowiol (Calbiochem).

The endogenous network activity-driven and evoked live staining assay was performed with the synaptotagmin 1 antibody (Syt1 Ab) that binds to the luminal domain of the vesicle protein. The coverslips were washed once with pre-warmed extracellular imaging

solution (low Tyroide´s buffer). Under endogenous network activity conditions the antibody was applied in the same solution for 20 minutes at 37ºC, while for evoked conditions the neurons were incubated for 4 min with high tyroides buffers 50 mM KCl contained (Lazarevic et al., 2011). Then, the coverslips were washed twice using tyroides buffer, following fixed with 4%PFA and processed as it is mentioned above. For surface staining of the AMPA receptor, neurons were incubated with antibodies recognizing an extracellular common epitope of GluA1, A2, A3 and A4 in neuronal cell media for 30 min at 4ºC to block membrane trafficking. After a short wash with tyroides buffer completed with 1% BSA (Bovine serum albumin), the secondary antibody was applied in cell media at 4ºC for 10 min. Following, the cells were washed again with modified tyroides buffer and processed for immunostaining as described above.

Images were acquired using a Zeiss Axio Imager A2 microscope (Zeiss) with Cool Snap EZ camera (Photometrics) using the VisiView software (Visitron Systems GmbH). Immunopositive boutons were analyzed along the proximal regions (between 10-50 μm) of the dendritic prolongations from the soma. More than 5 fields were acquired per coverslip and at least 7 fields were considered in each experiment to be analyzed. Images were analyzed using the free software ImageJ (NIH, http://rsb.info.nih.gov/ij/) and the OpenView software obtained from Dr. Noam Ziv (Tsuriel et al., 2006). 11x11 pixel squares were determined as ROIs semi-automatically, masked by the channel containing the presynaptic marker Synaptophysin1 (sphy), Synapsin1, 2 (syn1,2), or vesicular glutamate transporter (VGlut) for excitatory neurons (B2E).

#### 2.2.2.7 Patch clamp recordings of cultured neurons

Whole-cell patch-clamp experiments were performed on hippocampal primary cultures from WT or Pclo-mutant mice on 19-21 DIV at a concentration of 25.000 cells/18 mm coverslips (collaboration with Cr. Yulia Klyeva). Patch pipettes from borosilicate glass had a pipette resistance of 4-6 MΩ, the series resistance was <20 MΩ and the resting membrane potential was measured immediately after establishment of the whole-cell configuration. Extracellular solution contained in mM: 145 NaCl, 2.5 KCl, 2 MgCl2, 2 CaCl2, 10 HEPES, and 10 D-glucose (pH 7.4 adjusted with NaOH). Intracellular solution for recording of evoked EPSC (eEPSCs) and action potentials contained in mM: 140 K-gluconate, 1 MgCl2, 2 CaCl2, 4 NaATP, 10 EGTA, 10 Hepes, and 0.4 GTP (pH 7.25

adjusted with KOH). Input resistance and parameters of action potentials were calculated from I/V curve in neurons kept at -60 mV by application of current steps (1s, from -250 pA to 600 pA with 50 pA increment). For measurements of mEPSCs we used an intracellular solution of the following composition in mM: 115 Cs methylsufonate, 10 CsCl, 5 NaCl, 20 TEAchloride, 2 MgCl2, 2 CaCl2, 10 HEPES, 0.6 EGTA, 2 Mg-ATP, 0.3 Na-GTP, pH 7.2-7.3, Na-channels and GABAA-receptors were blocked by adding to the bath solution of tetrodotoxin (TTX,1 µM, Tocris, Bristol, UK) and bicucullinemethioidide (Bicu, 10 µM, Abcam, Cambrige, UK) respectively. Miniature inhibitory postsynaptic currents (mIPSCs) were recorded with intracellular solution of following composition in mM: 118 KCl, 9 EGTA, 10 HEPES, 4 MgCl2, 1CaCl2, 2 Mg-ATP, 0.3 Na-GTP, (pH 7.2-7.3 adjusted with KOH), Na-channels, AMPA and NMDA-receptors were blocked by adding to the bath solution of TTX, 6,7-dinitroquinoxaline-2,3-dione (DNQX, 10 µM) and D-2-amino-5-phosphonopentanoic acid (APV, 25 µM; both toxins from Tocris, Bristol, UK) respectively. The holding potential for miniature excitatory postsynaptic currents (mEPSCs) and mIPSCs recordings was -60 and -70 mV respectively. Analysis of AP properties, mEPSCs and mIPSC were carried out using Mini Analysis Program (Synaptosoft, USA). At least 300 mEPSCs and 500 mIPSCs were analyzed per cell.

Data were acquired at 23-27°C, using an EPC10 Patch-clamp amplifier (HEKA, Germany), filtered at 3 kHz and sampled at 10-40 kHz using Patch Master 2.32 software and analyzed by the use of Fit-master software v2.65 (both from HEKA, Lambrecht, Germany).

### 2.2.3 Statistical analysis

All results of quantitative analyses are given as mean ± s.e.m calculated from each cell analyzed. Statistical analyses were performed using GraphPad Prism 5 software using the test indicated in each figure and in all cases, statistical significances are marked as *$p<0.05$, **$p<0.01$ and ***$p<0.001$.

# 3 Results

## 3.1 Bassoon and Piccolo as regulators of neurotransmitter release

### 3.1.1 A role for Piccolo in the neurotransmission

#### 3.1.1.1 Piccolo deletion impairs synaptic vesicle recycling and reduces mEPSCs frequency

Although recently new data on the role of Piccolo have been published its function in nerve terminals is still only partly understood. Piccolo is a presynaptic scaffolding protein paralogous to Bassoon; both share ten regions of homology (Fenster et al., 2000). The region 7 contains a PxxP motif, which in the case of Bassoon has been reported to facilitate the recruitment of $Ca_v2.1$ to transmitter release sites and to contribute to the regulation of synaptic transmission (Davydova et al., 2014). Although Piccolo contains a similar motif, its function has not been analyzed to date.

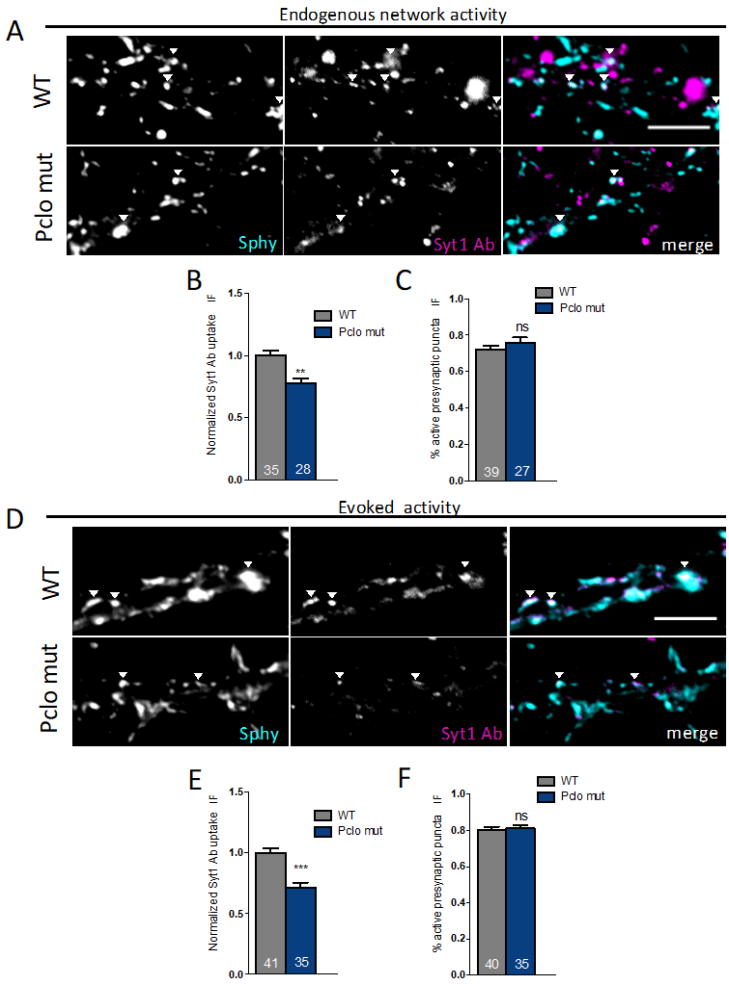


**Figure 6: Piccolo-mutant neurons exhibit impaired presynaptic function.** (A) Syt1 Ab uptake assay: representative images of WT and Piccolo-mutant neurons (20DIV) from the proximal part of the dendrite (20-50 µm from the soma), analyzed under endogenous network activity conditions. Sphy was used to label presynaptic terminals. The right images show merged images of Sphy (cyan) and Syt1 Ab (magenta). Scale bar 5µm. (B) Quantification of averaged Syt1 Ab uptake assay immunofluorescence values per cell as shown in A. (C) Quantification of active presynaptic puncta in Syt1 Ab assay under endogenous network activity conditions. (D) Representative images under evoked activity conditions. (E) Quantification of Syt1 Ab uptake assay immunofluorescence as shown in D. (F) Quantification of active presynaptic puncta in Syt1 Ab assay after 4 min 50mM KCl stimulation Values are averages from three independent experiments and are normalized to control. The numbers within the columns indicate the number of cells analyzed per condition. Bars represent mean values; whiskers, SEM. The statistical significance was assessed using a t-test. ns = p>0.05; ** = p<0.01; *** = p<0.001.

To do so, I used Piccolo-mutant mice (referred to here as Pclo mut) hippocampal cultures, in which the deletion of exon 14 of the *Piccolo* gene ablosished the expression of the pre-

synaptic protein almost completely (<5% compared to WT) (Mukherjee et al., 2010). In order to assess whether these mice display impairment of presynaptic functions, a Synaptotagmin 1 antibody (Syt1 Ab) uptake assay was performed in WT and Piccolo-mutant hippocampal primary neurons. The labeled antibody binds to the luminal domain of the SV protein synaptotagmin1, which is internalized into synaptic vesicle after exo-/endocytosis. The amount of the internalized antibody serves as a measure for the SV recycling efficiency at individual synapses. The incubation was performed under endogenous network activity driven conditions for 20 min, and during chemical stimulation (50 mM KCl for 4min) to measure evoked activity conditions, which leads to the release of the total recycling pool of vesicles (Alibi and Tsien, 2012). In addition to the Syt1 Ab antibody,

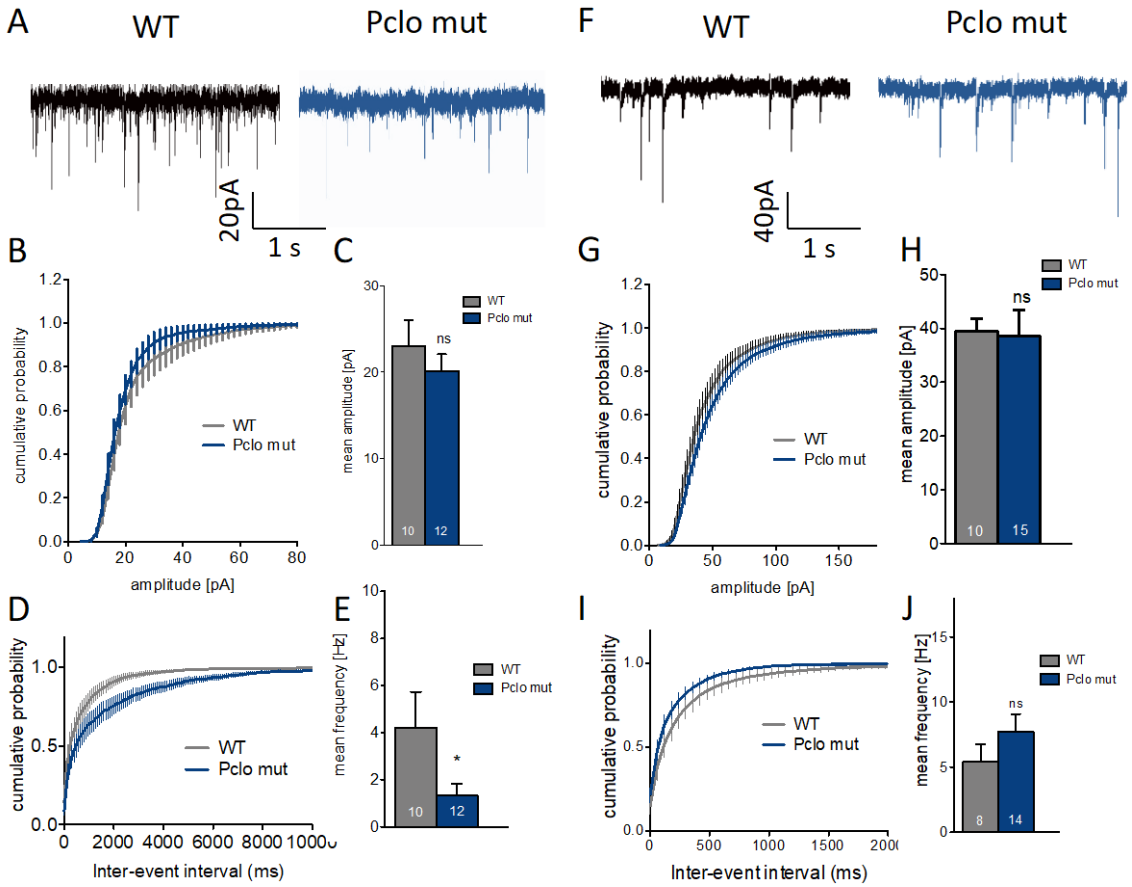


**Figure 7: Piccolo-mutant neurons show decreased frequency of mEPSC.** (A) Representative traces of AMPA-mEPSC recoded in WT and Pclo mut cultures at 19DIV. (B) Cumulative distributions of the mEPSC amplitudes in WT and Pclo mut cultures (C) Mean amplitude of the mEPSC from WT and Pclo mut mice. Data in B, C are mean ± s.e.m. (D) Cumulative distributions of the mEPSC inter-event intervals in WT and Pclo mutant neurons at 19-21 DIV. (E) Quantification of the mean frequency of WT and Pclo mutant mice ±s.e.m. (F) Representative traces of GABA-mIPSC recoded in WT and Pclo mut cultures at 19DIV. (G) Cumulative distributions of the mIPSC amplitudes in WT and Pclo mut cultures (H) Mean amplitude of the mIPSC from WT and Pclo mut mice. Data in G, H are mean±SEM . (I) Cumulative distributions of the mIPSC inter-event intervals in WT and Pclo mutant neurons at 19-21 DIV. (J) Quantification of the mean frequency of WT and Pclo mutant mice ±s.e.m. Statistical differences were assessed by Student's t-test (C, H; $p>0.5$) or non-parametric Mann-Whitney u-test (E, J; $p<0.05$) in comparison of both genotypes. Number of cells indicated in the bars. Data obtained in collaboration with Dr. Yulia Klyueva.

the neurons were labeled with synaptophysin (sphy) to mark presynapses. Analyses were done at the proximal part of dendrites (20-50 µm from the soma), where functional adaptations take place in primary hippocampal cultures (Lee et al., 2013). Under both conditions, the Piccolo-mutant neurons displayed a significant reduction in the Syt1 Ab uptake (Endogenous network activity: Figure 6A, B; Pclo mut 77.64 ± 3.8% of the WT; Evoked activity: Figure 6C, D; Pclo mut 71.63 ± 3.9% of the WT). In contrast, the number of puncta positive for the SV-associated protein synaptotagmin 1 (Syt1), used as an indicator of activity, was not changed between genotypes either upon endogenous network activity (Figure 6C; WT: 0.71 ± 0.022; Pclo mut: 0.77 ± 0.025) nor under chemical stimulation (Figure 6F; WT: 0.80 ± 0.021, Pclo mut: 0.79 ± 0.017).Eneko

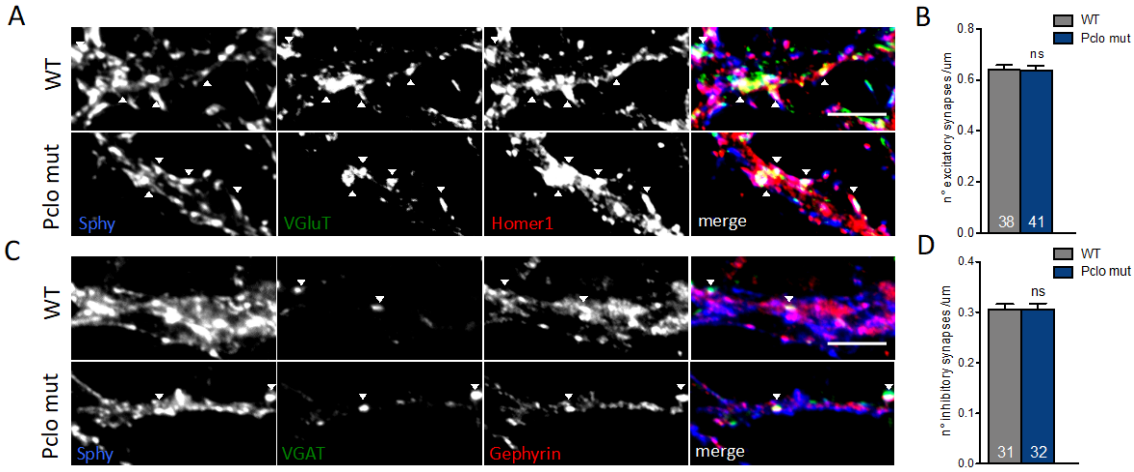


**Figure 8: Piccolo does not disturb the number of excitatory or inhibitory synapses.** (A, C) Example of immunostainings for excitatory (A) and inhibitory (C) synapses of WT and Pclo mutant neurons. The right images are overlay images with VGluT (green) and Homer1 (red) in synaptophysin(Sphy)-positive puncta to identify excitatory synapses. For inhibitory VGAT (green) and Gephyrin (red) were used. Scale bar, 5µm. (B, D) Quantification of excitatory (B) or excitatory (D) synapses per µm in the proximal segment of the dendrites. Values are averages from three independent experiments and are normalized to control (18-19 DIV). The number of cells analyzed is indicated within the bars. Bars represent mean values; whiskers, s.e.m.. The statistical significance was assessed using a t-test. ns=p>0.05.

In order to assess whether presynaptic impairment in the absence of Piccolo affects also the postsynaptic function, I collaborated with my colleague Dr. Yulia Klyueva to measure AMPA receptor-mediated miniature excitatory postsynaptic currents (mEPSC) using whole-cell voltage clamp recordings of mature hippocampal WT and Piccolo-deficient neurons (19-21DIV). Piccolo-mutant neurons showed a decreased frequency of mEPSCs (Figure 7D, E; WT: 3.202 ± 1.045 Hz, Pclo mut: 1.342 ± 0.4746 Hz) while the amplitude was not changed (Figure 7B, C; WT 23.05 ± 3.04 pA, Pclo mut 20.16 ± 1.94 pA), confirming the Syt1 Ab uptake results. In parallel, I examined whether the deletion of Piccolo altered the basic inhibitory transmission in mature hippocampal neurons. Analysis of the GABA-mediated miniature inhibitory postsynaptic currents (mIPSC) amplitude between

WT and Piccolo-mutant mice were not changed (Figure 7G, H; WT: 5.41 ± 1.37Hz; Pclo mut: 7.73 ± 1.36Hz). Moreover, cumulative distribution of the mIPSC inter-event intervals appeared slightly, but not significantly increased in Pclo mut compared to WT (Figure 7I, J; WT: 38.55 ± 4.83 pA; Pclo mut: 42.80 ± 4.09 pA). This suggests that presynaptic function is impaired in excitatory, but not in inhibitory synapses of Piccolo-deficient neurons. The reduced mEPSC frequency might be due to a reduction in the number of excitatory synapses in mature Piccolo-mutant cultures. In order to address this question, I performed triple immunostaining to determine whether the number of excitatory or inhibitory synapses was changed in Piccolo absence. To identify excitatory synapses, the primary cultures were labelled with antibodies against VGlut1 and Homer1, whereas vesicular GABA Transporter (VGat) and Gephyrin were used for inhibitory synapses (Figure 8A, C). The quantitative analysis revealed no significant changes between WT and Piccolo-mutant excitatory (Figure 8A, B; WT: 0.64 ± 0.01840 and Pclo mut: 0.63 ± 0.021) and inhibitory (Figure 8C, D; WT: 0.30 ± 0.01144 and Pclo mut: 0.30 ± 0.012) synapses.

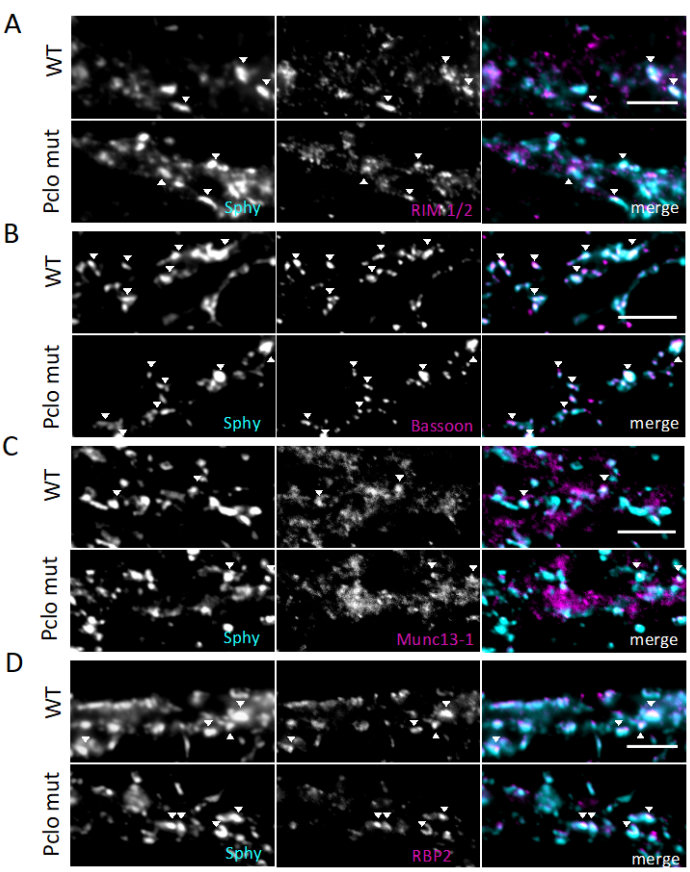


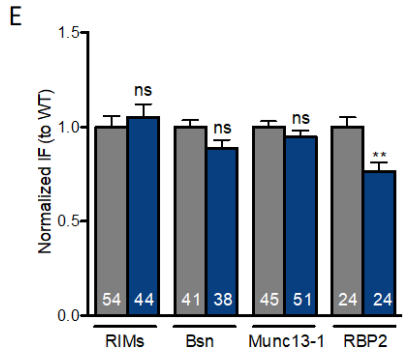


**Figure 9: Quantification of presynaptic protein levels in hippocampal Piccolo-mutant neurons.** (A-D) Immunostainings examples of various presynaptic proteins in WT and Piccolo-mutant hippocampal neurons. The center images (presynaptic proteins of interest; magenta) were overlaid with synaptophysin (Sphy; cyan). Images on the right are the overlay result. Scale bar 5 µm. (E) Quantification of the components of the presynapse was done in the proximal region of the dendrite (between 10-50 µm of the first portion of the dendrite branch). Values are averages from, at least, three independent experiments and are normalized to control (18-19 DIV). Only immunofluorescence of Sphy positive puncta were taking into account The number of cells analyzed is indicated within the bars. Bars represent mean values; whiskers, s.e.m..The statistical significance was assessed using a t-test. ns=p>0.05, **p<0.01

These results indicate that the differences observed in the Syt1 AB uptake assay and the electrophysiological results from Piccolo-mutant neurons are not due to changes of the

number of excitatory/ inhibitory synapses or active presynaptic boutons, but rather to modifications of Pr at the level of individual synapses. Changes in either evoked $Ca^{2+}$ influx into the presynapse and/or SV recycling have been reported to modulate the Pr (Murthy et al., 2001; Zhao et al., 2011; Jeans et al., 2017).

### 3.1.1.2 Piccolo deficiency barely affects the composition of the CAZ

There is a tight correlation between active zone size and the Pr (Holderith et al., 2012; Michel et al., 2015). In order to address whether the molecular composition of the presynapses is affected in Piccolo-mutant neurons, I performed quantitative immunostainings against some CAZ proteins, which have been published to organize the release machinery, such as RIMs, Bassoon, Munc13-1, and RBP2 (Figure 9A-D). The cultures were immunostained with specific antibodies, and the fluorescence intensity was measured at individual synapses defined by synaptophysin puncta, comparing Piccolo-mutant synapses and WT hippocampal cultures. No significant changes were detected in the immunostaining intensity of RIMs, Bassoon and Munc13-1 (Figure 9E; RIMs: Pclo mut is 104.9% ± 6.1% of the WT; Bassoon: Pclo mut: 93.85 ± 4.9% of the WT; Munc13-1: Pclo mut: 97.93 ± 3.4% of the WT), which is in line with previous publications (Mukherjee et al., 2010). However, RBP2 was found significantly decreased in Piccolo-mutant synapses (Figure 9E; RBP2: Pclo mut: 74.74 ± 4.6% of the WT). Thus, the lack of Piccolo in nerve terminals affects specifically the localization of RBP2.

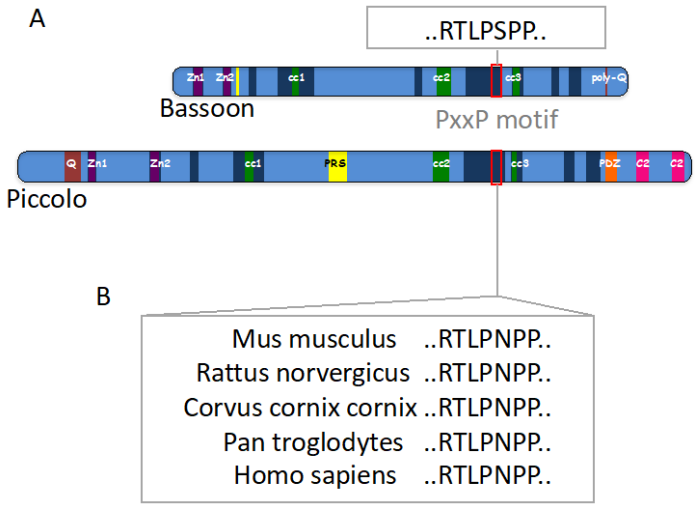


**Figure 10: PxxP motif contained in Pclo is conserved across evolution.** (A) Scheme of the PxxP-motif contained in Bsn and Pclo highlighted in red. (B) Scheme of the PxxP motif sequence conserved among species. The information comes from a protein BLAST in www.nacbi.nlm.nih.gov/BLAST/

### 3.1.1.3 RBPs may link Piccolo to calcium channels

RBPs harbour three SH3 domains, which can connect presynaptic scaffold proteins to the pore-forming subunit of $Ca^{2+}$ channels (Hibino et al., 2002). Indeed, my lab showed that Bassoon via a PxxP motif located in the 7$^{th}$ PBH region can bind to

RBPs, and ultimately, to calcium channels (Davydova et al., 2014). Based on the structural similarities between Piccolo and Bassoon, I was keen to know whether Piccolo could exert similar functions like Bassoon in the recruitment of VGCC. A protein BLAST revealed that the PxxP sequence contained in the 7$^{th}$ PBH region of Piccolo is conserved among different species (Figure 10B). It might suggest that this sequence is important for some yet undiscovered functions.

To explore whether RBP binds Piccolo in heterologous cells, I co-expressed EGFP-Pclo 27 (aa3602-3787) or its non-binding mutant (EGFP-27*), where a 3-amino-acid mutation was introduced into the RBP-binding interface (RTLPNPP/ATLANPA), together with full-length RBP2 tagged with a myc flag in HEK293T cells. Anti-GFP microbeads were used to co-immunoprecipitate (co-IP) over-expressed Piccolo and RBP2. The mutation completely prevented binding, while there was strong co-IP of RBP2 with Pclo27 with the intact PxxP motif (Figure 11A), suggesting that RBP2 may serve as a link between $Ca^{2+}$ channels and the presynaptic scaffold. To test whether RBP2 is responsible for simultaneous integration of Piccolo and VGCC, I performed a triple co-IP from HEK293T cells expressing Piccolo fragments (aa3602-3792) containing PxxP motif (mRFP-Pclo), $Ca_V2.1$ (EGFP- $Ca_V2.1$) or $Ca_V2.2$ (EGFP- $Ca_V2.2$) and myc-tagged full-length RBP2 using specific GFP antibodies. The signal of mRFP-Pclo was detected only when RBP2 was simultaneously co-expressed with the EGFP-$Ca_V2$s fragments (Figure 11B), confirming that RBP2 might serve as a link between Piccolo and VGCC in vitro. On the other hand, I observed stronger co-IP with $Ca_V2.1$, meaning a preferential binding of Piccolo to this channel subtype. I discarded this idea when the differences in the co-IP signals were

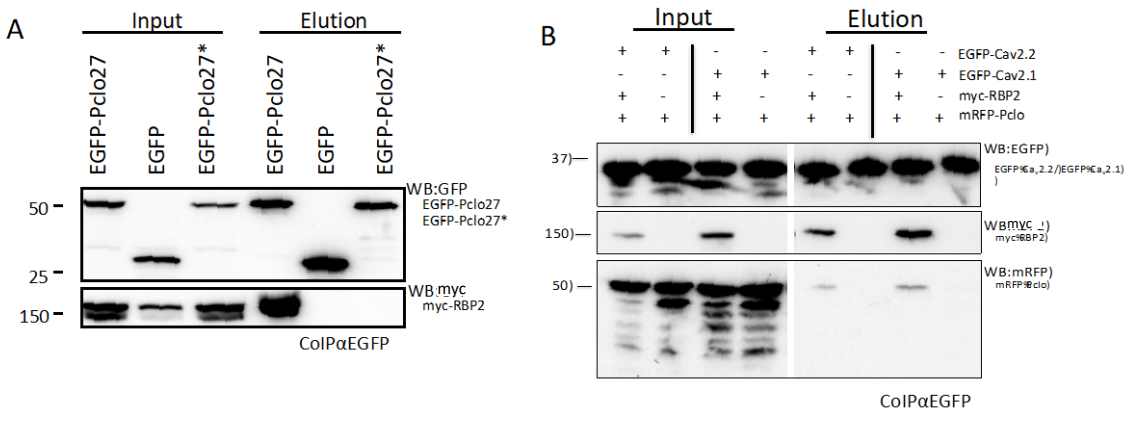


**Figure 11: RBP2 could potentially link Piccolo with VGCC.** (A) Myc-RBP2 can be co-immunoprecipitated with GFP antibodies when co-expressed with EGFP- Pclo27 (aa3602-3787), but not with EGFP-Pclo27* (RTLPNPP/ATLANPA) or with EGFP alone. Antibodies used for immunodetection on Western blots, position of bands corresponding to proteins of interest and size markers are indicated. (B) Co-expression of RBP2 is required to co-precipitate Piccolo fragments (aa3602-3792; mRFP-Pclo) enclosing the PxxP motif with $Ca_V2.2$ (first two columns) or $Ca_V2.1$ (second two columns) from HEK293T cell lvsates with anti-GFP antibodies.

attributed to variations of the RBP2 expression, which depended on the Piccolo-VGCC fragments co-IP.

### 3.1.1.4 Voltage-gated calcium channel levels and function in Piccolo-mutant neurons

$Ca^{2+}$ entering into the nerve terminal through $Ca_V2.1$ and $Ca_V2.2$ is one of the first events responsible for initiating the neurotransmitter release at fast conventional synapses (Olivera et al., 1994; Dunlap et al., 1995). The magnitude of $Ca^{2+}$ entry correlates with the number of $Ca^{2+}$ channels and SV exocytosis rate (Neher et al., 2008; Zhao et al., 2011; Lazarevic et al., 2011; Jeans et al., 2017). Protein-protein interactions are crucial to adequate $Ca^{2+}$ responses necessary for successful neurotransmission. Considering the

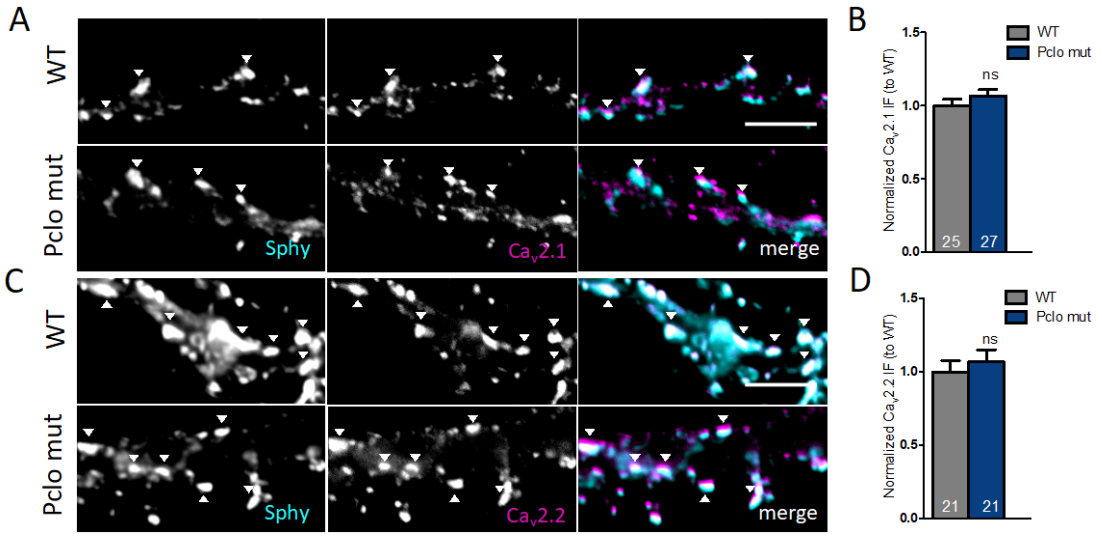


**Figure 12: Quantification of presynaptic calcium channel protein levels in hippocampus.** (A, C) Examples of immunostainings for $Ca_V2.1$ and $Ca_V2.2$ in WT and Piccolo-mutant hippocampal neurons (18-19DIV). The right images were overlay with Sphy (cyan), and $Ca_V2.1$ and $Ca_V2.2$(magenta). Scale bar, 5µm. (B, D) Quantification of the immunofluorescence in the proximal part of the dendrites (between the first 10-50 µm). Values from three independent experiments (normalized to WT). The number of cells analyzed is indicated within the bars. Bars represents mean values; whiskers, SEM. The statistical significance was assessed using a t-test. ns=p>0.05. The $Ca_V$ 2.2 experiments were done in collaboration with Dr. Carolina Montenegro.

decrease of the RBP2 fluorescence intensity levels observed in Piccolo-mutant neurons (Figure 9), similar to Bassoon-lacking synapses (Davydova et al., 2014), I hypothesized that Piccolo might be involved in the positional priming of $Ca^{2+}$ channels at the AZ plasma membrane. While RIM localizes both subtypes of VGCC (Kaeser et al., 2011), Bassoon specifically recruits $Ca_V2.1$ (Davydova et al., 2014). Therefore, I sought to find out whether Piccolo would localize $Ca_V2.2$. To this end, I performed immunostaining using antibodies against $Ca_V2.1$ and $Ca_V2.2$ to see whether the levels of both $Ca^{2+}$ channels were impaired in absence of the presynaptic scaffold Piccolo. Fluorescence intensities were not

changed neither for $Ca_V2.1$ (Figure 12B; Pclo mut: 105.9 ± 4.5% of the WT) nor $Ca_V2.2$ (Figure 12D; Pclo mut: 106.7 ± 8.1% of the WT). These results suggest that Piccolo, in contrast to Bassoon, was not involved in the recruitment of VGCC.

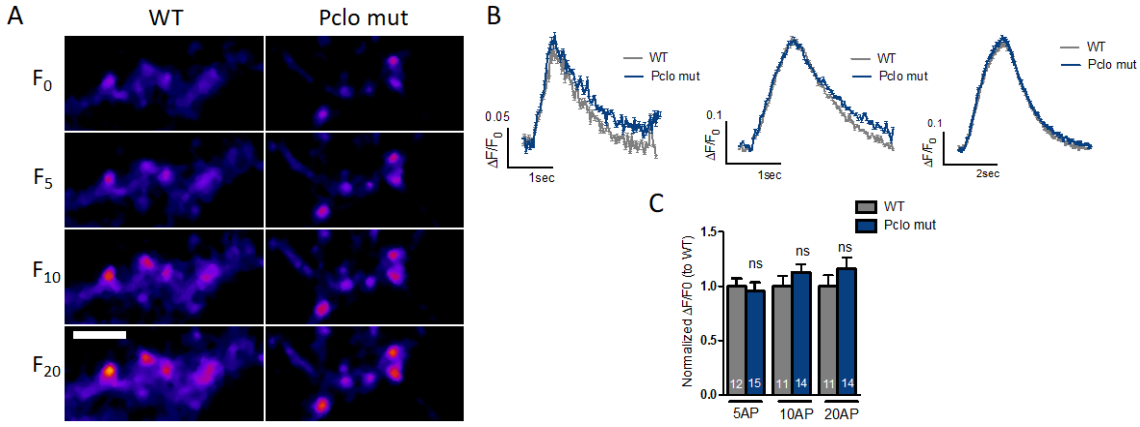


**Figure 13: Piccolo-mutation does not change evoked presynaptic $Ca^{2+}$ influx.** (A) Representative images depicting the fluorescence response of mature hippocampal neurons (19DIV) from WT and Piccolo mutant, expressing Sy-GCaMP5G before stimulation ($F_0$) and upon stimulation with 5 ($F_5$) 10 ($F_{10}$) and 20 ($F_{20}$) pulses at 20Hz. Scale bar 2µm. (B) Representative traces of responses by 5, 10 and 20 pulses of WT (grey) and Piccolo mutant (blue) hippocampal neurons. (C) Quantification of the average responses ± s.e.m. of the $Ca^{2+}$ sensor from ≥ two individual experiments to 5, 10, and 20 pulses of WT and Piccolo mutant neurons. Statistical significance was assessed by Student t-test, ns=p>0.05.

Despite Piccolo seems not to be involved in the recruitment of $Ca^{2+}$ channels at the release sites, it might regulate channel properties. To address this question, I took advantage of the genetically-encoded fluorescent $Ca^{2+}$ indicator GCaMP5G (based on Akerboom et al., 2012). This sensor was fused to the C-terminus of the SV protein synaptophysin (sphy) to restrict the expression of it within the presynaptic terminals (referred here as sy-GCaMP5G) . Neurons infected at 4DIV were imaged at 17 DIV or later to let hippocampal neurons reach the mature state. Then, the responses of this cells as immunofluorescence brightness peaks, in response to 5, 10 and 20 pulses at 20Hz stimulation were recorded. Consequent analysis between genotypes revealed that Piccolo did not influence the evoked $Ca^{2+}$ influx in primary hippocampal neurons (Figure 13A, B, C; Pclo mut at 5AP: 95.54 ± 7.8% of the WT; Pclo mut at 10AP: 112.4 ± 7.6% of the WT; Pclo mut 20AP: 115.9 ± 10% of the WT). These results are in line with previously

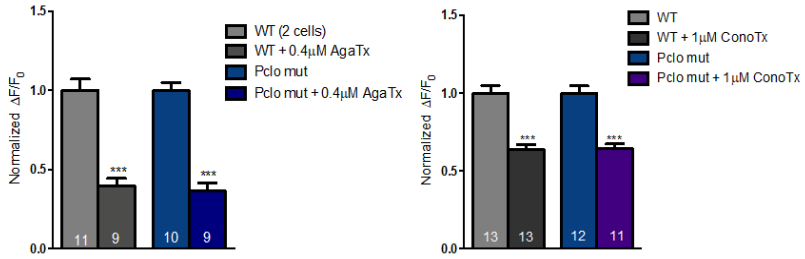


**Figure 14: No specific sub-type contribution of VGCC in Piccolo-mutant neurons.** Quantification of WT and Piccolo-mutant hippocampal neurons (18-19DIV) GCaMP5G responses upon 5 pulses stimulation before and after AgaTx application for 8min (left) and ConoTx for 10min (right). Data was normalized to each control. The bars represent average responses ± s.e.m. of the $Ca^{2+}$ sensor from three individual experiments. Statistical differences were assessed by Student t-test, ***=p<0.001.

reported unchanged VGCC levels in this thesis, and therefore, opposite to my initial hypothesis. Furthermore, it clarified previous assumptions about Piccolo´s role in the overall presynaptic $Ca^{2+}$ entry at the plasma membrane. However, whether the presynaptic protein contributes to subtype-specific presynaptic $Ca^{2+}$ transients remained was unknown. To answer this question, I selectively suppressed P/Q-type influx with the spider toxin Agatoxin (AgaTx), while the cone snail Conotoxin (ConoTx) was used to inhibit N-type contribution. The blockers were bath applied for 8 and 10 min, respectively, after a first acquisition to compare treated with non-treated responses to verify the state of the drugs (short drug lifetime). AgaTx and ConoTx significantly decreased the $Ca^{2+}$ entry in either in WT or in Piccolo-mutants (Figure 14; Left: AgaTx: WT: 39 ± 4 %; Pclo mut: 36 ± 5.1 %; Right: ConoTx: WT: 63 ± 3.1%; Pclo mut: 64± 2.9%), supporting previous results in the overall $Ca^{2+}$ responses in Piccolo-mutant presynapses. Accordingly, I conclude that Piccolo neither regulate the localization nor the functional characteristics of VGCC in hippocampal neurons.

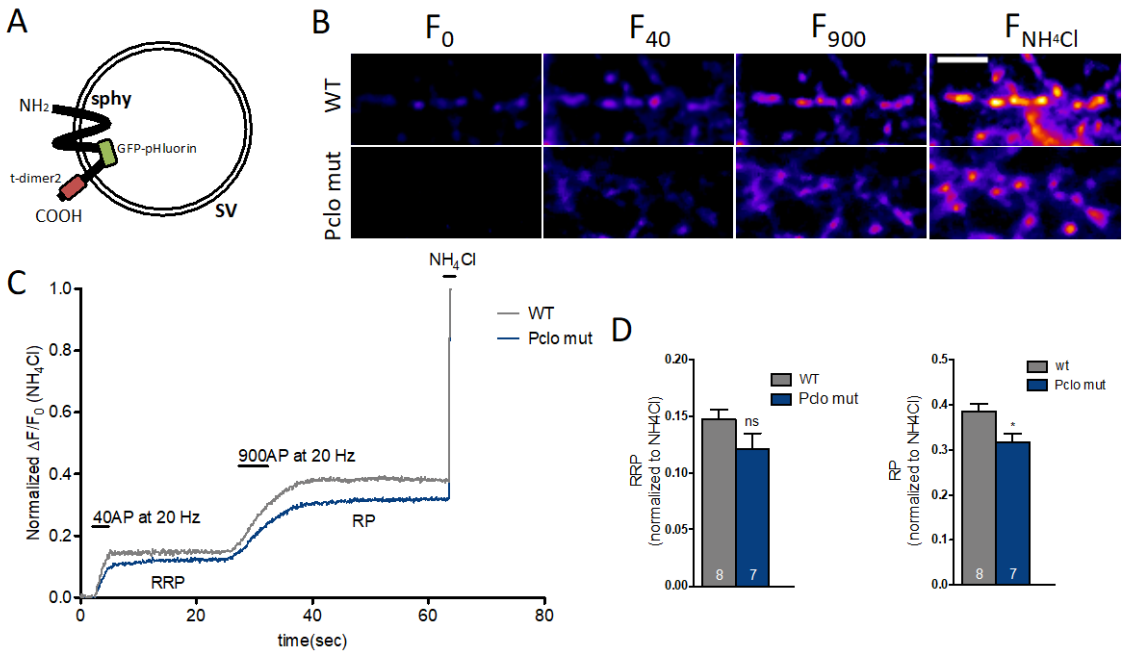


**Figure 15: Reduced SV pool sizes in Piccolo-mutant neurons.** (A) Scheme showing the supercliptic SynaptopHluorin construct. The supereclitic GFP-pHluorin is inserted between the third and the fourth transmembrane domain of synaptophysin and the dimeric RFP (tdimer2) is fused to the C- terminal part of synaptophysin. (B) Representative images of mature WT and Piccolo-mutant neurons at basal state ($F_0$), after 40AP ($F_{40}$), 900AP ($F_{900}$) and the $NH_4Cl$ pulse ($F_{NH4Cl}$). Scale bar 2µm. (C) Represent traces of the experiments described in B. (D) Quantification of Synaptophysin-pHluorin signal normalized to NH4Cl signal (mean ± s.e.m.) from two independent experiments. Number of analyzed cells indicated within the columns. Student´s t-test was used for statistics; ns= p>0.05, *=p<0.05. These experiments were performed by Dr Carolina Montenegro.

### 3.1.1.5 Does Piccolo affect the synaptic vesicle cycle?

The correlation between the Pr and the size of the SV pools has been demonstrated by several groups (Dobrunz and Stevens, 1997; Murthy et al., 2001; Thiagarajan et al., 2005; Branco et al., 2008; Zhao et al., 2011). Using the Syt1 Ab uptake, I showed the impairment of the presynaptic function in Piccolo-mutant neurons. In order to know whether the presynaptic scaffold regulates the SV pool sizes, I took advantage of the genetically-encoded pH-sensitive probe called Synaptophysin-pHluorin (SynpHy). This tool is a fusion protein made from a pH-sensitive GFP-pHluorin inserted in the intraluminal domain of the SV protein Sphy ( Figure 15A; Rose et al., 2013). Due to low pH in the lumen of SV (5.5), the SynpHy fluorescence remains quenched. Upon stimulation and exocytosis, vesicles fuse with the plasma membrane and the fluorescence rapidly increases due to exposure to the basic extracellular medium (pH 7.4). Subsequent endocytosis and vesicle re-acidification produced a fluorescent decay of the signal. To measure the size of the different SVs pools, I employed the 'alkaline trapping' method using bafilomycin A (BafA). This drug is a reversible inhibitor of the vesicular proton pump (V-type ATPase), which was applied to prevent the vesicle re-acidification after SV exocytosis (Sankaranarayanan et al., 2001). SVs exocytosis was triggered by continuous stimulation with 40 pulses at 20 Hz to ensure the release of the RRP, followed by 900 pulses at 20Hz to ensure the exocytosis of the TRP, with two minutes in between for recovery of the cells. At the end of the experiment 60mM $NH_4Cl$ was applied to the extracellular medium, which alkalinizes the SV lumen and therefore de-quenches the entire pHluorin-expressing vesicle pool. The 'alkaline trapping' allowed us to determine the maximum green fluorescence signal and thereby to correct for differences in the expression levels between individual synapses (Figure 17B, C). Analyzed SV exocytosis revealed a decrease in TRP (Figure 15D; Pclo mut: 82.19 ± 5.2% of the WT) in Piccolo-mutant cells, while in the RRP no significant difference was observed

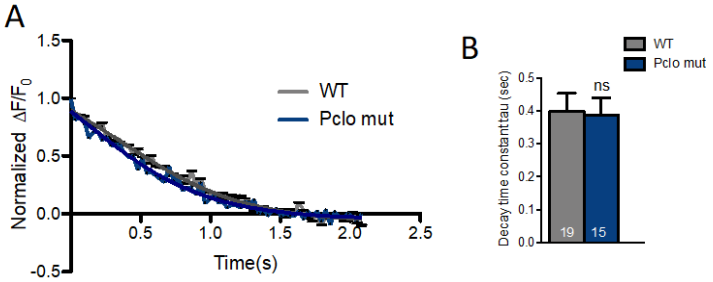


**Figure 16: Sy-GCaMP5G fluorescence decay time constant is not change in Piccolo-mutant neurons.** (A) Representative peak normalized traces fit to one-exponential decay model (grey-WT and blue-Pclo mut lines). (B) Decay time constant quantification from 4 independent experiments. Student´s t-test was used to compare the responses. Number of cells indicated in the bars. Bars represents mean values; whiskers, SEM; number of cell analyzed indicated in the bars. The statistical significance was assessed using a t-test, ns=p>0.05.

(Figure 15D; 82.28 ± 9.2 % of the WT), supporting previous results obtained in the Syt1 Ab uptake assay. Additionally, these results are in line with a recent publication, where no changes in the RRP and a decreased TRP were observed upon Piccolo deletion in rats (Ackermann et al., 2018). They proposed that via Pra1, Piccolo impairs RAB5 function, and consequently the endosome sorting affecting the SV replenishment.

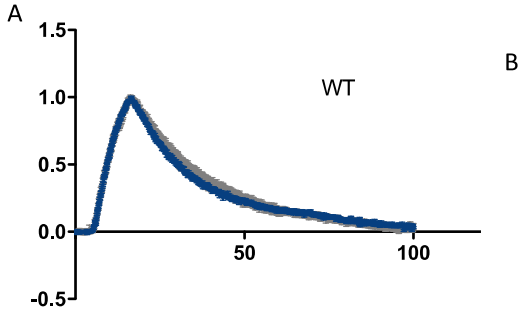


**Figure 17: Piccolo deletion has no consequence in SV endocytosis.** (A) Normalized fluorescence changes of sy- pHluorin in WT and Pclo mutant hippocampal neurons (19DIV). (B) Decay time constant quantification from 2 independent experiments. Bars represents mean values; whiskers, SEM; number of cells analyzed indicated in the bars. The statistical significance was assessed using a t-test, ns=p>0.05.

It has been reported that upon changes of the $Ca^{2+}$ transients, the SV recycling is modulated (Sankaranayanan and Ryan, 2001; Dittman and Ryan, 2009; Wu et al., 2009; Wu et al., 2014a; Wu et al., 2014b). The members of the Syt family have been proposed to promote the SV recycling (Haucke et al., 2000; Jarousse and al., 2003; Yao et al., 2012; Liu et al., 2014; Wang et al., 2016). Since Pclo serves as a low-affinity $Ca^{2+}$ sensor within the presynapse (Gerber et al., 2001), it might contribute to the vesicle recycling. Thus, I wondered whether the clearance of $Ca^{2+}$ from the presynaptic terminals lacking Pclo could affect SV recycling. I analyzed the fluorescence decay rate of the evoked $Ca^{2+}$ influx responses from Figure 15 and 16. The decays were normalized to the maximum value of the peak, and the outcome traces were fitted to a single exponential equation. Comparison between decay constant tau of WT and Piccolo-mutant neurons resulted in no significant difference (Figure 16A, B; WT: 0.3986 ± 0.055 sec; Pclo mut: 0.3927 ± 0.049 sec), indicating that the $Ca^{2+}$ did not play any role in the mechanism of SV pool size regulation. Therefore, I used a precise tool to measure the SV endocytosis in Piccolo-mutant cultures, the SynpHy.

Several studies have demonstrated that Piccolo interacts with actin-binding proteins including the actin-binding protein 1 (Abp1; Fenster et al., 2003), Profilin2 (Waites et al., 2011), Daam1 (Wagh et a., 2015) or Trio (Terry-Lorenzo et al., 2016). The interplay with Pra1 (Fenster et al., 2000) and/or GIT1 (Kim et al., 2003) supports its role in the SV endocytosis. To see whether Piccolo impairs the SV recycling in my model, I used the

genetically encoded tool SypHy to measure the endocytic rate. Upon 200AP at 20Hz stimuli, I evoked the SV exocytosis de-quenching the fluorescence of the pHluorin, while consequent endocytosis and vesicle re-acidification causes a decay of the fluorescence.

I determined the decay time constant of WT and Piccolo-mutant neurons by fitting the normalized decay curves to one exponential function. Comparison of both decay times showed no significant differences (Figure 17A, B; Pclo mut: 93.85 ± 8.7% of the WT), suggesting that the endocytosis is not affected in my model.

These results are in line with a recent publication where is it shown that Piccolo deletion impairs the formation of early endosomes not affecting the initial steps of the endocytosis (Ackermann et al., 2018). To test whether my model exhibits the same deficits in endosome formation, I quantified the protein levels of the early endosome antigen 1 (EEA1). In my analysis, the levels of EEA1 were decreased in Piccolo-mutant neurons (Figure 18B right; Pclo mut: 81,79 ± 3.5% of the WT). These results support the role of Piccolo in SV replenishment, as it was hypothesized.

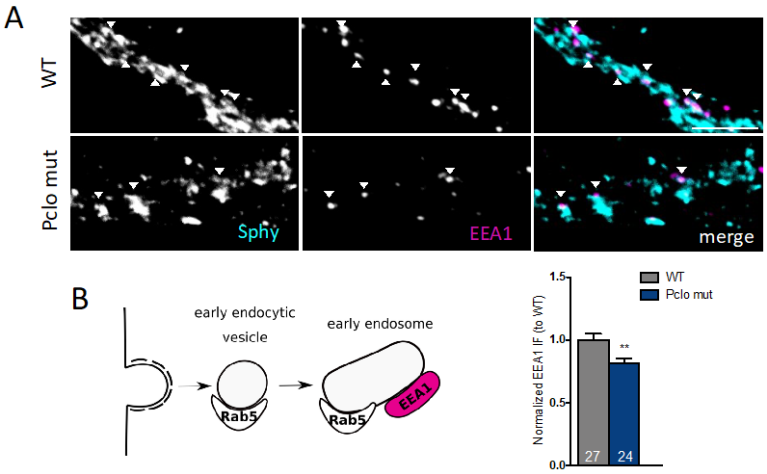


**Figure 18: Endosome marker levels are decreased in Piccolo-mutant presynapses.** (A) Representative images of the proximal segment (the first 10-50 µm of the neuron branch) of WT and Pclo mut neurons (14DIV) stained with early endosome antigen 1 (EEA1). Sphy was used to label presynaptic terminals. The right images were overlayed with Sphy (cyan and EEA1 (magenta). Scale bar, 5µm. (B) (Left) Schematic representation depicts when Rab5 and EEA1 associate to generate early endosomes. (Right) Quantification of EEA1 levels as shown in A. Values are normalized to each control, and are averages from two independent experiments. The numbers within the columns indicate the number of cells analyzed per genotype. Bars represents mean values; whiskers, SEM. The statistical significance was assessed using a t-test. ** = $p<0.01$.

### 3.1.2 Bassoon deletion enhances presynaptic calcium influx in hippocampal neurons

Findings of my group demonstrated differential recruitment of $Ca_v2.1$ via RBPs at the plasmatic membrane in Bassoon KO hippocampal neurons (here referred to as $Bns^{gt}$) (Davydova et al., 2014). These neurons show decreased signals in Syt1 Ab uptake assays during endogenous network activity, and exhibit an impaired frequency of mEPSCs. I

wondered how Bassoon deletion interfered in the presynaptic function, and in particular its role in the regulation of VGCC-mediated $Ca^{2+}$ entry. First, I reproduced previous data showing that Synapsin 1,2 (syn1, 2) positive $Bsn^{gt}$ presynapses exhibited an impairment of the Syt1 Ab signal under endogenous network-driven conditions (Figure 19A, B; $Bsn^{gt}$: 68.72 ± 2.7 % of the WT). Additionally, by inducing chemical depolarization, Syt1 Ab uptake is also significantly decreased in $Bsn^{gt}$ neurons (Figure 19C, D; $Bsn^{gt}$: 67.22 ± 3.2 % of the WT). These data support previous works showing the importance of Bassoon within the presynaptic terminal.

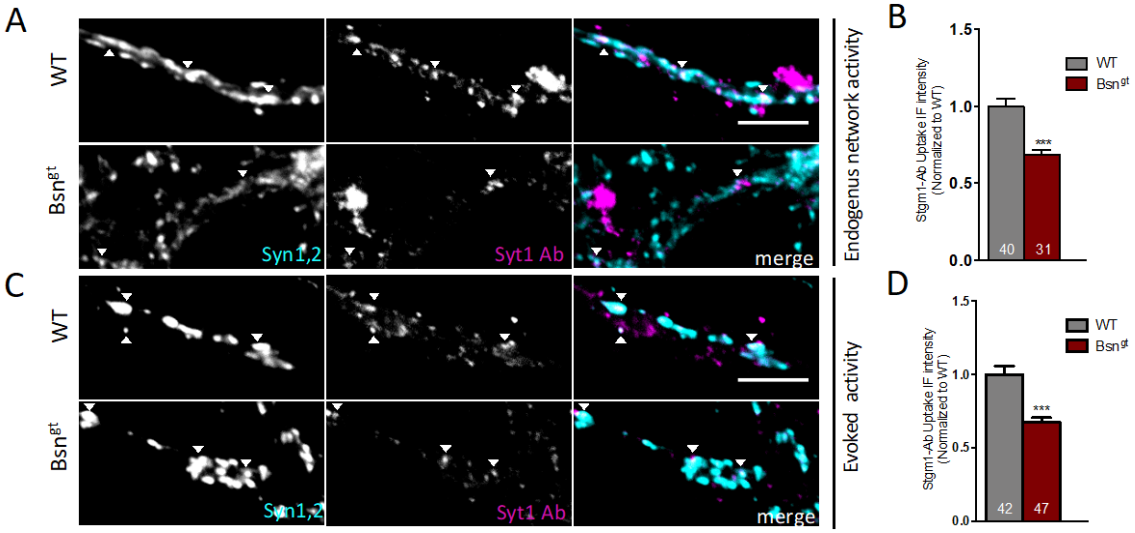


**Figure 19: Bassoon lacking neurons show impaired presynaptic function.** (A) Syt1 Ab uptake assay representative images of WT and $Bsn^{gt}$ neurons (20DIV) from the proximal part of the dendrite (between 10-50 µm of the neuron branch) analyzed under endogenous network activity condition. SyHhy was used to label presynaptic terminals. The right images were overlayed with synapsin 1,2 (cyan) and Syt1 Ab (magenta). Scale bar 5µm. (B) Quantification of Syt1 Ab uptake assay as shown in A. (C) Representative images under evoked activity conditions. (D) Quantification of Syt1 Ab uptake assay as shown in B. Values are averages from ≥ three independent experiments and are normalized to control. The numbers within the columns indicate the number of cells analyzed per condition. Bars represent mean values; whiskers, SEM. The statistical significance was assessed using t-test. *** = $p<0.001$. Experiment conducted in collaboration with Dr. Carolina Montenegro.

Second, taking advantage of the genetically encoded $Ca^{2+}$ sensor sy-GCaMP5G, I wanted to see whether the absence of Bsn modulated the presynaptic $Ca^{2+}$ influx. Measuring $Ca^{2+}$ entry upon 5, 10 and 20 pulses at 20Hz, I observed an increase of the presynaptic $Ca^{2+}$ in $Bsn^{gt}$ neurons compared to WT (Figure 20A, B, C; $Bsn^{gt}$ at 5AP: 137.8 ± 9.3% of the WT; $Bsn^{gt}$ at 10AP: 140.6 ± 9.4% of the WT; $Bsn^{gt}$ at 20AP: 140.2 ± 9.2% of the WT). This data suggests that the deficiency in Syt1 Ab uptake shown in $Bsn^{gt}$ synapses is not due to VGCC-mediated $Ca^{2+}$ income, but more likely to the modulation of other steps of the SV cycle, e.g. endocytosis, exocytosis or the size of the SV pool sizes.

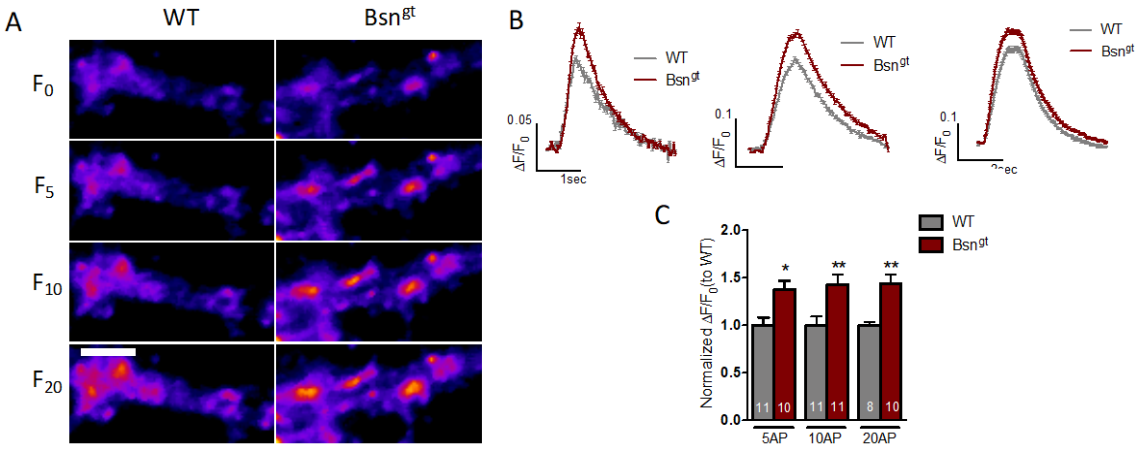


**Figure 20: Enhanced evoked presynaptic $Ca^{2+}$ influx in $Bsn^{gt}$ neurons.** (A) Representatives images depicting the fluorescence response of mature hippocampal neurons (18-19DIV) from WT and $Bsn^{gt}$, expressing Sy-GCaMP5G before stimulation ($F_0$) and upon stimulation with 5 ($F_5$), 10 ($F_{10}$) and 20 ($F_{20}$) pulses at 20Hz. Scale bar 2µm. (B) Representative traces of responses by 5, 10 and 20 pulses of WT (grey) and $Bsn^{gt}$ (red) hippocampal neurons. (C) Quantification of the average responses ± s.e.m. of the calcium sensor from ≥ two individual experiment to 5, 10, and 20 pulses of WT and $Bsn^{gt}$ neurons. Statistics were assessed by Student t-test, **=p<0.01.

Third, it is completely unknown how Bassoon deletion generates the changes in overall evoked presynaptic $Ca^{2+}$ influx. Thus, I dissected the contribution of each VGCC subtype in hippocampal neurons. To address this question, AgaTx and ConoTx were bath applied to block N-type or P/Q-type $Ca^{2+}$ income. After AgaTx application a similar reduction was observed in both genotypes (Figure 21A (left); WT/AgaTx: 48.11 ± 5.1% of WT; $Bsn^{gt}$/AgaTx: 48.11 ± 5.1% of $Bsn^{gt}$). However, while ConoTx application caused a 38% reduction in WT neurons , a 49% was registered in $Bsn^{gt}$ neurons (Figure 21A (right); WT/ConoTx: 62 ± 2.8% of WT; $Bsn^{gt}$/ConoTx: 51 ± 3.1% of $Bsn^{gt}$). These results may explain the changes in the overall presynaptic $Ca^{2+}$ entry of $Bsn^{gt}$ obtained before, and are in agreement with previous publications, which showed a relative enhancement of the $Ca_V2.2$-mediated contribution (Davydova et al., 2014).

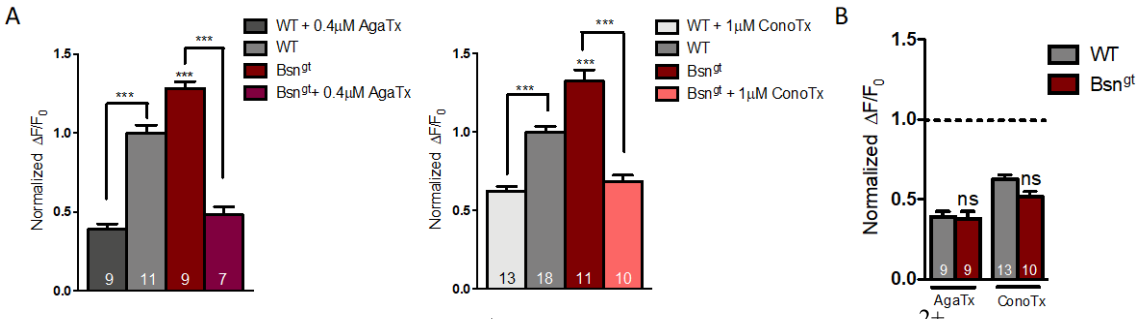


**Figure 21: VGCC subtype contribution in $Bsn^{gt}$ synapses.** (A) Quantification of evoked $Ca^{2+}$ income of WT and $Bsn^{gt}$ hippocampal neurons (19-20DIV) upon 5 pulses stimulation, before and after drug application, AgaTx for 8min (left), and ConoTx for 10min (right). Data was normalized to each control. (B) Comparison of the relative effect of AgaTx and ConoTx in WT and $Bsn^{gt}$ neurons. The bars represent average responses ± s.e.m. of the calcium sensor from three individual experiments. Statistical differences were assessed by Student t-test for A, and one-way ANOVA with Bonferroni´s posttest for B. ***=p<0.001; ns= p>0.05.

### 3.1.3 Evoked calcium influx in Bassoon/Piccolo double mutant presynapses

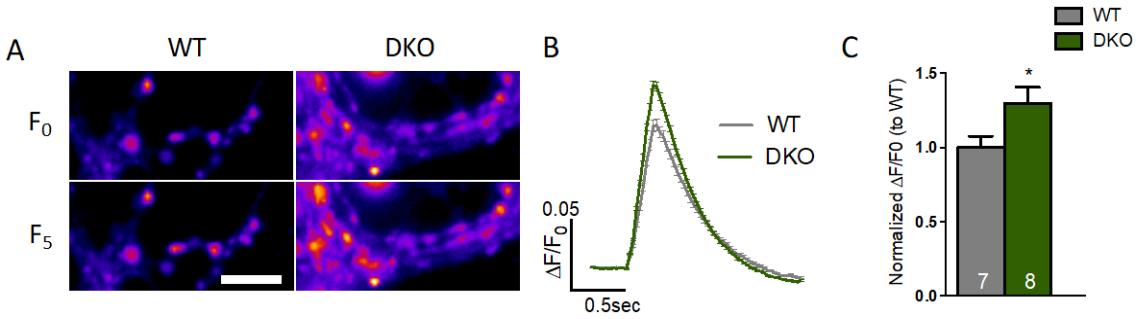


**Figure 22: Double-KO enhances evoked presynaptic $Ca^{2+}$ influx.** (A) Representatives images depicting the fluorescence response of mature hippocampal neurons (18DIV) of WT and DKO, expressing Sy-GCaMP5G before stimulation ($F_0$) and upon stimulation with 5 pulses ($F_5$) at 20Hz. (B) Representative traces of responses by 5 pulses of WT (grey) and Double-KO (green) hippocampal neurons. (B) Quantification of the average responses ± s.e.m. of the calcium sensor from two individual experiment to 5pulses. Statistical was assessed by Student t-test, *=p<0.05

In parallel to the previous presynaptic $Ca^{2+}$ imaging experiments shown, I measured the evoked presynaptic $Ca^{2+}$ income in Bassoon/Piccolo double-mutant primary cultures of hippocampal neurons (here referred as DKO). Taking advantage of the previously described genetically-encoded tool, I observed a significant increase $Ca^{2+}$ magnitudes in DKO presynapses in comparison with WT (Figure 24; Double-KO: 129.9 ± 10.7% of the WT). (Figure 22; Double-KO: 129.9 ± 10.7% of the WT). Surprisingly, a 30% increase was registered when both scaffolds were deleted, similar increase registered in $Bsn^{gt}$ neurons (~37%). Therefore, the fact that Piccolo is missing, in addition to Bassoon, has no additive effect. Despite my first hypothesis suggesting a contributory role of Piccolo to the regulation of VGCC function, only Bassoon seems to play that role in hippocampus. In summary, the absence of either Piccolo or Bassoon has consequences for the neurotransmitter release. While Piccolo is more involved in processes regulating the SV cycle, Bassoon is postulated as an important piece for the neurotransmission machinery. Besides

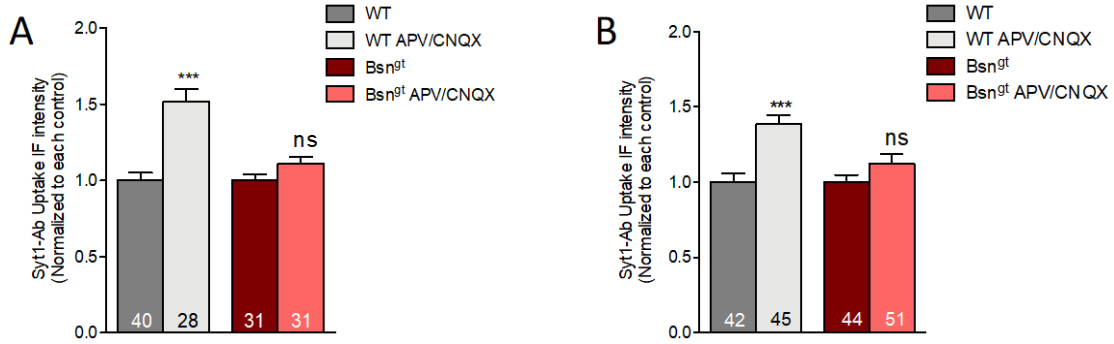


**Figure 23: Bassoon deletion impairs presynaptic function upon chronic silencing.** (A)Quantification of the Syt1 Ab uptake assay in WT, WT silenced, $Bsn^{gt}$ and $Bsn^{gt}$ silenced upon endogenous network activity conditions, and (B)chemical depolarization (20-21DIV). Values are normalized to each control. Values are averages from ≥ three independent experiments and are normalized to each control. The numbers within the columns indicate the number of cells analyzed per condition. Bars represents mean values; whiskers, SEM. The statistical significance was assessed using a t-test. *** = p<0.001, ns=p>0.05. Experiment conducted in collaboration with Dr. Carolina Montenegro.

its contribution to presynaptic $Ca^{2+}$ influx, it seems to be important for the SV cycle too. I showed that both scaffolds, Bassoon and Piccolo, are important proteins for the well-functioning of the synapses.

## 3.2 Bassoon and Piccolo are molecular regulators during homeostatic plasticity

### 3.2.1 Bassoon is required for presynaptic homeostatic plasticity adaptive mechanisms

Several studies reported that changes in evoked $Ca^{2+}$ income, specifically through P/Q-type influx, underlie presynaptic homeostatic adaptations (Zhao et al., 2011; Davis and Müller, 2015; Jeans et al., 2017). Although it is not clear whether changes in the number or the function regulate the homeostasis. Bsn, the presynaptic scaffold, has been reported to contribute to the recruitment of $Ca_v2.1$ to the release sites (Davydova et al., 2014). Additionally, in this thesis, it has been shown that it contributes to the presynaptic $Ca^{2+}$ VGCC-mediated entry. Therefore, I was keen to know whether Bsn was a key molecular player during homeostatic plasticity mechanisms. To study the role of Bsn during homeostatic adaptations, I treated mature hippocampal neurons (20DIV) with 50µM D-APV5 (NMDA receptor antagonist) and 10µM CNQX (AMPA-receptor antagonist) for 48h in order to induce chronic silencing.

Quantification of Syt1 Ab uptake after prolonged blocking excitatory synaptic activity block revealed that APV/CNQX-treated neurons showed a large increase of the fluorescence signal, but Bassoon deficient neurons were not able to do so either during basal network-driven activity (Figure 23A; WT APV/CNQX: 151.9 ± 8.2% of WT; $Bsn^{gt}$ APV/CNQX: 111 ± 4.2% of $Bsn^{gt}$) nor upon chemical depolarization (Figure 23B; WT APV/CNQX: 138.7 ± 5.5% of WT; $Bsn^{gt}$ APV/CNQX: 112 ± 6.3% of $Bsn^{gt}$). This data emphasizes the importance of Bassoon in mechanisms of homeostatic adaptation.

In order to face perturbation of neuronal activity, neurons can homeostatically regulate excitatory or inhibitory synapses. While inhibitory synapses can undergo homeostatic plasticity (reviwed in Turrigiano 2011), excitatory synapses are the most studied model. I analyzed whether the importance of Bsn during homeostatis is preserved in excitatory

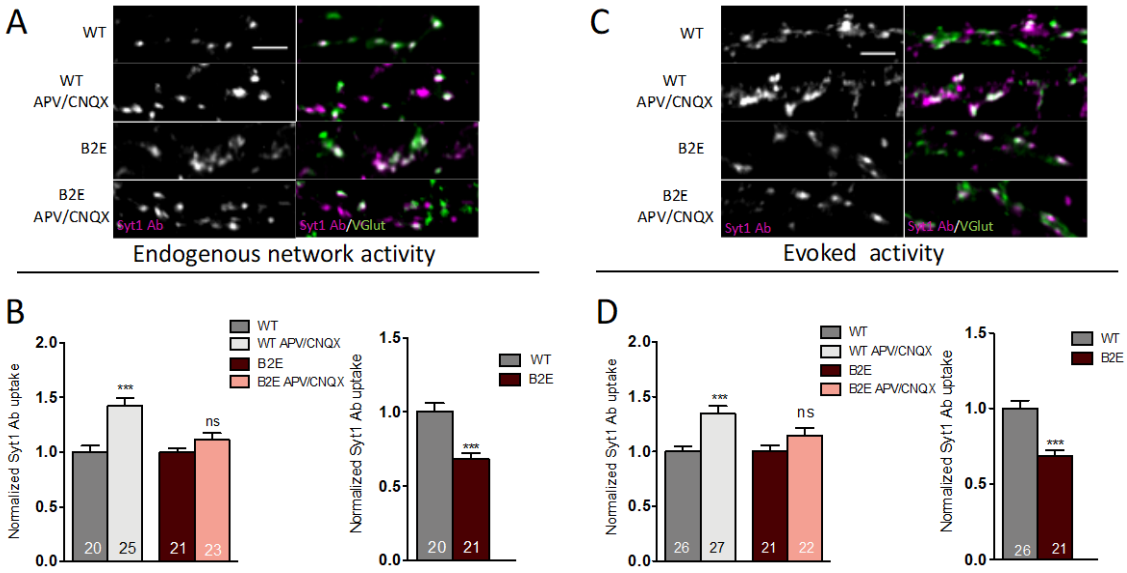


**Figure 24: Impaired homeostasis in excitatory Bassoon-deleted presynapses.** (A) Representative images of Syt1 Ab uptake assay under endogenous network activity conditions of WT and B2E hippocampal neurons, silenced (APV/CNQX-treated) and not-silenced (20-22DIV). VGlut (green) was used to label glutamatergic presynaptic terminals, where Syt1 Ab immunofluorescence signal (magenta) was quantified. Scale bar, 5µm. (B) Normalized Syt1 Ab uptake assay quantification to each non-silenced genotype (left), and comparison between non-silenced WT and B2E neurons (right). (C) Representative images of Syt1 Ab uptake assay after chemical depolarization (D) Quantification of Syt1 Ab uptake assay immunofluorescence signal under evoked conditions as shown in C (left). Comparison between non-silenced WT and B2E neurons (right). Values are averages from two independent experiments. The normalization is done either to each non-silenced genotype or to the WT. The numbers within the columns indicate the number of cells analyzed per condition. Bars represents mean values; whiskers, SEM. The statistical significance was assessed using a t-test. *** = $p<0.001$, ns=$p>0.05$. Graphs A and C were provided by Dr. Carolina Montenegro, while the analysis of the images (B and D) was done in collaboration with Dr. Montenegro.

neurons. To test this, I used a conditional Bassoon mutant mice generated in my lab. This mouse model selectively loose Bassoon in glutamatergic forebrain neurons. It was generated by gene ablation through the empty spiracle homebox-1 (Emx1) promoter-driven lox-P/Cre recombinase system (referred here as B2E; Annamneedi et al., 2018). In parallel to previous experiments, quantification of Syt1 Ab uptake assay fluorescence intensity in vesicular glutamate transporter 1 (VGlut1)-positive presynaptic boutons of B2E compared to WT was done. As previously, analyzed signals showed that neurons lacking Bsn were not able to rise the presynaptic function after chronic silencing upon either endogenous network activity nor evoked (Figure 24; Endogenous network activity: WT APV/CNQX: 142 ± 7.4% of the WT and $Bsn^{gt}$ APV/CNQX: 111 ± 6.3% of the $Bsn^{gt}$; Evoked activity: WT APV/CNQX: 134 ±7.1% of the WT and $Bsn^{gt}$ APV/CNQX: 114 ± 7.1% of the $Bsn^{gt}$). This result supports the importance of Bassoon during presynaptic homeostatic adaptations, and shows the relevance of Basson in excitatory synapses independent of the inhibitory neurons.

Continuous manipulation of the global network activity leads to changes in the postsynaptic receptor population (Turrigiano et al., 1998; Shi et al., 2001; Matsuzaki et al., 2004; Harms et al., 2005; Plant et al., 2006; Ehlers et al., 2007). To explore whether Bsn induced changes in the postsynaptic machinery composition, I measured the surface population of AMPA receptor. The neurons were immunolabeled with an antibody that recognizes a common extracellular epitope for all AMPA isoforms (1-4, named here as panGluA). Using the Syt1 Ab uptake assay, the presynaptic function was monitored (Figure 25B; WT APV/CNQX: 151 ± 8.2% of the WT; $Bsn^{gt}$ APV/CNQX: 111 ± 4.2% of the $Bsn^{gt}$), used as control. I confirmed that Bassoon does not impair the surface AMPA receptor fraction in silenced neurons (Figure 25C; WT APV/CNQX: 151 ± 11% of the WT; $Bsn^{gt}$ APV/CNQX: 149 ± 10% of the $Bsn^{gt}$). These results suggest that Bassoon does not elicit

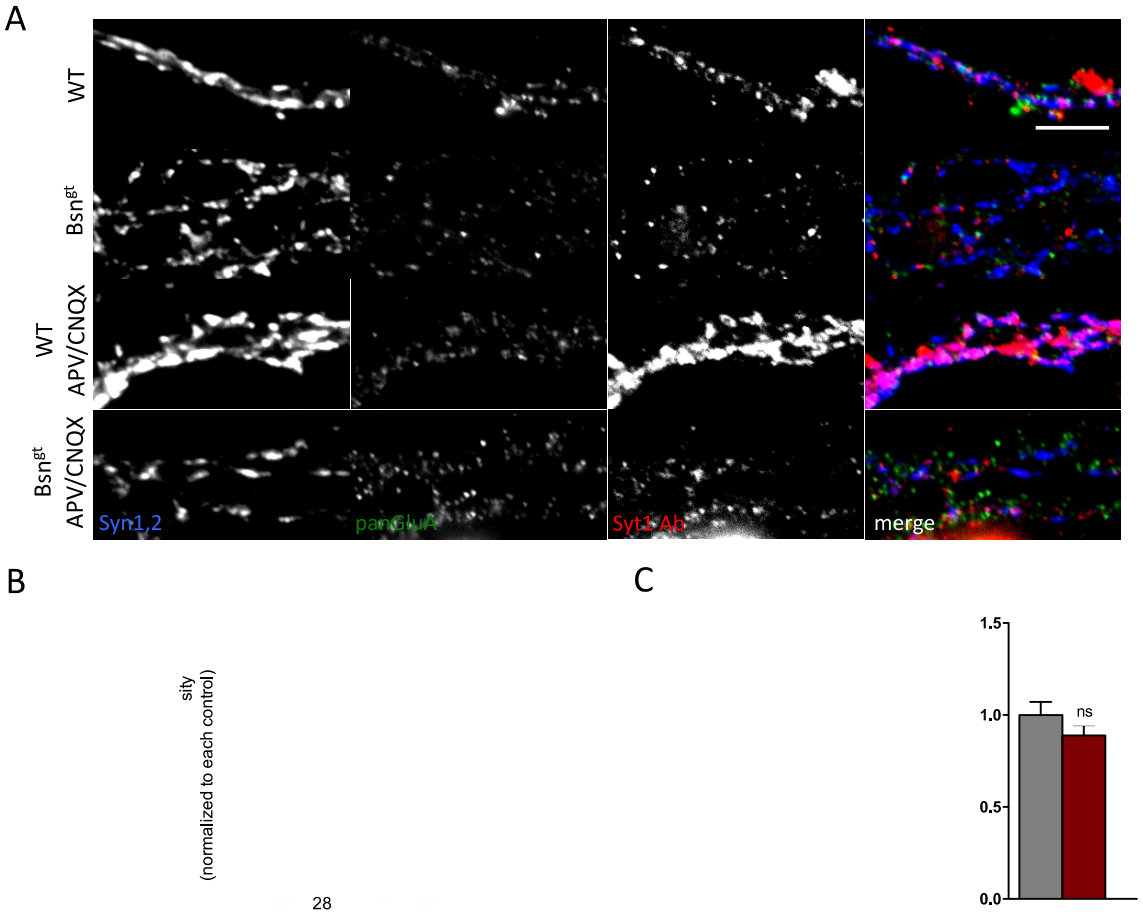


**Figure 25: Bassoon does not affect the surface receptor population on the postsynapse during homeostatic plasticity.** (A) Representative images of panGluA and Syt1 Ab uptake assay signals assay in WT and $Bsn^{gt}$, silenced and non-silenced hippocampal neurons (20-22DIV). Synapsin1,2 was used to label presynaptic terminals in which the panGluA and Syt1 Ab signals were quantified. The right images represent the overlaid result of panGluA (green), Syt1 Ab (red) and the presynaptic marker (blue). Scale bar, 5µm (B) Quantification of the Syt1 Ab uptake immunofluorescence signal under endogenous network activity (left). The normalization is done to each non-silenced genotype. Normalization of $Bsn^{gt}$ to WT is used as control for the experiment (right). (C) Quantification of the panGluA immunofluorescence signal of silenced and non-silenced WT and $Bsn^{gt}$ cells. Values are averages from three independent experiments. The numbers within the columns indicate the number of cells analyzed per condition. Bars represent mean values; whiskers, SEM. The statistical significance was assessed using a t-test. *** = $p<0.001$, ns=$p>0.05$.

changes in the postsynaptic receptor population due to chronic changes in network activity.

Based on the relevance of Bassoon for $Ca^{2+}$ channel number and function, I wondered whether the impairments of the presynaptic homeostatic scaling in Bassoon lacking neurons were due to deficiencies of the $Ca^{2+}$ income during homeostatic plasticity adaptations. To test this, I took advantage of the genetically encoded $Ca^{2+}$ sensor sy-GCaMP5G. As previously published, chronic silencing induced a significant increase in the presynaptic $Ca^{2+}$ entry. In contrast, $Bsn^{gt}$ neurons were not able to show such enhancement after the treatment (Figure 26A; WT APV/CNQX: 144.9 ± 8.9% of the WT; $Bsn^{gt}$ APV/CNQX: 109.7 ± 5.6% of the $Bsn^{gt}$). For this experiment, the differences between WT and $Bsn^{gt}$ (Figure 26B; $Bsn^{gt}$: 135.4 ± 7.1% of the WT) were used as quality control. Overall, the data accentuate the role of the presynaptic scaffold, not only during neurotransmitter release, but during homeostatic plasticity in the presynaptic terminals. Thus, my results suggest that Bassoon elicits changes in the SV cycle and presynaptic $Ca^{2+}$ influx not affecting the postsynapse.

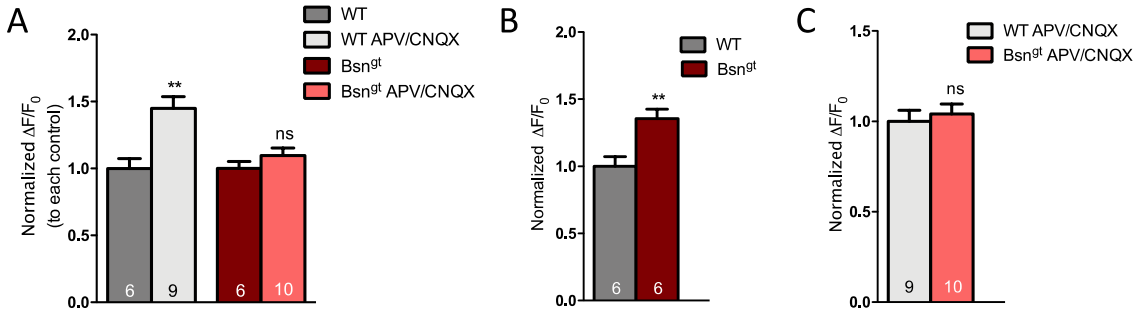


**Figure 26: Bassoon is required for presynaptic $Ca^{2+}$ influx during homeostatic plasticity.** (A) Control quantification of the average responses ± s.e.m. of the $Ca^{2+}$ sensor from two individual experiments upon 5 pulses at 20Hz of WT and $Bsn^{gt}$ hippocampal neurons (20-22DIV), silenced and non-silenced. (B) Responses of non-silenced WT and $Bsn^{gt}$ $Ca^{2+}$ wave amplitude used as control (Normalized to WT). (C) Average responses of silenced WT and $Bsn^{gt}$ neurons (Normalized to WT APV/CNQX). Number of cells analyzed indicated within the bars. Statistical significance was assessed by Student t-test, **=p<0.01, ns=p>0.05.

### 3.2.2 Piccolo regulates synaptic vesicle recycling during homeostatic plasticity

RBP has been reported to stabilize homeostatic plasticity through modulation of presynaptic $Ca^{2+}$ income and SV pools dynamics (Müller et al., 2015). Since Piccolo-mutant neurons showed decreased levels of RBP2, I was keen to know if the presynaptic scaffold is important for the presynaptic homeostatic plasticity too. To first explore the role of Piccolo during changes of the overall network, I performed Syt1 Ab uptake assays in

silenced neurons. WT neurons significantly increased their uptake upon endogenous network activity, whereas Piccolo-mutant neurons did not (Figure 27B, C; Basal: WT APV/CNQX: 146.2 ± 3.8% of the WT, Pclo mut APV/CNQX: 111.7 ± 7% of the Pclo mut). To test whether this effect relies on presynaptic modulation mechanisms, I performed Syt1 Ab uptake during a short chemical depolarization. The results confirmed previous experiments, showing that Piccolo-mutant neurons were not able to upregulate the antibody uptake (Figure 27B, C; WT APV/CNQX: 147.5 ± 6.2% of the WT, Pclo mut APV/CNQX: 109 ± 6.1% of the Pclo mut). These results confirm the importance of Piccolo during homeostatic adaptations.

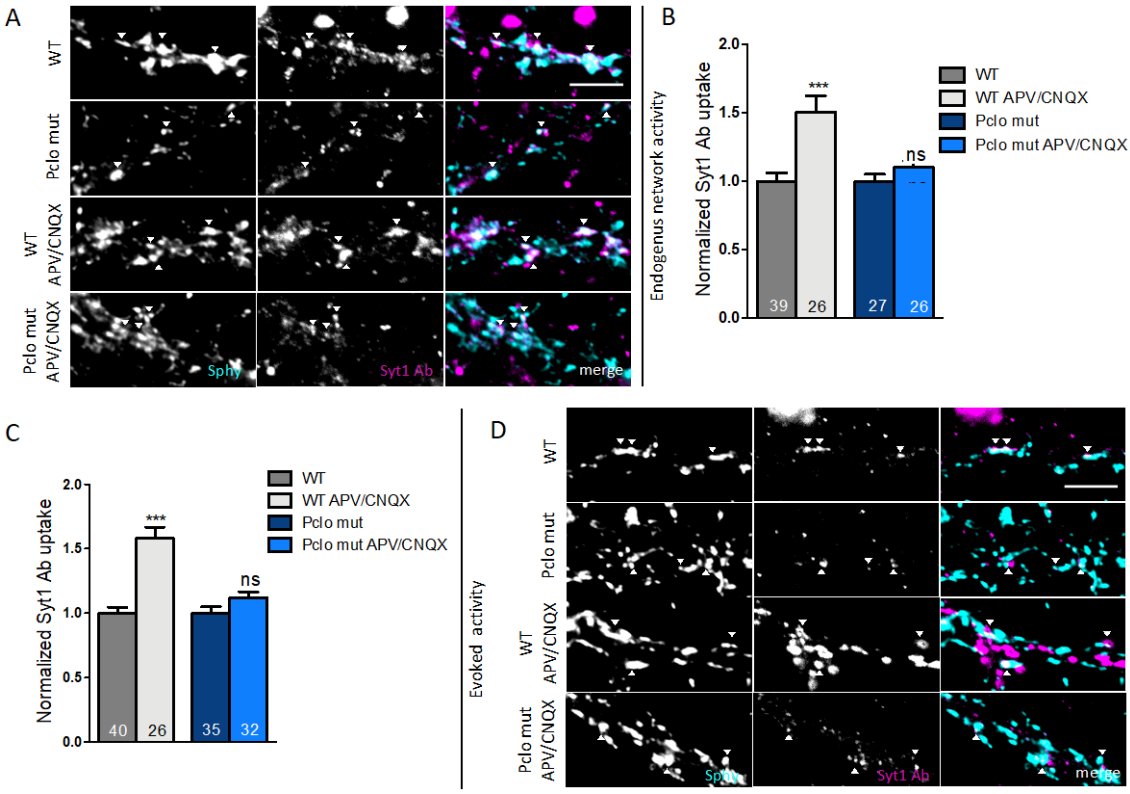


**Figure 27: Piccolo plays an important role in the SV recycling during homeostasis.** (A, D) Representative images of WT, Pclo mutant and their respective silenced cells (20-22DIV) of the analyzed Syt1 Ab uptake assay under endogegus network activity conditions (A) and chemical depolarization (D) in the proximal part of the dendrite (first 20-50). Sphy was used as a presynaptic marker to mask the Syt1 Ab signal. The right images are overlay with sphyt (cyan) and Syt1 Ab (magenta). Scale bar, 5µm. (B, C) Quantification of the Syt1 Ab uptake assay in WT, WT silenced, Pclo mut and Pclo mut silenced upon basal conditions (B), and chemical depolarization (C). Values are normalized to each control. Values are averages from three independent experiments and are normalized to WT. The numbers within the columns indicate the number of cell analyzed per condition. Bars represent mean values; whiskers, SEM. The statistical significance was assessed using a t-test. *** = $p<0.001$, ns=$p>0.05$.

Although several studies associated homeostatic adaptations with changes of the SV pools sizes (Murthy et al., 2001; Moulder et al., 2006; Müller et al., 2012), others reported that the microdomains generated by the VGCC are the key in these processes (Thanawala and Regehr, 2013; Jeans et al., 2017). While Piccolo was shown, to bind VGCC through

RBP2, in vitro, no functional consequences were discovered. However, I wondered whether the presynaptic proteins is necessary for the well-functioning of VGCC upon chronic silencing. Once more, taking advantage of the $Ca^{2+}$ sensor, I measured the peaks of fluorescence after stimulation. The quantification of the $\Delta F/F_0$ signal revealed that Pclo does not interfere with the presynaptic $Ca^{2+}$ income during homeostatic plasticity (Figure 28A; WT APV/CNQX: 158 ± 7.3% of the WT, Pclo mut APV/CNQX: 155.8 ± 7.6% of the Pclo mut). Control conditions showed no differences, supporting the veracity of the results (Figure 28B; Pclo mut: 104.8 ± 5.9% of the WT). This data demonstrated the importance of Piccolo during homeostasis, highlighting the relevance of the scaffold in the SV recycling, but not in the presynaptic $Ca^{2+}$ influx.

A B

**Figure 28: Piccolo does not affect presynaptic $Ca^{2+}$ imaging after chronic silencing.** (A) Analyzed average responses ± s.e.m. of the $Ca^{2+}$ sensor from three individual experiments to 5 pulses at 20Hz of WT, Pclo mutant neurons and silenced genotypes (normalized to each non-treated genotype) (20-22DIV). (B) Comparison between WT and Pclo mut used as control (normalized to WT). Number of cells analyzed indicated within the bars. Statistical significance was assessed by Student t-test, ***=p<0.0001,

In summary, these results showed, for the first time, two molecular players of the homeostatic plasticity in mammals. To date, only RIMs and RBPs have been identified in Drosophila (Müller et al., 2012, 2015). Bassoon seems to be important in multiple homeostatic mechanisms including SV recycling and VGCC-mediated $Ca^{2+}$ entry, whereas Piccolo is more in volved in the regulation of the SV cycle.

# 4 Discussion

## 4.1 The contribution of Bassoon and Piccolo to the neurotransmitter release

The correct signal transmission between neurons is the fundamental principle for a healthy brain function. The presynaptic active zone, the niche of Bassoon and Piccolo, has a major role orchestrating an efficient neurotransmitter release, which is one of the crucial steps of the neuronal communication. Understanding the molecular mechanisms behind neurotransmission, and those who govern them, underlie the development of new strategies to fight brain diseases. Although the role of Piccolo in these processes is not fully understood, initial genome-wide association studies have connected Pclo to psychiatric and developmental disorders such as depressive and bipolar disorders (Sullivan et al., 2009; Choi et al., 2011; Minelli et al., 2012; Woudstra et al., 2013; Giniatullina et al., 2015). Additionally, a recent study has discovered a non-sense mutation in the Piccolo gene in patients with a severe developmental disorder associated with intellectual and motor disabilities called pontocerebellar hypoplasia3 (Ahmed et al., 2015). In contrast, its paralogous presynaptic protein, Bassoon, has been linked to deafness, epilepsy and neurodegeneration (Marquez et al., 2009; Conroy et al., 2014; Wang et al., 2017). More recently, the Bassoon gene has been found mutated in patients with familiar and sporadic progressive supranuclear palsy-like disorder (Yabe et al., 2018). However, how the two presynaptic proteins contribute to the disease development is not known. In this study, I focused mainly on the mechanisms that contribute to the neurotransmitter release and presynaptic $Ca^{2+}$ influx regulation. I demonstrated that Piccolo tunes the SV cycling, whereas it does not contribute to the presynaptic $Ca^{2+}$ current modulation. Bassoon, in contrast, regulates both processes. My results extend the current knowledge about neurotransmission and the players that influence this important mechanism.

### 4.1.1 Decreased presynaptic performance in Piccolo-mutant synapses

There are several mechanisms by which neurons can release rapidly and reliably neurotransmitter from SV located in the presynapses. Positional priming has been proposed as one important process to influence neurotransmission. It is defined as the process that localizes $Ca^{2+}$ channels near "molecularly primed" vesicles (Neher and Sakaba, 2008).

This mechanism ensures the rapid and precise release of SV in response to VGCC opening. It modifies the coupling distance between the SV and the $Ca^{2+}$ nanodomains. RIMs and Bassoon have been reported to control the abundance and function of the VGCC in mammalian brain presynapses through direct (PDZ domain) or indirect binding via RBPs (Kaeser et al., 2011; Davydova et al., 2014). Here, I showed that the specific PxxP motif in Piccolo (RTLPNPP) can bind to RBP2 and may serve as a bridge to connect with VGCC. A decrease of the RBP2 fluorescence intensity was observed in Piccolo-mutant single synapses. In rodents, the deletion of RBPs leads to no major phenotype other than unstable synaptic transmission (Acuna et al., 2015, 2016), whereas in flies, it causes a severe disfunction of the SV exocytosis (Liu et al., 2011). In the system used here, it seems it has no major consequences.

Functional analysis showed that Piccolo does not influence either the number or the function of VGCC, which is at odds with the possible implication of Piccolo in the positional priming of $Ca^{2+}$ channels. Thus, I aimed to study the functionality of the RTLPNPP motif in Piccolo and its implication in the binding between RBP2 and VGCC. Schneider and collaborators, (2015) proposed that within synapses two types of channel populations could be found, the mobile and the immobile. While the extrasynaptic region is mostly constituted by a mobile fraction, within synapses only 35%-45% of the channels are immobile. Piccolo might contribute to reducing the mobility of certain populations of $Ca^{2+}$ channels. It might limit the movement of the synaptic population avoiding its diffusion to the extrasynaptic regions. However, whether Piccolo has an impact in the lateral mobility of VGCC requires further investigation.

Although no changes were observed in my functional analysis of Picolo-deficient hippocampal neurons, I cannot exclude a different outcome in other systems. In central auditory synapses lacking Piccolo changes in the levels of certain VGCC-associated CAZ proteins were reported (Butola et al., 2017). Specifically, while Bassoon is upregulated, RIMs were downregulated, suggesting a possible compensatory effect of Bassoon. Nevertheless, Davydova et al., (2014) virtually positioned Bassoon in the first SH3 domain, RIM1 in the second, and VGCC bound to the third. Thus, it might be that Piccolo binds preferentially to the first RPB domain instead of Bassoon in the auditory system. However, Collins et al., (2005) showed that p38 MAPK phosphorylates the serine in position 5 of Bassoon´s PxxP motif (RTLPSPP), which might prevent the biding of the scaffold to the first SH3 domain. Therefore, the loss of Piccolo might generate a decompensation of the

complex and its components. Based on this, it would be interesting to know whether the function and/or the levels of VGCC are impaired in Piccolo-lacking central auditory synapses. Recent work proposed that Fife, a Drosophila Piccolo-RIM-related protein, functions as $Ca^{2+}$ channel anchorage (Bruckner et al., 2017). It organizes the AZ keeping the nanometer distance between vesicles and channels for reliable neurotransmission. These results might support the idea of the putative role of Pclo in the positional priming of VGCC.

### 4.1.2 Piccolo impairs the synaptic vesicle replenishment

The data presented in this dissertation suggest a role for Piccolo in the recycling of SVs at hippocampal synapses.

As already outlined in the Introduction, based on ultrastructural properties, biochemical characteristics and functional studies, three major pathways have been proposed for SV retrieval: clathrin-mediated endocytosis, 'kiss-and-run', and bulk endocytosis. Clathrin-mediated endocytosis is the most studied mechanism, up to date, numerous studies support the importance of clathrin-mediated endocytosis for the recycling of the SVs. The impairment of the function of clathrin leads to a decrease of the endocytosis (Gonzalez-Gaitan and Jackle, 1997; Granseth et al., 2006; Jockusch et al., 2005; van der Bliek and Meyerowitz, 1991). However, the partial or complete loss of clathrin function does not block synaptic transmission (Gu et al., 2008; Wu et al., 2014). On the other hand, 'Kiss-and-run' is a precisely and coordinated pathway to recover the vesicles (Aravanis et al., 2003; Fesce et al., 1994). It is a faster and less energy-demanding process than its predecessor. This process has been proved to be crucial at fast synapses with a high demand of SV needed to maintain high firing rates, like in the Calyx of Held. Bulk endocytosis, instead, is a system to retrieve SV through large invaginations of plasma membrane upon intense neurotransmission.

Recent publications on C.elegans and mouse synapses reported a novel mechanism that retrieves SVs within 50 to 100 ms after synaptic stimulation referred as "ultrafast endocytosis". This process follows the same principle as bulk endocytosis, it retrieves SV through membrane invaginations with the engagement of actin and dynamin (Watanabe et al., 2013a; Watanabe et al., 2013b).

Based on the pHluorin imaging and Syt1 Ab uptake experiments, I have revealed a major deficit in the SV retrieval of Piccolo-mutant neurons, leading to depletion of TRP. With

pHluorin imaging I could not show that Piccolo affects negatively SV endocytosis, however, this does not mean that Piccolo is not involved in other processes. Due to limited temporal resolution, pHluorin imaging is not suitable to study fast modes of SV endocytosis such as 'kiss and run' and the recently described ultrafast endocytosis. Thus, additional methods and further experiments are needed to dig up the role of Piccolo in the diverse types of vesicle recycling. Considering the deficits shown by Syt1 Ab uptake in Piccolo-mutant neurons, the reported functions of Piccolo during the SV cycle together with its role in the activity-dependent assembly of presynaptic F-actin (Leal-Ortiz et al., 2008; Mukherjee et al, 2010; Waites et al., 2011; Waites et al., 2013; Wagh et al., 2015; Butola et al., 2017) and the published interaction with actin-binding proteins, including Pra1, Profilin-2, Daam1, Abp1 and Trio, and its role (Wang et al., 1999; Fenster et al., 2000; Kim et al., 2003; Waites et al., 2011; Terry-Lorenzo et al., 2016), there are several possibilities for its putative role in the reformation of the SVs.

Vesicle sorting, not directly from the plasma membrane, but from endosome structures has been suggested to contribute to SV recycling. This process has been strongly implicated in the restoration of the RRP (Hoopmann et al., 2010). Nevertheless, in Piccolo-mutant neurons no significant reduction in the size of the RRP was observed. Endosome-like structures have been also implicated in SV recycling during bulk endocytosis. It has been shown that bulk endocytosed vesicles might undergo a reexo-/reendocytosis cycle after 10-15 min of strong stimulation (Evans and Cousin, 2007), contributing to the replenishment of the RP. Furthermore, while the RRP was unaltered in Piccolo-mutant neurons, I observed a reduction in the size of the RP, suggesting that Piccolo might have a role during bulk endocytosis.

RAB proteins, a subgroup of the Ras family of small GTPases, are essential regulators of numerous intracellular membrane trafficking events during the SV cycle as molecular modulators of the exchange of a GDP-bound 'off-state' and a GTP-bound 'on-state' (reviwed in Barr, 2013; Binotti et al., 2016). Together, RAB3 and RAB27B are involved in SV exocytosis, while RAB27B additionally participates in the SV recycling. RAB5 has a role during SV biogenesis and retrieval. Furthermore, RAB35, together with RAB5, has been proposed to contribute to SV replenishment of the SV pools through early endosomal compartments. My preliminary data regarding EEA1 levels suggests that Piccolo

might contribute to this SV replenishment mechanism, which goes in line with previous reported works about Piccolo´s functionality during SV retrieval (Ackermann et al., 2018). Through the action of Pra1, Piccolo might influence the function of RAB5, which would cause defects in endosome formation, and therefore, in the RP size. The decrease of RAB5 activity impairs the maturation of early endosomes, and therefore, affects SV replenishment (Wucherpfennig et al., 2003). Although this hypothesis would fit with my results, further experiments are needed to prove the contribution of Piccolo to the RAB5 function in my model.

Another aspect that might be considered is the regulation of the SV mobilization between SV pools. It has been shown that posttranslational modification of proteins, such as phosphorylation, modulates SV dynamics (Chi et al., 2003; Gelsomino et al., 2013). Synapsin phosphorylated at site 1 ($Ser^{9}$) by PKA, increases the RP size, decreasing the association between the vesicle protein to SV and/or F-actin (Hosaka et al., 1999; Menegon et al., 2006). CaMKI- and IV-mediated phosphorylation at site 1 ($Ser^{9}$) also modulate the mobilization of SVs (Chi et al., 2003). CDK5 at site 7 ($Ser^{551}$) generates a decrease in the RP size blocking the mobilization of SVs from RtP (Kim and Ryan, 2010; Verstegen et al., 2014). CaMKII was identified as a binding partner for synapsin1 on SV (Benfenatti et al., 1992), which mediates SV dispersion (Chi et al., 2001). It has been reported that the loss of Pclo leads to increase of the SV exocytosis rate through CaMKII-mediated synapsin 1 phosphorylation (Leal-Ortiz et al., 2008). As a consequence of this interaction, Pclo might deregulate the SV pools sizes. However, the effects of the aforementioned presynaptic enzymes cannot be discarded, and should be considered for further research.

### 4.1.3 Bassoon is necessary for synaptic vesicle recycling

Several studies demonstrated the importance of Bassoon in neurotransmitter release. Many of them reported the relation of the presynaptic scaffold protein with the SV cycle. Hallermann et al., (2010) showed that while the spontaneous excitatory currents between Bassoon-lacking neurons are not impaired, the protein makes the vesicle reloading at cerebellar mossy fiber-to-granule cell synapses more dynamic. These findings might be supported by a decreased RRP observed in previous studies (Khimich et al., 2005; Frank et al., 2010; Jing et al., 2013). Moreover, evidences suggest that Bassoon plays a role in vesicle replenishment at the endbulb synapses of central auditory synapses (Mendoza-

Schulz et al, 2014), which goes in line with my Stg1 Ab uptake results in hippocampal neurons. However, the mechanism which underlies this effect is still unknown.

Although the deficiency of Bassoon in presynapses could lead to defects in SV endocytosis, the mobilization of vesicles between SV pools cannot be excluded as a mechanism behind the defects shown by the Sty1 Ab uptake assay in $Bns^{gt}$ synapses. In my lab, we observed that CDK5 activity is impaired in this type of neurons (Montenegro-Venegas, Pina-Fernández et al., unpublished). CDK5 is an important protein that has been shown to participate in neurotransmission, neural development, and postsynaptic signal integration (Tan et al., 2003; Lagace et al., 2008; Kim and Ryan, 2010; Ou et al., 2010). In nerve terminals, this enzyme has been shown to play a role in SV endocytosis, exocytosis, and presynaptic $Ca^{2+}$ influx (Tomizawa et al., 2002; Anggono et al., 2006; Kim and Ryan, 2010; Su et al., 2012; Kim and Ryan, 2013). Specially, Tomosyn I CDK5-mediated phosphorylation has been shown to regulate the RRP and RP size (Cazares et al, 2016). Tomo1 proteins, which interact with Synapsin 1a/b, mediate via Rab3A-GTP the mobilization of vesicles within pools. Furthermore, amphiphysin 1, dynamin 1 and synaptojanin are SV recycling -associated proteins reported as substrate of CDK5 (Floyd et al., 2001; Tomizawa et al., 2003; Tan et al., 2003). Roscovitine, a potent CDK5 antagonist, decreases second round of SV endocytosis after stimulation by blocking the phosphorylation of dynamin1 on $Ser^{774}$ and $Ser^{778}$ (Tan et al., 2003). Moreover, experiments in p35- (CDK5 activator) deficient animals showed that CDK5 activity inhibits SV endocytosis, consistent with amphiphysin and dynamin1 CDK5-dependent phosphorylation interruption (Tomizawa et al., 2003). Albeit the importance of CDK5 in the SV cycle has been largely proved, it is unclear if the kinase displays a major role in $Bsn^{gt}$ neurons SV cycle. Furthermore, it is not clear whether the SV endocytosis and/or SV dynamics cause the defects of vesicle replenishment in Bassoon-deficient presynapses. While the role of Piccolo in vesicle cycling has been explored, less is known about Bassoon´s function in this context. Thus, further experiments are needed to dissect the defects shown here and the contribution of Bassoon to this mechanism.

### 4.1.4 The presynaptic calcium influx are influenced by Bassoon

A recent study reported that the interplay between presynaptic $Ca^{2+}$ channels and the presynaptic scaffold causes an impairment in neurotransmission (Davydova et al., 2014). However, how the presynaptic $Ca^{2+}$ influx is affected is not known yet. Thus, I studied

the presynaptic $Ca^{2+}$ influx in $Bsn^{gt}$ hippocampal neurons. Surprisingly, I found that the influx of $Ca^{2+}$ into the presynaptic terminal is enhanced in $Bsn^{gt}$ neurons. I hypothesize that this effect might be a neuronal compensatory mechanism triggered to rescue impaired neurotransmission in $Bsn^{gt}$ neurons.

While the main source of $Ca^{2+}$ ions that elicits the neurotransmitter release comes from the extracellular pool, those contained in intracellular organelles are also an important source that contributes to neuronal excitability (Fitzjohn and Collingridge 2002; Bardo et al., 2006; Baker et al., 2013; Segal, 2018; Heine et al., 2019). Despite the mitochondria containing high $[Ca^{2+}]_i$ (Rizzuto et al., 2012), the endoplasmatic reticulum is the main compartment for intracellular $Ca^{2+}$ storage (Verheatsky, 2004; Juan-Sanz et al., 2017). A critical role of the presynaptic endoplasmatic reticulum in the control of neurotransmission has been described recently (Juan-Sanz et al., 2017; reviewed in Heine et al., 2019). From my results, I cannot exclude the contribution of the endoplasmatic reticulum as a net source of AP-driven $Ca^{2+}$, perhaps via $Ca^{2+}$-induced calcium release (Verhratsky and Shmigol, 1996; Stavermann et al., 2015). Nevertheless, the tight coupling of neurotransmitter release and $Ca^{2+}$ entry dictates the VGCC-driven character of the exocytosis (Llinás et al., 1992; Stanley, 1997). In contrast, distant sources of $Ca^{2+}$ unlikely contribute to this process, but to short-term and long-term plasticity (reviwed in Baker et al., 2013; Padamsey et al., 2019). In order to understand how the absence of Bsn affects the presynaptic $Ca^{2+}$ influx, AgaTx and ConoTx were applied. I observed that the $Ca_v2.2$ contribution was slightly higher, whereas the $Ca_v2.1$ was unchanged in spite of the decreased immunoreactivity already mentioned. However, a preceding publication demonstrated that the loss of Bsn reduces the $Ca_v2.1$-driven synaptic transmission and it is compensated by a functional recruitment of $Ca_v2.2$. This effect is explained by a differential recruitment of $Ca_v2.1$ at the release sites by Bassoon (Davydova et al., 2014). Several publications showed that the accumulation of $Ca_v2.1$ in the presynaptic terminal does not alter synaptic transmission (Cao and Tsien, 2010; Schneider et al., 2015; Lubbert et al., 2017), therefore, the number of channels seems not to be a critical factor for the neurotransmission but for the regulation of their activity. VGCC function is controlled by multiple mechanisms such as the interaction with SNARE proteins or G proteins, and protein phosphorylation. Syntaxin1A and SNAP25 through the synprint domain interact with $Ca_v2.2$ regulating its function (Bezprozvanny et al., 1995; Wiser et al., 1996; Catterall et al., 2008). Phosphorylation of the $Ca_v2.2$ synprint domain by PKC or CaMKII has been

shown to prevent the negative regulation via SNARE proteins (Yokoyama et al., 1997). Furthermore, CaMKII interferes with $Ca_v2.1$ function via direct association rather than phosphorylation (Jiang et al., 2008). Additionally, as previously mentioned, CDK5 is an important enzyme in the synaptic regulation, which also interferes with the VGCC functioning. CDK5 enhances the presynaptic $Ca^{2+}$ influx through $Ca_v2.2$ C-terminal phosphorylation (Su et al., 2012), while phosphorylation of the α1 subunit of $Ca_v2.1$ leads to channel activity down-regulation (Tomizawa et al., 2002). Also, another study indicated that the inhibition of CDK5 activity induces large potentiation of $Ca_v2.2$ activity and it does not affect $Ca_v2.1$ (Kim and Ryan, 2013). Therefore, it is evident that CDK5 modulates VGCC function. These studies indicate that many presynaptic SNARE proteins, scaffolds, and enzymes regulate the VGCC function and dynamics. However, the functional link between Bsn and the presynaptic $Ca^{2+}$ channels requires a further investigation. Moreover, alternative splicing of $Ca^{2+}$ channels can generate thousands of combinations with differential properties and expression patterns, depending on the requirements of the neurons (Maximov and Bezprozvanny, 2002; Liao and Soong, 2010; Lipscombe, 2015; Thalhammer et al., 2017). For example, the mutually exclusive alternative splicing of exon 37 of $Ca_v2.2$, which generates larger or smaller N-type influx based on which exon is expressed (Bell et al., 2004). However, this phenomenon is not restricted to the $Ca_v2.2$ subtype. $Ca_v2.1$ has been reported to experience the same mechanism in exons 37 and 47 with similar consequences (Adams et al., 2009; Thalhammer et al., 2017). Thalhammer et al., (2017) showed that while $Ca_v2.1$[EFa] promotes synaptic depression, $Ca_v2.1$[EFb] favors synaptic facilitation. Importantly, they described that the colocalization between Bassoon and the $Ca_v2.1$[EFa] isoform was higher than with $Ca_v2.1$[EFb]. It suggests that Bassoon might have more affinity for one splice variant than for the other, and therefore, this fact might contribute to the channel dynamics and to the release properties of the neurons.

Splicing of exon 47 leads to a shortening of the $Ca_v2.1$ α-subunit C-terminus (Krovetz et al., 2000; Soong et al., 2002), which contains binding motifs necessary for modulation and/or localization of $Ca^{2+}$ channels, including the SH3 for RBPs binding (Hibbino et al., 2002), and the motif through which, directly or indirectly, RIM interacts with the channels (Hibbino et al., 2002; Kaeser et al., 2011; Davydova et al., 2014). A recent study demonstrated that this alternative splicing of $Ca_v2.1$ shapes synapse-specific Pr at the channel dynamics level, sharpening the distance between vesicles and channels (Heck et

al., 2019). While the $Ca_v2.1_{\triangle 47}$, which lacks the C-terminal, increases the Pr and displays more variable channel-vesicle distances, the $Ca_v2.1_{+47}$ isoforms enhance synaptic short-term depression, and preserve the defined distance between the channels and SV. The presence of the scaffolding protein Bassoon might contribute to keep the stability within nanodomains and maintain the effective channel-vesicle distance in order to ensure the fast and precise vesicle release. Instead, when the scaffold is missing, the transition from nanodomains to microdomains might happen. Nevertheless, how Bassoon contributes to the synapse fine-tuning in $Ca^{2+}$ channels alternative splicing terms, is yet an intricate question to answer. Due to the infinite combinations generated after alternative splicing, it would be interesting to see which isoforms are predominant in Bassoon-lacking pre-synaptic boutons. Although RIM interacts directly with $Ca_v2.1_{+47}$ isoforms, which might support the defined channel-vesicle distance, the contribution of Bassoon is not yet certain. It would be interesting to know whether Bassoon, despite its interplay with $Ca_v2.1_{+47}$ in a non-directly manner, contributes to fix the channels at certain distance of the vesicles. Lastly, Piccolo and Bassoon have been involved in the shuttling of the C-terminal binding protein1 (CtBP1) (Ivanova et al., 2015), a well-established transcriptional co-repressor in neurons (Chinnadurai, 2007; 2009), between synapses and the nucleus. When both pre-synaptic scaffolds are deleted from synapses, CtBP1 is only present in the nucleus. This finding links both large presynaptic proteins with the transcriptional control of genes. I hypothesize that the absence of Bassoon causes the shuttling of CtBP1 into the nucleus having an effect on alternative splicing mechanisms of $Ca_v$s. Moreover, the expression and modulation of VGCC in the plasma membrane in neurons are auxiliary subunit-dependent (reviewed in Buraei and Yang, 2010; Dolphin, 2012, 2016; Bikbaev et al., 2020). In Purkinje cells, α*2*δ2 subunit increases the $Ca^{2+}$ influx of the $Ca_v2.1$-β4, but not single channel conductance (Barclayet al.2001; Brodbecket al., 2002). α*2*δ1 and α*2*δ2 contain the perfect MIDAS motif, which is required for increasing $Ca^{2+}$ ions (Cantiet al., 2005; Hoppa et al., 2012), and $Ca_v2.2$ location on the cell surface (Cassidy et al.2014). Mutation of this motif decreases α*2*δ subunit trafficking itself (Cantiet al., 2005; Cassidyet al., 2014) with consequences in $Ca^{2+}$ influx of α*2*δ1 and α*2*δ2-coupled $Ca^{2+}$ channels (Hoppa et al., 2012; Canti et al., 2005). In contrast, α*2*δ3 and α*2*δ4, which do not contain perfect MIDAS motifs (Whittaker & Hynes, 2002), seem to enhance $Ca^{2+}$ income too, but it may display a more modest trafficking role (Davies et al., 2010). Bassoon, through CtBP1,

might interfere with the alternative splicing of the α*2*δ auxiliary subunit, which may modulate the functional properties of $Ca^{2+}$ channels.

### 4.1.5 Bassoon and Piccolo deletion does not sum in the dysregulation of voltage-gated calcium channels

I have shown how important these two scaffolds, individually, are for $Ca^{2+}$ channels' function, but I also wanted to investigate whether the deletion of both proteins is crucial for VGCC-diven $Ca^{2+}$ influx. In other words, does the deletion of Piccolo, on top of Bassoon lack, have additive effects? Previous studies reported opposite results: while Mukherjee and collaborators (2010) showed that evoked and spontaneous neurotransmission were unchanged, Ivanova and colleagues (2015) showed that upon basal network-driven activity the Syt1 Ab uptake was reduced. The differences between models might explain the disparity in the results. While Mukherjee and collaborators used a knock-down strategy, Ivanova et al. worked with a constitutive mouse model which is mutant for both presynaptic proteins. Based on the differences in the Syt1 Ab uptake assay shown by Ivanova and colleagues, the same animal model was used in my study. Contrary to what was expected, once more, my experiments showed that the double-mutant synapses have enhanced AP-evoked presynaptic $Ca^{2+}$ income. Since the increase seen for $Bsn^{gt}$ neurons is comparable to the one registered in the double mutant, the contribution of Pclo to the VGCC-driven $Ca^{2+}$ influx could be totally excluded in hippocampal neurons. On the other hand, the increase registered in $Ca^{2+}$-imaging, anew, does not fit with the Stg1 Ab uptake assay results previously mentioned, suggesting that, most likely, the SV cycle is impaired when both scaffolds are missing. The proteasomal activity has been proposed as a negative regulator of the neurotransmitter release through the SV recycling (Jiang et al, 2010; Ivanova et al, 2016). While acute inhibition of proteasomes increases the Pr, prolonged ubiquitin-proteasome system (UPS) blockage enhances the RP size (Willeumier et al, 2006; Rinetti & Schweizer, 2010). Since in Bassoon- and Piccolo-mutant synapses the SV clusters are destabilized by the ubiquitination of SV proteins (Waites et al., 2013), the UPS might have a key role in these synapses. Indeed, I identified Bassoon as a novel interacting partner of PSMB4, a β subunit of 20S core proteasome (Montenegro-Venegas et al., unpublished). I demonstrated that acute pharmacological inhibition of proteasome recovered the defect in the size of SV pool sizes. However, future experiments are required to disentangle this question in the double mutant.

Altogether, until now, my study explored the roles of Piccolo and Bassoon in processes governing neurotransmission. In conclusion, my findings revealed new aspects of the regulation of VGCC and SV cycling, and open new questions about how the two CAZ proteins regulate these processes (Figure 30).

## 4.2 Bassoon and Piccolo during homeostatic plasticity

Learning and memory require the formation of neuronal networks in the brain. A key process underlying this mechanism is synaptic plasticity. Synaptic plasticity is a higher-level process in which the strength of excitatory synapses is altered in response to the pattern of activity at the synapse.

The data presented in the second part of my dissertation contribute to the better understanding of how some of the molecular mechanisms underlying presynaptic homeostatic plasticity are ruled. I identified Bassoon and Piccolo as two molecular players in the homeostatic plasticity adaptations in mammalian neurons. Bassoon seems to be important for SV recycling and presynaptic $Ca^{2+}$ influx during prolonged network inactivation, whereas Piccolo modulates the SV replenishment.

### 4.2.1 Bassoon is necessary for presynaptic homeostatic plasticity adaptations

As previously described, chronic silencing induces upregulation of the presynaptic function through the reorganization of the release machinery (Lazarevic et al., 2011), SV recycling (Bacci et al., 2001; Burrone et al., 2002; Thiagarajan et al., 2005; Moulder et al., 2006; Han and Stevens, 2009; Kim et al., 2010), and changes in the Pr (Murthy et al., 2001; Zhao et al., 2011). However, at present, no molecular players underlying these adaptations are known in mammals.I identified Bassoon as a crucial protein for adaptive homeostatic adjustment of presynaptic efficacy in mice hippocampal neurons. Multiple studies highlighted the importance of the SV cycle, the presynaptic $Ca^{2+}$ influx, and the postsynaptic receptor dynamics as key factors by which homeostatic plasticity is supported (Murthy et al., 2001; Thiagarajan et al., 2005; Branco et al., 2008; Kim and Ryan, 2010; Lazarevic et al., 2011; Zhao et al., 2011; Jeans et al., 2017; Thalhammer et al., 2017). I have shown that Bassoon is important for two mechanisms that take place within the nerve terminal.

Firstly, upon chronic silencing, neurons increase the amplitude of mEPSCs to maintain the firing rate (Turrigiano et al., 1998). The AMPA receptor content in spines is adjusted to counterbalance the changes in the overall network activity (Watt et al., 2000; Sutton et al., 2006; Ibata et al., 2008; Gainey et al., 2009). As expected, Bassoon did not interfere with the AMPA receptor dynamics, restricting its range of action to the presynapses. Secondly, based on Syt1 Ab uptake, Bassoon impairs the SV recycling after chronic silencing. Mechanistically, homeostatic adaptations comprise modulation of SV pools (mainly RRP (Murthy et al., 2001; Moulder et al., 2006). However, dynamic mobilization of vesicles from the RtP has been attributed to the activity of CDK5 during homeostasis (Kim and Ryan, 2010). The balance between CDK5 and calcineurin B, a protein a phosphatase, seems to determine the size of the largest SV pool. Considering the importance of CDK5 in my model (Montenegro-Venegas, Pina-Fernandez et al., unpublished), I hypothesize that the blockage of its activity can rescue the reported presynaptic upscaling. Thirdly, changes in the VGCC-driven $Ca^{2+}$ influx tune homeostatic plasticity.

Several groups proposed that the increase shown after chronic silencing is mainly $Ca_v2.1$-dependent (Zhao et al, 2011; Lazarevic et al., 2011; Jeans et al., 2017; Thalhammer et al., 2017). Moreover, new publicartions suggest that the enhancement after chronic silencing is based on the unitary conductance of individual channels (Jeans et al., 2017; Thalhammer et al., 2017) and not in the number of channels (Jarvis and Zamponi, 2007; Lazarevic et al., 2011). Thalhammer and collaborators (2017) showed that alternative splicing of $Ca_v2.1$ exon 47 is a key factor controlling homeostasis. They proposed that the balance between isoforms shapes presynaptic plasticity. Increasing the contribution of the $Ca_v2.1$[EFa] isoform, which displays higher synaptic efficacy, the neurons endure the upregulation of the presynaptic $Ca^{2+}$ influx after chronic silencing. I showed that Bassoon was required for a correct upscaling of the $Ca^{2+}$ income within the presynaptic terminal, which might be due to an impairment in the recruitment of $Ca_v2.1$ at the release sites. Therefore, it might suggest that i) Bassoon specifically anchors $Ca^{2+}$ channels with certain functional properties to favor the development of nanodomains; ii) via CtBP1, Bassoon shapes the population and the recruitment of $Ca_v2.1$ to the presynapses; iii) CDK5-mediated phosphorylation of $Ca^{2+}$ channels regulates their intrinsic properties. i) The higher co-localization between the presynaptic scaffold and $Ca_v2.1$[EFa] suggests that the scaffold might be preferentially bound to this subtype of $Ca_v2.1$. Moreover, it might serve the

creation of nanodomains that ensure the fast and precise release of neurotransmitters. Bassoon absence might deregulate the balance between Ca channel splice isoforms and support the transition from nanodomains to microdomains. Alternatively, ii) since Bassoon/Piccolo-deficient neurons failed in the CtBP1 shuttling to the nucleus during chronic silencing (Ivanova et al., 2015), it might deregulate the expression of any $Ca^{2+}$ channel subunit with consequences in the channel's dynamics or kinetics, such as α2δ (Cottrell et al., 2018; Dahimene et al., 2018). iii) The effects of CDK5 during homeostatic plasticity have been already described in this thesis(see page 63). Because this enzyme is important for the homeostatic adaptations and for $Bsn^{gt}$ neurons, it might influence $Ca^{2+}$ channels properties.

### 4.2.2 Piccolo is required for correct homeostasis

My data suggest that Piccolo is crucial for the homeostatic adaptations through the SV replenishment, but not for the VGCC-mediated $Ca^{2+}$ influx. The homeostatic potentiation of the presynaptic function during chronic silencing requires an increase of Pr (Murthy et al., 2001), supported by an augmented SV recycling (Bacci et al., 2001; Burrone et al., 2002; Thiagarajan et al., 2005; Moulder et al., 2006; Han and Stevens, 2009). Based on Stg1 Ab uptake, I showed that Piccolo maintains the increase of the SV pools contributing to the SV replenishment during silencing. Since I reported the decrease of EEA1 levels, it can be concluded that the failure of the RAB-dependent SV replenishment is the cause of the impairment during homeostatic plasticity in Piccolo-mutant neurons.

At mammalian central synapses, $Ca^{2+}$ entry regulates the SV pool sizes (Schneggenburger et al., 1999; Thanawala and Regehr, 2013). Thus, major changes in the Pr are likely to be $Ca^{2+}$ influx-dependent. Recent work highlights the importance of the microdomain generated by each $Ca^{2+}$ channel during homeostatic plasticity (Jeans et al., 2017). Considering the potential of Piccolo to bind indirectly VGCC, I expected it to have a role in supporting the creation of nanodomains. Nevertheless, Bassoon is placed as the binding partner of the first SH3 domain, while RIM1 and $Ca_V$s occupy second and third SH3 domains (Wang et al., 2000; Hibino et al., 2002; Davydova et al., 2014). Thus, I aimed to study Piccolo´s location. Based on the structural similarities between Bassoon and Piccolo, I would expect Piccolo to bind to the SH3I in RBPs. It seems that besides a competition

may exist for the first domain, Bassoon is the presynaptic protein that preferentially occupied that domain. The RBP-interacting PxxP motifs in Bassoon and Piccolo differ in the aa in position 5, which in Bassoon is serine, but asparagine in Piccolo (RTLPSPP vs RTLPNPP). Collins et al., (2005) showed in vivo that p38 MAPK could in particular phosphorylate this serine of Bassoon ($Ser^{2893}$). This finding could lead to the idea that phosphorylation may regulate which of both scaffolding proteins interacts with RBPs during homeostatic plasticity, and could explain why in my analysis Piccolo-mutant neurons do not statistically differ from the WT. This kinase is activated by some forms of synaptic plasticity (Imprey et al., 1999), it might get activated during presynaptic homeostatic plasticity. However, if the kinase gets activated, the $Ca_v2.2$ is inhibited (Wilk-Blaszczak et al., 1998; Brust et al., 2006), which is not crucial because the enhancement of presynaptic $Ca^{2+}$ influx is $Ca_v2.1$-mediated (Lazarevic et al., 2011; Zhao et al., 2011; Jeans et al., (2017)

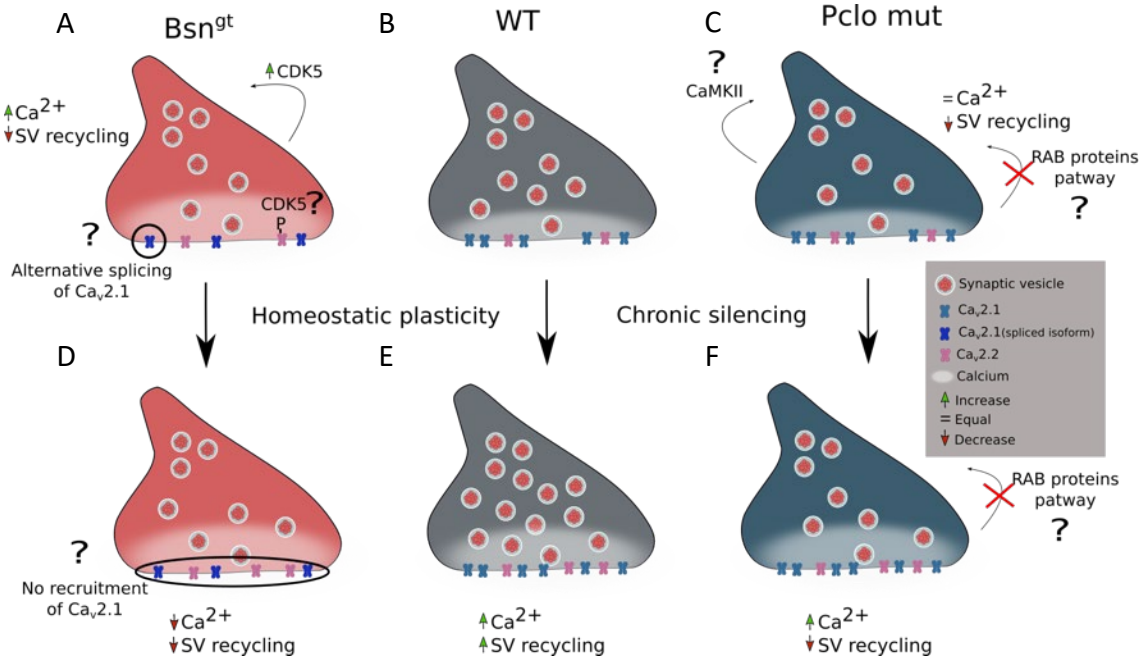


**Figure 29: Proposed role of Piccolo and Bassoon in neurotransmission and synaptic plasticity.** (A) $Bsn^{gt}$ presynapses show higher presynaptic $Ca^{2+}$ income and decreased SV recycling compared to WT (B). $Ca_v2.2$-mediated $Ca^{2+}$ entry is enhanced, while the $Ca_v2.1$ are comparable to control. CDK5 activity and alternative splicing could be the mechanisms behind these processes. (C) Piccolo-mutant terminals do not exert changes in either number or function of VGCC, the SV replenishment is impaired, and most likely, RAB proteins can be the cause of the dysfunction. (Down row) Homeostatic plasticity adaptations in $Bsn^{gt}$, WT and Piccolo-mutant neurons. While the chronic silencing treatment increases evoked presynaptic $Ca^{2+}$ influx and SV recycling in WT presynapses (E), $Bsn^{gt}$ neurons (D) may have post the potential to recruit more $Ca^{2+}$ channels after silencing, and therefore, lack the ability for hemostatic adaptation. Instead, Piccolo-mutant presynapses (F) the VGCC function is not impaired, but the SV recycling is, whether the RAB proteins are involved is not yet clear.

At present, only RIM and RBP have been identified as molecular players during homeostatic plasticity in Drosophila (Muller et al., 2012; Müller et al., 2016). In this thesis,

Piccolo and Bassoon have been shown for the first time to be crucial for homeostatic plasticity adaptations in vertebrates. Both scaffolds play similar and/or unique roles in the Pr increase after prolonged network silencing. Overall, Piccolo and Bassoon modulate the SV recycling, whereas only Bassoon is crucial for AP-evoked $Ca^{2+}$ influx during homeostasis (see the model in Figure 30). The mechanisms underlying these findings are still not fully understood, therefore future work is required to unravel the unknown.

# 5 Abbreviations

| | |
|---|---|
| Aa | Amino acid |
| Abp1 | Actin-binding protein 1 |
| AgaTX | ω-Agatoxin IVA |
| AMPA | α-amino-3-hydroxy-5-methyl-4-isoxazolepropionic acid |
| AP | Action potential |
| APS | Ammonium persulfate |
| APV | D-2-amino-5-phosphonovalerate |
| Ara C | Cytosine β-D-Arabinofuranoside |
| ATP | Adenosine triphosphate |
| AZ | Active zone |
| BafA | Bafilomycin A |
| BSA | Bovine serum albumin |
| Bsn | Bassoon |
| $Bsn^{gt}$ | Bassoon gene trap |
| CaMK | Calcium/calmodulin-dependent protein kinase |
| cAMP-GEFII | cAMP- guanidine nucleotide exchange factor II |
| CAST | cytomatrix at the active zone-associated structural protein |
| CAZ | Cytomatrix at the active zone |
| CDK | Cyclin-dependent kinase |
| CME | Clathrin-mediated endocytosis |
| CNQX | 6-Cyano-7-nitroquinoxaline-2,3 dione disodium |
| co-IP | Co-immunoprecipitate |
| ConoTX | ω-Conotoxin GVIA |
| D-APV5 | D-(-)-2-Amino-5- phosphonopentanoic acid |
| D-PLL | Poly-D-lysine |
| $dH_2O$ | Distilled water |
| DIV | Days in vitro |
| DMEM | Dulbecco´s modified eagle medium |
| DNA | Deoxyribonucleic acid |
| DNase | Deoxyribonuclease |
| dNTP | Deoxynucleotide |
| EDTA | Ethylenediaminetetraacetic acid |

| | |
|---|---|
| EEA1 | Early endosome antigen 1 |
| EGFP | enhanced green fluorescent protein |
| EGTA | ethylene glycol-bis(β-aminoethyl ether)-N,N,N′,N′-tetraacetic acid |
| EMCCD | Electron- multiplying CCDs |
| Emx1 | empty spiracle homebox-1 |
| ET | Emission transmission |
| FCS | Fetal calf serum |
| GABA | gamma-aminobutyric acid |
| GFP | Green fluorescent protein |
| $G_{\alpha}$ | Gs protein alpha subunit |
| HBSS | Hanks Balanced Salt solution |
| HEK293-T | Human embryonic kidney cells |
| HEPES | 4-(2-hydroxyethyl)-1-piperazineethanesulfonic acid |
| KO | Knockout |
| L-PLL | Poly-L-Lysine |
| mEPSC | Miniature excitatory postsynaptic currents |
| mRFP | Red fluorescent protein |
| P0 | Postnatal day 0 |
| PBH | Piccolo-Bassoon homology |
| PBS | Phosphate-buffered saline |
| PBS-T | Phosphate-buffered saline-tween |
| Pclo | Piccolo |
| Pclo mut. | Piccolo mutant |
| PCR | Polymerase chain reaction |
| PDZ | Post synaptic density protein (PSD95), Drosophila disc large tumor suppressor, (Dlg1) and zonula occludens-1 protein (zo-1) |
| PFA | Paraformaldehyde |
| PKA | Protein Kinase A |
| Pr | Release probability |
| PRA1 | Rab acceptor protein 1 |
| PSD95 | Postsynaptic density protein 95 |
| RBP | RIM-binding protein |
| RIM | Rab3-interacting molecule |

| | |
|---|---|
| ROI | Region of interest |
| RP | Recycling pool |
| Rpm | Revolutions per minute |
| RRP | Readily releasable pool |
| $R_tP$ | Resting pool |
| S.e.m. | Standard error of the mean |
| SDS | Sodium Dodecyl Sulfate |
| SNAP25 | Synaptosomal-associated protein 25 |
| SNARE | Soluble NSF attachment protein receptor |
| SNR | Signal to noise ratio |
| Sphy | Synaptophysin |
| SV | Synaptic vesicle |
| sy-GCaMP5G | Synaptophysin- GCaMP5G |
| Syn1, 2 | Synapsin 1,2 |
| Synprint | Synaptic protein interaction site |
| SynpHy | Synaptophysin-pHluorin |
| Syt1 ab | Synaptotagmin 1 antibody |
| TAE | Tris-acetate- ethylenediaminetetraacetic acid |
| TEMED | Tetramethylethylenediamine |
| Tris-HCl | Tris-hydrochloride |
| TRP | Total recycling pool |
| TTX | Tetrodotoxin |
| U | Unit |
| VGAT | Vesicular GABA Transporter |
| VGCC | Voltage-gated calcium channel |
| VGluT1 | Vesicular glutamate transporter 1 |
| WT | Wild-type |
| $\Delta F/F_0$ | Delta fluorescent/initial brightness |

# 6 Bibliography

Ackermann, F., Schink, K. O., Bruns, C., Izsvak, Z., Hamra, K., Rosenmund, C., & Garner, C. C. (2018). Critical role for Piccolo in synaptic vesicle retrieval. *bioRxiv*.

Ackermann, F., Waites, C. L., & Garner, C. C. (2015). Presynaptic active zones in invertebrates and vertebrates. *EMBO Rep, 16*(8), 923-938. doi:10.15252/embr.201540434

Acuna, C., Liu, X., & Sudhof, T. C. (2016). How to Make an Active Zone: Unexpected Universal Functional Redundancy between RIMs and RIM-BPs. *Neuron, 91*(4), 792-807. doi:10.1016/j.neuron.2016.07.042

Adams, D. J., Callaghan, B., & Berecki, G. (2012). Analgesic conotoxins: block and G protein-coupled receptor modulation of N-type (Ca(V) 2.2) calcium channels. *Br J Pharmacol, 166*(2), 486-500. doi:10.1111/j.1476-5381.2011.01781.x

Ahmed, M. Y., Chioza, B. A., Rajab, A., Schmitz-Abe, K., Al-Khayat, A., Al-Turki, S., . . . Mochida, G. H. (2015). Loss of PCLO functionunderlies pontocerebellar hypoplasia type III. Neurology, 84(17), 1745-1750. doi:10.1212/WNL.0000000000001523.

Ahmed, S. P., Bittencourt-Hewitt, A., & Sebastian, C. L. (2015). Neurocognitive bases of emotion regulation development in adolescence. *Dev Cogn Neurosci, 15*, 11-25. doi:10.1016/j.dcn.2015.07.006

Akerboom, J., Chen, T. W., Wardill, T. J., Tian, L., Marvin, J. S., Mutlu, S., ... & Gordus, A. (2012). Optimization of a GCaMP calcium indicator for neural activity imaging. *Journal of neuroscience*, *32*(40), 13819-13840.

Alabi, A. A., & Tsien, R. W. (2012). Synaptic vesicle pools and dynamics. *Cold Spring Harb Perspect Biol, 4*(8), a013680. doi:10.1101/cshperspect.a013680

Altmüller, F., Pothula, S., Annamneedi, A., Nakhaei-Rad, S., Montenegro-Venegas, C., Pina-Fernández, E., ... & Ahmadian, M. R. (2017). Aberrant neuronal activity-induced signaling and gene expression in a mouse model of RASopathy. *PLoS genetics*, *13*(3), e1006684.

Altrock, W. D., Tom Dieck, S., Sokolov, M., Meyer, A. C., Sigler, A., Brakebusch, C., ... & Brandt, C. (2003). Functional inactivation of a fraction of excitatory synapses in mice deficient for the active zone protein bassoon. *Neuron*, *37*(5), 787-800.

Angenstein, F., Hilfert, L., Zuschratter, W., Altrock, W. D., Niessen, H. G., & Gundelfinger, E. D. (2008). Morphological and metabolic changes in the cortex of mice lacking the functional presynaptic active zone protein bassoon: a combined 1H-NMR spectroscopy and histochemical study. *Cereb Cortex, 18*(4), 890-897. doi:10.1093/cercor/bhm122

Anggono, V., Smillie, K. J., Graham, M. E., Valova, V. A., Cousin, M. A., & Robinson, P. J. (2006). Syndapin I is the phosphorylation-regulated dynamin I partner in synaptic vesicle endocytosis. *Nature neuroscience*, *9*(6), 752.

Annamneedi, A., Caliskan, G., Muller, S., Montag, D., Budinger, E., Angenstein, F., . . . Stork, O. (2018). Ablation of the presynaptic organizer Bassoon in excitatory neurons retards dentate gyrus maturation and enhances learning performance. *Brain Struct Funct, 223*(7), 3423-3445. doi:10.1007/s00429-018-1692-3

Araki, Y., Zeng, M., Zhang, M., & Huganir, R. L. (2015). Rapid dispersion of SynGAP from synaptic spines triggers AMPA receptor insertion and spine enlargement during LTP. *Neuron, 85*(1), 173-189. doi:10.1016/j.neuron.2014.12.023

Augustine, G. J., Charlton, M. P., & Smith, S. J. (1987). Calcium action in synaptic transmitter release. *Annual review of neuroscience*, *10*(1), 633-693.

Bacci, A., Coco, S., Pravettoni, E., Schenk, U., Armano, S., Frassoni, C., ... & Matteoli, M. (2001). Chronic blockade of glutamate receptors enhances presynaptic release and downregulates the interaction between synaptophysin-synaptobrevin–vesicle-associated membrane protein 2. *Journal of Neuroscience*, *21*(17), 6588-6596.

Bachli, E., & Gundelfinger, M. (2017). *Praxis (Bern 1994), 106*(15), 807-813. doi:10.1024/1661-8157/a002740

Baker, K. D., Edwards, T. M., & Rickard, N. S. (2013). The role of intracellular calcium stores in synaptic plasticity and memory consolidation. *Neuroscience & Biobehavioral Reviews*, *37*(7), 1211-1239.

Balaji, T., Ramanathan, M., Srinivasan, M., & Menon, V. P. (2008). Distribution of cyclooxygenase-1 and cyclooxygenase-2 in the mouse seminal vesicle. *Journal of Applied Biomedicine (De Gruyter Open)*, *6*(2).

Bardo, S., Cavazzini, M. G., & Emptage, N. (2006). The role of the endoplasmic reticulum Ca2+ store in the plasticity of central neurons. *Trends in pharmacological sciences*, *27*(2), 78-84.

Bell, T. J., Thaler, C., Castiglioni, A. J., Helton, T. D., & Lipscombe, D. (2004). Cell-specific alternative splicing increases calcium channel current density in the pain pathway. *Neuron, 41*(1), 127-138. doi:10.1016/s0896-6273(03)00801-8

Benfenati, F., Valtorta, F., Rubenstein, J. L., Gorelick, F. S., Greengard, P., & Czernik, A. J. (1992). Synaptic vesicle-associated Ca2+/calmodulin-dependent protein kinase II is a binding protein for synapsin I. *Nature*, *359*(6394), 417.

Bernstein, G. M., & Jones, O. T. (2007). Kinetics of internalization and degradation of N-type voltage-gated calcium channels: role of the alpha2/delta subunit. *Cell Calcium, 41*(1), 27-40. doi:10.1016/j.ceca.2006.04.010

Bezprozvanny, I. (1995). Scheller RH, and Tsien RW. *Functional impact of syntaxin on gating of N-type and Q-type calcium channels. Nature*, *378*, 623-626.

Bhattacharya, S., Herrera-Molina, R., Sabanov, V., Ahmed, T., Iscru, E., Stober, F., . . . Montag, D. (2017). Genetically Induced Retrograde Amnesia of Associative Memories After Neuroplastin Ablation. *Biol Psychiatry, 81*(2), 124-135. doi:10.1016/j.biopsych.2016.03.2107

Boucrot, E., Ferreira, A. P., Almeida-Souza, L., Debard, S., Vallis, Y., Howard, G., . . . McMahon, H. T. (2015). Endophilin marks and controls a clathrin-independent endocytic pathway. *Nature, 517*(7535), 460-465. doi:10.1038/nature14067

Branco, T., Staras, K., Darcy, K. J., & Goda, Y. (2008). Local Dendritic Activity Sets Release Probability at Hippocampal Synapses. *Neuron, 59*(3), 475-485. doi:10.1016/j.neuron.2008.07.006

Branco, T., Staras, K., Darcy, K. J., & Goda, Y. (2008). Local dendritic activity sets release probability at hippocampal synapses. *Neuron*, *59*(3), 475-485.

Brown, R. E., & Milner, P. M. (2003). The legacy of Donald O. Hebb: more than the Hebb synapse. *Nature Reviews Neuroscience*, *4*(12), 1013.

Bruckner, J. J., Zhan, H., Gratz, S. J., Rao, M., Ukken, F., Zilberg, G., & O'Connor-Giles, K. M. (2017). Fife organizes synaptic vesicles and calcium channels for high-probability neurotransmitter release. *J Cell Biol*, *216*(1), 231-246.

Buraei, Z., & Yang, J. (2010). The ss subunit of voltage-gated Ca2+ channels. *Physiol Rev, 90*(4), 1461-1506. doi:10.1152/physrev.00057.2009

Burrone, J., Li, Z., & Murthy, V. N. (2006). Studying vesicle cycling in presynaptic terminals using the genetically encoded probe synaptopHluorin. *Nature protocols*, *1*(6), 2970.

Butola, T., Wichmann, C., & Moser, T. (2017). Piccolo Promotes Vesicle Replenishment at a Fast Central Auditory Synapse. *Front Synaptic Neurosci, 9*, 14. doi:10.3389/fnsyn.2017.00014

Bykhovskaia, M. (2011). Synapsin regulation of vesicle organization and functional pools. *Semin Cell Dev Biol, 22*(4), 387-392. doi:10.1016/j.semcdb.2011.07.003

Canti, C., Nieto-Rostro, M., Foucault, I., Heblich, F., Wratten, J., Richards, M. W., . . . Dolphin, A. C. (2005). The metal-ion-dependent adhesion site in the Von Willebrand fac-

tor-A domain of 2 subunits is key to trafficking voltage-gated Ca2+ channels. *Proceedings of the National Academy of Sciences, 102*(32), 11230-11235. doi:10.1073/pnas.0504183102

Castiglioni, A. J., Raingo, J., & Lipscombe, D. (2006). Alternative splicing in the C-terminus of CaV2.2 controls expression and gating of N-type calcium channels. *J Physiol, 576*(Pt 1), 119-134. doi:10.1113/jphysiol.2006.115030

Catterall, W. A. (2000). Structure and regulation of voltage-gated Ca2+ channels. *Annual review of cell and developmental biology*, *16*(1), 521-555.

Catterall, W. A. (2011). Voltage-gated calcium channels. *Cold Spring Harb Perspect Biol, 3*(8), a003947. doi:10.1101/cshperspect.a003947

Catterall, W. A., & Few, A. P. (2008). Calcium channel regulation and presynaptic plasticity. *Neuron, 59*(6), 882-901. doi:10.1016/j.neuron.2008.09.005

Catterall, W. A., & Few, A. P. (2008). Calcium channel regulation and presynaptic plasticity. *Neuron*, *59*(6), 882-901.

Cazares, V. A., Njus, M. M., Manly, A., Saldate, J. J., Subramani, A., Ben-Simon, Y., . . . Stuenkel, E. L. (2016). Dynamic Partitioning of Synaptic Vesicle Pools by the SNARE-Binding Protein Tomosyn. *J Neurosci, 36*(44), 11208-11222. doi:10.1523/JNEUROSCI.1297-16.2016

Chai, Z., Wang, C., Huang, R., Wang, Y., Zhang, X., Wu, Q., . . . Zhou, Z. (2017). CaV2.2 Gates Calcium-Independent but Voltage-Dependent Secretion in Mammalian Sensory Neurons. *Neuron, 96*(6), 1317-1326 e1314. doi:10.1016/j.neuron.2017.10.028

Chen, J., Billings, S. E., & Nishimune, H. (2011). Calcium Channels Link the Muscle-Derived Synapse Organizer Laminin 2 to Bassoon and CAST/Erc2 to Organize Presynaptic Active Zones. *Journal of Neuroscience, 31*(2), 512-525. doi:10.1523/jneurosci.3771-10.2011

Chen, X., Tomchick, D. R., Kovrigin, E., Araç, D., Machius, M., Südhof, T. C., & Rizo, J. (2002). Three-dimensional structure of the complexin/SNARE complex. *Neuron*, *33*(3), 397-409.

Chinnadurai, G. The transcriptional corepressor CtBP: a foe of multiple tumor suppressors. *Cancer research* 69.3 (2009): 731-734.

Chinnadurai, G. Transcriptional regulation by C-terminal binding proteins. *The international journal of biochemistry & cell biology* 39.9 (2007): 1593-1607.

Choi, K. H., Higgs, B. W., Wendland, J. R., Song, J., McMahon, F. J., & Webster, M. J. (2011). Gene Expression and Genetic Variation Data Implicate PCLO in Bipolar Disorder. *Biological Psychiatry, 69*(4), 353-359. doi:10.1016/j.biopsych.2010.09.042

Choi, K. H., Higgs, B. W., Wendland, J. R., Song, J., McMahon, F. J., & Webster, M. J. (2011). Gene expression and genetic variation data implicate PCLO in bipolar disorder. Biol Psychiatry, 69(4), 353-359. doi:10.1016/j.biopsych.2010.09.042.

Clayton, E. L., Evans, G. J., & Cousin, M. A. (2007). Activity-dependent control of bulk endocytosis by protein dephosphorylation in central nerve terminals. *The Journal of physiology*, *585*(3), 687-691.

Cohen, J. E., Lee, P. R., Chen, S., Li, W., & Fields, R. D. (2011). MicroRNA regulation of homeostatic synaptic plasticity. *Proc Natl Acad Sci U S A, 108*(28), 11650-11655. doi:10.1073/pnas.1017576108

Conroy, J., McGettigan, P. A., McCreary, D., Shah, N., Collins, K., Parry-Fielder, B., ... & Webb, D. (2014). Towards the identification of a genetic basis for L andau-K leffner s yndrome. *Epilepsia*, *55*(6), 858-865.

Cousin, M. A., & Robinson, P. J. (2001). The dephosphins: dephosphorylation by calcineurin triggers synaptic vesicle endocytosis. *Trends in neurosciences*, *24*(11), 659-665.

Cruz, J. C., & Tsai, L. H. (2004). Cdk5 deregulation in the pathogenesis of Alzheimer's disease. *Trends in molecular medicine*, *10*(9), 452-458.

Davydova, D., Marini, C., King, C., Klueva, J., Bischof, F., Romorini, S., . . . Fejtova, A. (2014). Bassoon specifically controls presynaptic P/Q-type Ca(2+) channels via RIM-binding protein. *Neuron, 82*(1), 181-194. doi:10.1016/j.neuron.2014.02.012

Delvendahl, I., Vyleta, N. P., von Gersdorff, H., & Hallermann, S. (2016). Fast, Temperature-Sensitive and Clathrin-Independent Endocytosis at Central Synapses. *Neuron, 90*(3), 492-498. doi:10.1016/j.neuron.2016.03.013

Deng, L., Kaeser, P. S., Xu, W., & Sudhof, T. C. (2011). RIM proteins activate vesicle priming by reversing autoinhibitory homodimerization of Munc13. *Neuron, 69*(2), 317-331. doi:10.1016/j.neuron.2011.01.005

Dick, O., tom Dieck, S., Altrock, W. D., Ammermüller, J., Weiler, R., Garner, C. C., ... & Brandstätter, J. H. (2003). The presynaptic active zone protein bassoon is essential for photoreceptor ribbon synapse formation in the retina. *Neuron*, *37*(5), 775-786.

Dittman, J., & Ryan, T. A. (2009). Molecular circuitry of endocytosis at nerve terminals. *Annu Rev Cell Dev Biol, 25*, 133-160. doi:10.1146/annurev.cellbio.042308.113302

Dobrunz, L. E., & Stevens, C. F. (1997). Heterogeneity of release probability, facilitation, and depletion at central synapses. *Neuron*, *18*(6), 995-1008.

Dobrunz, L. E., & Stevens, C. F. (1997). Heterogeneity of release probability, facilitation, and depletion at central synapses. *Neuron*, *18*(6), 995-1008.

Dolphin, A. C. (2012). Calcium channel auxiliary alpha2delta and beta subunits: trafficking and one step beyond. *Nat Rev Neurosci, 13*(8), 542-555. doi:10.1038/nrn3311

Dong, W., Radulovic, T., Goral, R. O., Thomas, C., Suarez Montesinos, M., Guerrero-Given, D., . . . Young, S. M., Jr. (2018). CAST/ELKS Proteins Control Voltage-Gated Ca(2+) Channel Density and Synaptic Release Probability at a Mammalian Central Synapse. *Cell Rep, 24*(2), 284-293 e286. doi:10.1016/j.celrep.2018.06.024

Dreosti, E., Odermatt, B., Dorostkar, M. M., & Lagnado, L. (2009). A genetically encoded reporter of synaptic activity in vivo. *Nature methods*, *6*(12), 883.

Dulubova, I., Sugita, S., Hill, S., Hosaka, M., Fernandez, I., Südhof, T. C., & Rizo, J. (1999). A conformational switch in syntaxin during exocytosis: role of munc18. *The EMBO journal*, *18*(16), 4372-4382.

Duman, R. S. (2004). Depression: a case of neuronal life and death? *Biol Psychiatry, 56*(3), 140-145. doi:10.1016/j.biopsych.2004.02.033

Dunlap, K., Luebke, J. I., & Turner, T. J. (1995). Exocytotic Ca2+ channels in mammalian central neurons. *Trends in neurosciences*, *18*(2), 89-98.

Dunlap, K., Luebke, J. I., & Turner, T. J. (1995). Exocytotic Ca2+ channels in mammalian central neurons. *Trends in neurosciences*, *18*(2), 89-98.

Ehlers, M. D., Heine, M., Groc, L., Lee, M. C., & Choquet, D. (2007). Diffusional trapping of GluR1 AMPA receptors by input-specific synaptic activity. *Neuron, 54*(3), 447-460. doi:10.1016/j.neuron.2007.04.010

Ertel, E. A., Campbell, K. P., Harpold, M. M., Hofmann, F., Mori, Y., Perez-Reyes, E., ... & Tsien, R. W. (2000). Nomenclature of voltage-gated calcium channels. *Neuron*, *25*(3), 533-535.

Fenster, S. D., & Garner, C. C. (2002). Gene structure and genetic localization of the PCLO gene encoding the presynaptic active zone protein Piccolo. *International journal of developmental neuroscience*, *20*(3-5), 161-171.

Fenster, S. D., Chung, W. J., Zhai, R., Cases-Langhoff, C., Voss, B., Garner, A. M., ... & Garner, C. C. (2000). Piccolo, a presynaptic zinc finger protein structurally related to bassoon. *Neuron*, *25*(1), 203-214.

Fenster, S. D., Chung, W. J., Zhai, R., Cases-Langhoff, C., Voss, B., Garner, A. M., ... & Garner, C. C. (2000). Piccolo, a presynaptic zinc finger protein structurally related to bassoon. *Neuron*, *25*(1), 203-214.

Fenster, S. D., Chung, W. J., Zhai, R., Cases-Langhoff, C., Voss, B., Garner, A. M., ... & Garner, C. C. (2000). Piccolo, a presynaptic zinc finger protein structurally related to bassoon. *Neuron*, *25*(1), 203-214.

Fernandez-Alfonso, T., & Ryan, T. A. (2008). A heterogeneous "resting" pool of synaptic vesicles that is dynamically interchanged across boutons in mammalian CNS synapses. *Brain Cell Biol, 36*(1-4), 87-100. doi:10.1007/s11068-008-9030-y

Fernandez-Busnadiego, R., Asano, S., Oprisoreanu, A. M., Sakata, E., Doengi, M., Kochovski, Z., . . . Lucic, V. (2013). Cryo-electron tomography reveals a critical role of RIM1alpha in synaptic vesicle tethering. *J Cell Biol, 201*(5), 725-740. doi:10.1083/jcb.201206063

Fitzjohn, S. M., & Collingridge, G. L. (2002). Calcium stores and synaptic plasticity. *Cell calcium*, *32*(5-6), 405-411.

Fountain, D. I., Knapp, L., Baugh, K., Posner, M., & Fenster, S. D. (2015). Piccolo paralogs and orthologs display conserved patterns of alternative splicing within the C2A and C2B domains. *Genes & Genomics, 38*(5), 407-419. doi:10.1007/s13258-015-0383-1

Frank, C. A. (2014). How voltage-gated calcium channels gate forms of homeostatic synaptic plasticity. *Front Cell Neurosci, 8*, 40. doi:10.3389/fncel.2014.00040

Frank, T., Rutherford, M. A., Strenzke, N., Neef, A., Pangrsic, T., Khimich, D., . . . Moser, T. (2010). Bassoon and the synaptic ribbon organize Ca(2)+ channels and vesicles to add release sites and promote refilling. *Neuron, 68*(4), 724-738. doi:10.1016/j.neuron.2010.10.027

Friedman, H. V., Bresler, T., Garner, C. C., & Ziv, N. E. (2000). Assembly of new individual excitatory synapses: time course and temporal order of synaptic molecule recruitment. *Neuron*, *27*(1), 57-69.

Fujimoto, K., Shibasaki, T., Yokoi, N., Kashima, Y., Matsumoto, M., Sasaki, T., . . . Seino, S. (2002). Piccolo, a Ca2+ sensor in pancreatic beta-cells. Involvement of cAMP-GEFII.Rim2. Piccolo complex in cAMP-dependent exocytosis. *J Biol Chem, 277*(52), 50497-50502. doi:10.1074/jbc.M210146200

Fukuda, M., Kobayashi, H., Ishibashi, K., & Ohbayashi, N. (2011). Genome-wide investigation of the Rab binding activity of RUN domains: development of a novel tool that specifically traps GTP-Rab35. *Cell structure and function*, 1107010083-1107010083.

Gainey, Melanie A., et al. Synaptic scaling requires the GluR2 subunit of the AMPA receptor. *Journal of Neuroscience* 29.20 (2009): 6479-6489.

Gandhi, S. P., & Stevens, C. F. (2003). Three modes of synaptic vesicular recycling revealed by single-vesicle imaging. *Nature*, *423*(6940), 607-613.

Gerber, S. H., Garcia, J., Rizo, J., & Südhof, T. C. (2001). An unusual C2-domain in the active-zone protein piccolo: implications for Ca2+ regulation of neurotransmitter release. *The EMBO journal*, *20*(7), 1605-1619.

Giniatullina, A., Maroteaux, G., Geerts, C. J., Koopmans, B., Loos, M., Klaassen, R., . . . Verhage, M. (2015). Functional characterization of the PCLO p.Ser4814Ala variant associated with major depressive disorder reveals cellular but not behavioral differences. Neuroscience, 300, 518-538. doi:10.1016/j.neuroscience.2015.05.047.

Graf, E. R., Valakh, V., Wright, C. M., Wu, C., Liu, Z., Zhang, Y. Q., & DiAntonio, A. (2012). RIM promotes calcium channel accumulation at active zones of the Drosophila neuromuscular junction. *J Neurosci, 32*(47), 16586-16596. doi:10.1523/JNEUROSCI.0965-12.2012

Granseth, B., Odermatt, B., Royle, S. J., & Lagnado, L. (2006). Clathrin-mediated endocytosis is the dominant mechanism of vesicle retrieval at hippocampal synapses. *Neuron, 51*(6), 773-786. doi:10.1016/j.neuron.2006.08.029

Granseth, B., & Lagnado, L. (2008). The role of endocytosis in regulating the strength of hippocampal synapses. *The Journal of physiology*, *586*(24), 5969-5982.

Gundelfinger, E. D., & Fejtova, A. (2012). Molecular organization and plasticity of the cytomatrix at the active zone. *Current Opinion in Neurobiology, 22*(3), 423-430. doi:10.1016/j.conb.2011.10.005

Gundelfinger, E. D., Reissner, C., & Garner, C. C. (2015). Role of Bassoon and Piccolo in Assembly and Molecular Organization of the Active Zone. *Front Synaptic Neurosci, 7*, 19. doi:10.3389/fnsyn.2015.00019

Hallermann, S., Fejtova, A., Schmidt, H., Weyhersmuller, A., Silver, R. A., Gundelfinger, E. D., & Eilers, J. (2010). Bassoon speeds vesicle reloading at a central excitatory synapse. *Neuron, 68*(4), 710-723. doi:10.1016/j.neuron.2010.10.026

Hammarlund, M., Palfreyman, M. T., Watanabe, S., Olsen, S., & Jorgensen, E. M. (2007). Open syntaxin docks synaptic vesicles. *PLoS biology*, *5*(8), e198.

Han, E. B., & Stevens, C. F. (2009). Development regulates a switch between post- and presynaptic strengthening in response to activity deprivation. *Proc Natl Acad Sci U S A, 106*(26), 10817-10822. doi:10.1073/pnas.0903603106

Han, Y., Kaeser, P. S., Sudhof, T. C., & Schneggenburger, R. (2011). RIM determines Ca(2)+ channel density and vesicle docking at the presynaptic active zone. *Neuron, 69*(2), 304-316. doi:10.1016/j.neuron.2010.12.014

Harms, K. J., Tovar, K. R., & Craig, A. M. (2005). Synapse-specific regulation of AMPA receptor subunit composition by activity. *J Neurosci, 25*(27), 6379-6388. doi:10.1523/JNEUROSCI.0302-05.2005

Haucke, V., Wenk, M. R., Chapman, E. R., Farsad, K., & De Camilli, P. (2000). Dual interaction of synaptotagmin with μ2-and α-adaptin facilitates clathrin-coated pit nucleation. *The EMBO Journal*, *19*(22), 6011-6019.

He, L., & Wu, L. G. (2007). Role of Ca2+ channels in short-term synaptic plasticity. *Current opinion in neurobiology*, *17*(3), 352-359.

Hebb DO (1949) The organization of behavior. *Wiley, New York*

Heine, M., Heck, J., Ciuraszkiewicz, A., & Bikbaev, A. (2019). Dynamic compartmentalization of calcium channel signalling in neurons. *Neuropharmacology*.

Heuser, J. E., & Reese, T. S. (1973). Evidence for recycling of synaptic vesicle membrane during transmitter release at the frog neuromuscular junction. *J Cell Biol, 57*(2), 315-344. doi:10.1083/jcb.57.2.315

Heyden, A., Ionescu, M.-C. S., Romorini, S., Kracht, B., Ghiglieri, V., Calabresi, P., . . . Gundelfinger, E. D. (2011). Hippocampal enlargement in Bassoon-mutant mice is associated with enhanced neurogenesis, reduced apoptosis, and abnormal BDNF levels. *Cell and Tissue Research, 346*(1), 11-26. doi:10.1007/s00441-011-1233-3

Hibino, H., Pironkova, R., Onwumere, O., Vologodskaia, M., Hudspeth, A. J., & Lesage, F. (2002). RIM binding proteins (RBPs) couple Rab3-interacting molecules (RIMs) to voltage-gated Ca2+ channels. *Neuron*, *34*(3), 411-423.

Hilfiker, S., Pieribone, V. A., Czernik, A. J., Kao, H. T., Augustine, G. J., & Greengard, P. (1999). Synapsins as regulators of neurotransmitter release. *Philosophical Transactions of the Royal Society of London. Series B: Biological Sciences*, *354*(1381), 269-279.

Hosaka, M., Hammer, R. E., & Südhof, T. C. (1999). A phospho-switch controls the dynamic association of synapsins with synaptic vesicles. *Neuron*, *24*(2), 377-387.

Hosoi, N., Holt, M., & Sakaba, T. (2009). Calcium dependence of exo- and endocytotic coupling at a glutamatergic synapse. *Neuron, 63*(2), 216-229. doi:10.1016/j.neuron.2009.06.010

Huang, H., Lin, X., Liang, Z., Zhao, T., Du, S., Loy, M. M., ... & Ip, N. Y. (2017). Cdk5-dependent phosphorylation of liprinα1 mediates neuronal activity-dependent synapse development. *Proceedings of the National Academy of Sciences*, *114*(33), E6992-E7001.

Huntwork, S., & Littleton, J. T. (2007). A complexin fusion clamp regulates spontaneous neurotransmitter release and synaptic growth. *Nat Neurosci, 10*(10), 1235-1237. doi:10.1038/nn1980

Ibata, Keiji, Qian Sun, and Gina G. Turrigiano. Rapid synaptic scaling induced by changes in postsynaptic firing. *Neuron* 57.6 (2008): 819-826.

Igarashi, M., & Watanabe, M. (2007). Roles of calmodulin and calmodulin-binding proteins in synaptic vesicle recycling during regulated exocytosis at submicromolar Ca2+ concentrations. *Neurosci Res, 58*(3), 226-233. doi:10.1016/j.neures.2007.03.005

Ikeda, K., & Bekkers, J. M. (2009). Counting the number of releasable synaptic vesicles in a presynaptic terminal. *Proc Natl Acad Sci U S A, 106*(8), 2945-2950. doi:10.1073/pnas.0811017106

Ivanova, D., Dirks, A., & Fejtova, A. (2016). Bassoon and piccolo regulate ubiquitination and link presynaptic molecular dynamics with activity-regulated gene expression. *J Physiol, 594*(19), 5441-5448. doi:10.1113/JP271826

Ivanova, D., Dirks, A., Montenegro-Venegas, C., Schone, C., Altrock, W. D., Marini, C., . . . Fejtova, A. (2015). Synaptic activity controls localization and function of CtBP1 via binding to Bassoon and Piccolo. *The EMBO Journal, 34*(8), 1056-1077. doi:10.15252/embj.201488796

Jarousse, N., Wilson, J. D., Arac, D., Rizo, J., & Kelly, R. B. (2003). Endocytosis of synaptotagmin 1 is mediated by a novel, tryptophan-containing motif. *Traffic*, *4*(7), 468-478.

Jeans, A. F., van Heusden, F. C., Al-Mubarak, B., Padamsey, Z., & Emptage, N. J. (2017). Homeostatic Presynaptic Plasticity Is Specifically Regulated by P/Q-type Ca(2+) Channels at Mammalian Hippocampal Synapses. *Cell Rep, 21*(2), 341-350. doi:10.1016/j.celrep.2017.09.061

Jiang, X., Lautermilch, N. J., Watari, H., Westenbroek, R. E., Scheuer, T., & Catterall, W. A. (2008). Modulation of Cav2.1 channels by calcium/calmodulin-dependent protein kinase II bound to the C-terminal domain. *Proceedings of the National Academy of Sciences of the United States of America, 105*, 341–346.

Jing, Z., Rutherford, M. A., Takago, H., Frank, T., Fejtova, A., Khimich, D., ... & Strenzke, N. (2013). Disruption of the presynaptic cytomatrix protein bassoon degrades ribbon anchorage, multiquantal release, and sound encoding at the hair cell afferent synapse. *Journal of Neuroscience*, *33*(10), 4456-4467.

Juan-Sanz, J., Holt, G. T., Schreiter, E. R., de Juan, F., Kim, D. S., & Ryan, T. A. (2017). Axonal endoplasmic reticulum Ca2+ content controls release probability in CNS nerve terminals. *Neuron*, *93*(4), 867-881.

Kaech, S., & Banker, G. (2006). Culturing hippocampal neurons. *Nature protocols*, *1*(5), 2406.

Kaeser, P. S., Deng, L., Wang, Y., Dulubova, I., Liu, X., Rizo, J., & Sudhof, T. C. (2011). RIM proteins tether Ca2+ channels to presynaptic active zones via a direct PDZ-domain interaction. *Cell, 144*(2), 282-295. doi:10.1016/j.cell.2010.12.029

Kahne, T., Richter, S., Kolodziej, A., Smalla, K. H., Pielot, R., Engler, A., . . . Gundelfinger, E. D. (2016). Proteome rearrangements after auditory learning: high-resolution profiling of synapse-enriched protein fractions from mouse brain. *J Neurochem, 138*(1), 124-138. doi:10.1111/jnc.13636

Kawabe, H., Mitkovski, M., Kaeser, P. S., Hirrlinger, J., Opazo, F., Nestvogel, D., . . . Brose, N. (2017). Correction: ELKS1 localizes the synaptic vesicle priming protein bMunc13-2 to a specific subset of active zones. *J Cell Biol, 216*(4), 1205. doi:10.1083/jcb.20160608603092017c

Kennedy, M. J., & Ehlers, M. D. (2006). Organelles and trafficking machinery for postsynaptic plasticity. *Annu. Rev. Neurosci.*, *29*, 325-362.

Khimich, D., Nouvian, R., Pujol, R., Tom Dieck, S., Egner, A., Gundelfinger, E. D., & Moser, T. (2005). Hair cell synaptic ribbons are essential for synchronous auditory signalling. *Nature*, *434*(7035), 889.

Kim, S. H., & Ryan, T. A. (2010). CDK5 Serves as a Major Control Point in Neurotransmitter Release. *Neuron, 67*(5), 797-809. doi:10.1016/j.neuron.2010.08.003

Kim, S. H., & Ryan, T. A. (2013). Balance of calcineurin Aalpha and CDK5 activities sets release probability at nerve terminals. *J Neurosci, 33*(21), 8937-8950. doi:10.1523/JNEUROSCI.4288-12.2013

Kim, S. H., & Ryan, T. A. (2013). Balance of calcineurin Aα and CDK5 activities sets release probability at nerve terminals. *Journal of Neuroscience*, *33*(21), 8937-8950.

Kim, S., Ko, J., Shin, H., Lee, J. R., Lim, C., Han, J. H., . . . Kim, E. (2003). The GIT family of proteins forms multimers and associates with the presynaptic cytomatrix protein Piccolo. *J Biol Chem, 278*(8), 6291-6300. doi:10.1074/jbc.M212287200

Kiyonaka, S., Wakamori, M., Miki, T., Uriu, Y., Nonaka, M., Bito, H., . . . Mori, Y. (2007). RIM1 confers sustained activity and neurotransmitter vesicle anchoring to presynaptic Ca2+ channels. *Nat Neurosci, 10*(6), 691-701. doi:10.1038/nn1904

Korthals, M., Langnaese, K., Smalla, K. H., Kahne, T., Herrera-Molina, R., Handschuh, J., . . . Thomas, U. (2017). A complex of Neuroplastin and Plasma Membrane Ca(2+) ATPase controls T cell activation. *Sci Rep, 7*(1), 8358. doi:10.1038/s41598-017-08519-4

Krovetz, H. S., Helton, T. D., Crews, A. L., & Horne, W. A. (2000). C-terminal alternative splicing changes the gating properties of a human spinal cord calcium channel α1A subunit. *Journal of Neuroscience*, *20*(20), 7564-7570.

Lacinová, L. (2005). Voltage-dependent calcium channels. *General physiology and biophysics*, *24*, 1-78.

Lagace, D. C., Benavides, D. R., Kansy, J. W., Mapelli, M., Greengard, P., Bibb, J. A., & Eisch, A. J. (2008). Cdk5 is essential for adult hippocampal neurogenesis. *Proceedings of the National Academy of Sciences*, *105*(47), 18567-18571.

Lang, D., Schott, B. H., van Ham, M., Morton, L., Kulikovskaja, L., Herrera-Molina, R., . . . Dunay, I. R. (2018). Chronic Toxoplasma infection is associated with distinct alterations in the synaptic protein composition. *J Neuroinflammation, 15*(1), 216. doi:10.1186/s12974-018-1242-1

Langnaese, K., Seidenbecher, C., Wex, H., Seidel, B., Hartung, K., Appeltauer, U., ... & Gundelfinger, E. D. (1996). Protein components of a rat brain synaptic junctional protein preparation. *Molecular brain research*, *42*(1), 118-122.

Lazarevic, V., Fienko, S., Andres-Alonso, M., Anni, D., Ivanova, D., Montenegro-Venegas, C., . . . Fejtova, A. (2017). Physiological Concentrations of Amyloid Beta Regulate Recycling of Synaptic Vesicles via Alpha7 Acetylcholine Receptor and CDK5/Calcineurin Signaling. *Front Mol Neurosci, 10*, 221. doi:10.3389/fnmol.2017.00221

Lazarevic, V., Pothula, S., Andres-Alonso, M., & Fejtova, A. (2013). Molecular mechanisms driving homeostatic plasticity of neurotransmitter release. *Front Cell Neurosci, 7*, 244. doi:10.3389/fncel.2013.00244

Lazarevic, V., Schone, C., Heine, M., Gundelfinger, E. D., & Fejtova, A. (2011). Extensive remodeling of the presynaptic cytomatrix upon homeostatic adaptation to network activity silencing. *J Neurosci, 31*(28), 10189-10200. doi:10.1523/JNEUROSCI.2088-11.2011

Leal-Ortiz, S., Waites, C. L., Terry-Lorenzo, R., Zamorano, P., Gundelfinger, E. D., & Garner, C. C. (2008). Piccolo modulation of Synapsin1a dynamics regulates synaptic vesicle exocytosis. *J Cell Biol, 181*(5), 831-846. doi:10.1083/jcb.200711167

Liao, P., & Soong, T. W. (2010). Understanding alternative splicing of Cav 1.2 calcium channels for a new approach towards individualized medicine. *Journal of biomedical research*, *24*(3), 181-186.

Lindskog, M., Li, L., Groth, R. D., Poburko, D., Thiagarajan, T. C., Han, X., & Tsien, R. W. (2010). Postsynaptic GluA1 enables acute retrograde enhancement of presynaptic function to coordinate adaptation to synaptic inactivity. *Proc Natl Acad Sci U S A, 107*(50), 21806-21811. doi:10.1073/pnas.1016399107

Lipscombe, D. (2015). Calcium Channel CaVα1 Splice Isoforms - Tissue Specificity and Drug Action.

Lira, M., Arancibia, D., Orrego, P. R., Montenegro-Venegas, C., Cruz, Y., Garcia, J., . . . Torres, V. I. (2018). The Exocyst Component Exo70 Modulates Dendrite Arbor Formation, Synapse Density, and Spine Maturation in Primary Hippocampal Neurons. *Mol Neurobiol*. doi:10.1007/s12035-018-1378-0

Liu, C., Bickford, L. S., Held, R. G., Nyitrai, H., Sudhof, T. C., & Kaeser, P. S. (2014). The Active Zone Protein Family ELKS Supports Ca2+ Influx at Nerve Terminals of Inhibitory Hippocampal Neurons. *Journal of Neuroscience, 34*(37), 12289-12303. doi:10.1523/jneurosci.0999-14.2014

Liu, K. S., Siebert, M., Mertel, S., Knoche, E., Wegener, S., Wichmann, C., ... & Bückers, J. (2011). RIM-binding protein, a central part of the active zone, is essential for neurotransmitter release. *Science*, *334*(6062), 1565-1569.

Llinas, R., Sugimori, M., & Silver, R. B. (1992). Microdomains of high calcium concentration in a presynaptic terminal. *Science*, *256*(5057), 677-679.

Lois, C., Hong, E. J., Pease, S., Brown, E. J., & Baltimore, D. (2002). Germline transmission and tissue-specific expression of transgenes delivered by lentiviral vectors. *Science*, *295*(5556), 868-872.

Ma, C., Li, W., Xu, Y., & Rizo, J. (2011). Munc13 mediates the transition from the closed syntaxin-Munc18 complex to the SNARE complex. *Nat Struct Mol Biol, 18*(5), 542-549. doi:10.1038/nsmb.2047

Maggio, N., Shavit Stein, E., & Segal, M. (2018). Cannabidiol regulates long term potentiation following status epilepticus: mediation by calcium stores and serotonin. *Frontiers in molecular neuroscience*, *11*, 32.

Marquez, A., Cenit, M. C., Nunez, C., Mendoza, J. L., Taxonera, C., Diaz-Rubio, M., ... & Urcelay, E. (2009). Effect of BSN-MST1 locus on inflammatory bowel disease and multiple sclerosis susceptibility. *Genes and immunity*, *10*(7), 631.

Maximov, A., & Bezprozvanny, I. (2002). Synaptic targeting of N-type calcium channels in hippocampal neurons. *Journal of Neuroscience*, *22*(16), 6939-6952.

Maximov, A., Südhof, T. C., & Bezprozvanny, I. (1999). Association of neuronal calcium channels with modular adaptor proteins. *Journal of Biological Chemistry*, *274*(35), 24453-24456.

Maycox, P. R., Link, E., Reetz, A., Morris, S. A., & Jahn, R. (1992). Clathrin-coated vesicles in nervous tissue are involved primarily in synaptic vesicle recycling. *The Journal of cell biology*, *118*(6), 1379-1388.

McEwen, J. M., & Kaplan, J. M. (2008). UNC-18 promotes both the anterograde trafficking and synaptic function of syntaxin. *Molecular biology of the cell*, *19*(9), 3836-3846.

Menegon, A., Bonanomi, D., Albertinazzi, C., Lotti, F., Ferrari, G., Kao, H. T., . . . Valtorta, F. (2006). Protein kinase A-mediated synapsin I phosphorylation is a central modulator of Ca2+-dependent synaptic activity. *J Neurosci, 26*(45), 11670-11681. doi:10.1523/JNEUROSCI.3321-06.2006

Menegon, A., Bonanomi, D., Albertinazzi, C., Lotti, F., Ferrari, G., Kao, H. T., ... & Valtorta, F. (2006). Protein kinase A-mediated synapsin I phosphorylation is a central modulator of Ca2+-dependent synaptic activity. *Journal of Neuroscience*, *26*(45), 11670-11681.

Miller, T. M. (1984). Endocytosis of synaptic vesicle membrane at the frog neuromuscular junction. *The Journal of Cell Biology, 98*(2), 685-698. doi:10.1083/jcb.98.2.685

Minelli, A., Scassellati, C., Cloninger, C. R., Tessari, E., Bortolomasi, M., Bonvicini, C., . . . Gennarelli, M. (2012). PCLO gene: its role in vulnerability to major depressive disorder. *J Affect Disord, 139*(3), 250-255. doi:10.1016/j.jad.2012.01.028

Mittelstaedt, T., & Schoch, S. (2007). Structure and evolution of RIM-BP genes: identification of a novel family member. *Gene, 403*(1-2), 70-79. doi:10.1016/j.gene.2007.08.004

Mohle, L., Israel, N., Paarmann, K., Krohn, M., Pietkiewicz, S., Muller, A., . . . Dunay, I. R. (2016). Chronic Toxoplasma gondii infection enhances beta-amyloid phagocytosis and clearance by recruited monocytes. *Acta Neuropathol Commun, 4*, 25. doi:10.1186/s40478-016-0293-8

Moser, T., & Beutner, D. (2000). Kinetics of exocytosis and endocytosis at the cochlear inner hair cell afferent synapse of the mouse. *Proceedings of the National Academy of Sciences*, *97*(2), 883-888.

Moulder, K. L., Jiang, X., Taylor, A. A., Olney, J. W., & Mennerick, S. (2006). Physiological activity depresses synaptic function through an effect on vesicle priming. *J Neurosci, 26*(24), 6618-6626. doi:10.1523/JNEUROSCI.5498-05.2006

Moulder, K. L., Meeks, J. P., Shute, A. A., Hamilton, C. K., de Erausquin, G., & Mennerick, S. (2004). Plastic elimination of functional glutamate release sites by depolarization. *Neuron*, *42*(3), 423-435.

Mukherjee, K., Yang, X., Gerber, S. H., Kwon, H. B., Ho, A., Castillo, P. E., . . . Sudhof, T. C. (2010). Piccolo and bassoon maintain synaptic vesicle clustering without directly participating in vesicle exocytosis. *Proc Natl Acad Sci U S A, 107*(14), 6504-6509. doi:10.1073/pnas.1002307107

Muller, M., Genc, O., & Davis, G. W. (2015). RIM-binding protein links synaptic homeostasis to the stabilization and replenishment of high release probability vesicles. *Neuron, 85*(5), 1056-1069. doi:10.1016/j.neuron.2015.01.024

Muller, M., Liu, K. S. Y., Sigrist, S. J., & Davis, G. W. (2012). RIM Controls Homeostatic Plasticity through Modulation of the Readily-Releasable Vesicle Pool. *Journal of Neuroscience, 32*(47), 16574-16585. doi:10.1523/jneurosci.0981-12.2012

Müller, M., Liu, K. S. Y., Sigrist, S. J., & Davis, G. W. (2012). RIM controls homeostatic plasticity through modulation of the readily-releasable vesicle pool. *Journal of Neuroscience*, *32*(47), 16574-16585.

Müller, Martin, Özgür Genç, and Graeme W. Davis. "RIM-binding protein links synaptic homeostasis to the stabilization and replenishment of high release probability vesicles. *Neuron* 85.5 (2015): 1056-1069.

Murthy, V. N., Schikorski, T., Stevens, C. F., & Zhu, Y. (2001). Inactivity produces increases in neurotransmitter release and synapse size. *Neuron*, *32*(4), 673-682.

Nagy, G., Milosevic, I., Fasshauer, D., Muller, E. M., de Groot, B. L., Lang, T., . . . Sorensen, J. B. (2005). Alternative splicing of SNAP-25 regulates secretion through nonconservative substitutions in the SNARE domain. *Mol Biol Cell, 16*(12), 5675-5685. doi:10.1091/mbc.e05-07-0595

Naraghi, M., & Neher, E. (1997). Linearized buffered Ca2+ diffusion in microdomains and its implications for calculation of [Ca2+] at the mouth of a calcium channel. *Journal of Neuroscience*, *17*(18), 6961-6973.

Neher, E., & Sakaba, T. (2008). Multiple roles of calcium ions in the regulation of neurotransmitter release. *Neuron*, *59*(6), 861-872.

Nishimune, H., Numata, T., Chen, J., Aoki, Y., Wang, Y., Starr, M. P., . . . Stanford, J. A. (2012). Active zone protein Bassoon co-localizes with presynaptic calcium channel, modifies channel function, and recovers from aging related loss by exercise. *PLoS One, 7*(6), e38029. doi:10.1371/journal.pone.0038029

O'Brien, R. J., Kamboj, S., Ehlers, M. D., Rosen, K. R., Fischbach, G. D., & Huganir, R. L. (1998). Activity-dependent modulation of synaptic AMPA receptor accumulation. *Neuron*, *21*(5), 1067-1078.

Okerlund, N. D., Schneider, K., Leal-Ortiz, S., Montenegro-Venegas, C., Kim, S. A., Garner, L. C., . . . Garner, C. C. (2017). Bassoon Controls Presynaptic Autophagy through Atg5. *Neuron, 93*(4), 897-913 e897. doi:10.1016/j.neuron.2017.01.026

Olivera, B. M., Miljanich, G. P., Ramachandran, J., & Adams, M. E. (1994). Calcium channel diversity and neurotransmitter release: the ω-conotoxins and ω-agatoxins. *Annual review of biochemistry*, *63*(1), 823-867.

Paillart, C., Li, J., Matthews, G., & Sterling, P. (2003). Endocytosis and vesicle recycling at a ribbon synapse. *Journal of Neuroscience*, *23*(10), 4092-4099.

Parthier, D., Kuner, T., & Korber, C. (2018). The presynaptic scaffolding protein Piccolo organizes the readily releasable pool at the calyx of Held. *J Physiol, 596*(8), 1485-1499. doi:10.1113/JP274885

Pavlos, N. J., & Jahn, R. (2011). Distinct yet overlapping roles of Rab GTPases on synaptic vesicles. *Small GTPases*, *2*(2), 13441-13453.

Pfeffer, S., & Aivazian, D. (2004). Targeting Rab GTPases to distinct membrane compartments. *Nature reviews Molecular cell biology*, *5*(11), 886.

Plant, K., Pelkey, K. A., Bortolotto, Z. A., Morita, D., Terashima, A., McBain, C. J., . . . Isaac, J. T. (2006). Transient incorporation of native GluR2-lacking AMPA receptors during hippocampal long-term potentiation. *Nat Neurosci, 9*(5), 602-604. doi:10.1038/nn1678

Pravettoni, E., Bacci, A., Coco, S., Forbicini, P., Matteoli, M., & Verderio, C. (2000). Different localizations and functions of L-type and N-type calcium channels during development of hippocampal neurons. *Dev Biol, 227*(2), 581-594. doi:10.1006/dbio.2000.9872

Radhakrishnan, A., Stein, A., Jahn, R., & Fasshauer, D. (2009). The Ca2+ affinity of synaptotagmin 1 is markedly increased by a specific interaction of its C2B domain with phosphatidylinositol 4,5-bisphosphate. *J Biol Chem, 284*(38), 25749-25760. doi:10.1074/jbc.M109.042499

Reichenbach, N., Herrmann, U., Kahne, T., Schicknick, H., Pielot, R., Naumann, M., . . . Tischmeyer, W. (2015). Differential effects of dopamine signalling on long-term memory formation and consolidation in rodent brain. *Proteome Sci, 13*, 13. doi:10.1186/s12953-015-0069-2

Richards, D.A., Guatimosim, C., and Betz, W.J. (2000). Two endocytic recycling routes selectively fill two vesicle pools in frog motor nerve terminals. *Neuron 27*, 551-559.

Richards, D.A., Rizzoli, S.O., and Betz, W.J. (2004). Effects of wortmannin and latrunculin A on slow endocytosis at the frog neuromuscular junction. *The Journal of physiology 557*, 77-91.

Richmond, J. E., Weimer, R. M., & Jorgensen, E. M. (2001). An open form of syntaxin bypasses the requirement for UNC-13 in vesicle priming. *Nature, 412*(6844), 338-341. doi:10.1038/35085583

Ricoy, U. M., & Frerking, M. E. (2014). Distinct roles for Cav2.1-2.3 in activity-dependent synaptic dynamics. *J Neurophysiol, 111*(12), 2404-2413. doi:10.1152/jn.00335.2013

Rinetti, Gina V., and Felix E. Schweizer. Ubiquitination acutely regulates presynaptic neurotransmitter release in mammalian neurons. *Journal of Neuroscience* 30.9 (2010): 3157-3166.

Rizzoli, S. O., & Betz, W. J. (2005). Synaptic vesicle pools. *Nat Rev Neurosci, 6*(1), 57-69. doi:10.1038/nrn1583

Rizzuto, R., De Stefani, D., Raffaello, A., & Mammucari, C. (2012). Mitochondria as sensors and regulators of calcium signalling. *Nature reviews Molecular cell biology*, *13*(9), 566.

Robitaille, R., Adler, E. M., & Charlton, M. P. (1990). Strategic location of calcium channels at transmitter release sites of frog neuromuscular synapses. *Neuron*, *5*(6), 773-779.

Rodman, J. S., & Wandinger-Ness, A. (2000). Rab GTPases coordinate endocytosis. *J Cell Sci*, *113*(2), 183-192.

Rosenmund, C., Rettig, J., & Brose, N. (2003). Molecular mechanisms of active zone function. *Curr Opin Neurobiol, 13*(5), 509-519. doi:10.1016/j.conb.2003.09.011

Rosenmund, C., Sigler, A., Augustin, I., Reim, K., Brose, N., & Rhee, J. S. (2002). Differential control of vesicle priming and short-term plasticity by Munc13 isoforms. *Neuron*, *33*(3), 411-424.

Saheki, Y., & De Camilli, P. (2012). Synaptic vesicle endocytosis. *Cold Spring Harb Perspect Biol, 4*(9), a005645. doi:10.1101/cshperspect.a005645

Samuels, B. A., Hsueh, Y. P., Shu, T., Liang, H., Tseng, H. C., Hong, C. J., ... & Tsai, L. H. (2007). Cdk5 promotes synaptogenesis by regulating the subcellular distribution of the MAGUK family member CASK. *Neuron*, *56*(5), 823-837.

Sankaranarayanan, S., & Ryan, T. A. (2001). Calcium accelerates endocytosis of vSNAREs at hippocampal synapses. *Nature neuroscience*, *4*(2), 129.

Schattling, B., Engler, J. B., Volkmann, C., Rothammer, N., Woo, M. S., Petersen, M., . . . Friese, M. A. (2019). Bassoon proteinopathy drives neurodegeneration in multiple sclerosis. *Nat Neurosci*. doi:10.1038/s41593-019-0385-4

Schneider, R., Hosy, E., Kohl, J., Klueva, J., Choquet, D., Thomas, U., . . . Heine, M. (2015). Mobility of calcium channels in the presynaptic membrane. *Neuron, 86*(3), 672-679. doi:10.1016/j.neuron.2015.03.050

Schoch, S., & Gundelfinger, E. D. (2006). Molecular organization of the presynaptic active zone. *Cell Tissue Res, 326*(2), 379-391. doi:10.1007/s00441-006-0244-y

Scholz, K. P., & Miller, R. J. (1995). Developmental changes in presynaptic calcium channels coupled to glutamate release in cultured rat hippocampal neurons. *Journal of Neuroscience*, *15*(6), 4612-4617.

Schulz, A. M., Jing, Z., Caro, J. M. S., Wetzel, F., Dresbach, T., Strenzke, N., ... & Moser, T. (2014). Bassoon-disruption slows vesicle replenishment and induces homeostatic plasticity at a CNS synapse. *The EMBO journal*, *33*(5), 512-527.

Shapira, M., Zhai, R. G., Dresbach, T., Bresler, T., Torres, V. I., Gundelfinger, E. D., ... & Garner, C. C. (2003). Unitary assembly of presynaptic active zones from Piccolo-Bassoon transport vesicles. *Neuron*, *38*(2), 237-252.

Sheng, Z. H., Rettig, J., Takahashi, M., & Catterall, W. A. (1994). Identification of a syntaxin-binding site on N-type calcium channels. *Neuron*, *13*(6), 1303-1313.

Sheng, Z. H., Yokoyama, C. T., & Catterall, W. A. (1997). Interaction of the synprint site of N-type Ca2+ channels with the C2B domain of synaptotagmin I. *Proceedings of the National Academy of Sciences*, *94*(10), 5405-5410.

Shepherd, J. D., Rumbaugh, G., Wu, J., Chowdhury, S., Plath, N., Kuhl, D., . . . Worley, P. F. (2006). Arc/Arg3.1 mediates homeostatic synaptic scaling of AMPA receptors. *Neuron, 52*(3), 475-484. doi:10.1016/j.neuron.2006.08.034

Shi, S. H., Hayashi, Y., Esteban, J. A., & Malinow, R. (2001). Subunit-specific rules governing AMPA receptor trafficking to synapses in hippocampal pyramidal neurons. *Cell*, *105*(3), 331-343.

Shibasaki, T., Sunaga, Y., & Seino, S. (2004). Integration of ATP, cAMP, and Ca2+ signals in insulin granule exocytosis. *Diabetes*, *53*(suppl 3), S59-S62.

Shimizu, H., Kawamura, S., & Ozaki, K. (2003). An essential role of Rab5 in uniformity of synaptic vesicle size. *Journal of cell science*, *116*(17), 3583-3590.

Sidor, C. A., O'Keefe, F. R., Damiani, R., Steyer, J. S., Smith, R. M., Larsson, H. C., . . . Maga, A. (2005). Permian tetrapods from the Sahara show climate-controlled endemism in Pangaea. *Nature, 434*(7035), 886-889. doi:10.1038/nature03393

Soong, T. W., DeMaria, C. D., Alvania, R. S., Zweifel, L. S., Liang, M. C., Mittman, S., ... & Yue, D. T. (2002). Systematic identification of splice variants in human P/Q-type channel α12. 1 subunits: implications for current density and Ca2+-dependent inactivation. *Journal of Neuroscience*, *22*(23), 10142-10152.

Stach, S., Benard, J., & Giurfa, M. (2004). Local-feature assembling in visual pattern recognition and generalization in honeybees. *Nature, 429*(6993), 758-761. doi:10.1038/nature02594

Stanley, E. F. (1993). Single calcium channels and acetylcholine release at a presynaptic nerve terminal. *Neuron*, *11*(6), 1007-1011.

Stanley, E. F. (1997). The calcium channel and the organization of the presynaptic transmitter release face. *Trends in neurosciences*, *20*(9), 404-409.

Stavermann, M., Meuth, P., Doengi, M., Thyssen, A., Deitmer, J. W., & Lohr, C. (2015). Calcium-induced calcium release and gap junctions mediate large-scale calcium waves in olfactory ensheathing cells in situ. *Cell calcium*, *58*(2), 215-225.

Stellwagen, D., & Malenka, R. C. (2006). Synaptic scaling mediated by glial TNF-alpha. *Nature, 440*(7087), 1054-1059. doi:10.1038/nature04671

Stenmark, H. (2009). Rab GTPases as coordinators of vesicle traffic. *Nature reviews Molecular cell biology*, *10*(8), 513.

Studer, N., Gundelfinger, R., Schenker, T., & Steinhausen, H. C. (2017). Implementation of early intensive behavioural intervention for children with autism in Switzerland. *BMC Psychiatry, 17*(1), 34. doi:10.1186/s12888-017-1195-4

Su, S. C., Seo, J., Pan, J. Q., Samuels, B. A., Rudenko, A., Ericsson, M., ... & Tsai, L. H. (2012). Regulation of N-type voltage-gated calcium channels and presynaptic function by cyclin-dependent kinase 5. *Neuron*, *75*(4), 675-687.

Sudhof, T. C. (2004). The synaptic vesicle cycle. *Annu Rev Neurosci, 27*, 509-547. doi:10.1146/annurev.neuro.26.041002.131412

Sudhof, T. C., & Rizo, J. (2011). Synaptic vesicle exocytosis. *Cold Spring Harb Perspect Biol, 3*(12). doi:10.1101/cshperspect.a005637

Südhof, T. C., & Rothman, J. E. (2009). Membrane fusion: grappling with SNARE and SM proteins. *Science*, *323*(5913), 474-477.

Sullivan, P. F., de Geus, E. J. C., Willemsen, G., James, M. R., Smit, J. H., Zandbelt, T., . . . Penninx, B. W. J. H. (2008). Genome-wide association for major depressive disorder: a possible role for the presynaptic protein piccolo. *Molecular Psychiatry, 14*(4), 359-375. doi:10.1038/mp.2008.125

Sullivan, P. F., de Geus, E. J., Willemsen, G., James, M. R., Smit, J. H., Zandbelt, T., ... & Coventry, W. L. (2009). Genome-wide association for major depressive disorder: a possible role for the presynaptic protein piccolo. *Molecular psychiatry*, *14*(4), 359.

Sutton, Michael A., and Erin M. Schuman. Dendritic protein synthesis, synaptic plasticity, and memory. *Cell* 127.1 (2006): 49-58.

Takahashi, E., Niimi, K., & Itakura, C. (2010). Interaction Between Ca v 2.1 α 1 and CaMKII in Ca v 2.1 α 1 Mutant Mice, Rolling Nagoya. *Journal of molecular neuroscience*, *41*(2), 223-229.

Takahashi, M., Seagar, M. J., Jones, J. F., Reber, B. F., & Catterall, W. A. (1987). Subunit structure of dihydropyridine-sensitive calcium channels from skeletal muscle. *Proceedings of the National Academy of Sciences*, *84*(15), 5478-5482.

Tan, T. C., Valova, V. A., Malladi, C. S., Graham, M. E., Berven, L. A., Jupp, O. J., ... & Larsen, M. R. (2003). Cdk5 is essential for synaptic vesicle endocytosis. *Nature cell biology*, *5*(8), 701

Tanabe, T., Takeshima, H., Mikami, A., Flockerzi, V., Takahashi, H., Kangawa, K., ... & Numa, S. (1987). Primary structure of the receptor for calcium channel blockers from skeletal muscle. *Nature*, *328*(6128), 313.

Taniguchi, M., Taoka, M., Itakura, M., Asada, A., Saito, T., Kinoshita, M., ... & Hisanaga, S. I. (2007). Phosphorylation of adult type Sept5 (CDCrel-1) by cyclin-dependent kinase 5 inhibits interaction with syntaxin-1. *Journal of Biological Chemistry*, *282*(11), 7869-7876.

Tarelli, F. T., Bossi, M., Fesce, R., Greengard, P., & Valtorta, F. (1992). Synapsin I partially dissociates from synaptic vesicles during exocytosis induced by electrical stimulation. *Neuron*, *9*(6), 1143-1153.

Terry-Lorenzo, R. T., Torres, V. I., Wagh, D., Galaz, J., Swanson, S. K., Florens, L., . . . Garner, C. C. (2016). Trio, a Rho Family GEF, Interacts with the Presynaptic Active Zone Proteins Piccolo and Bassoon. *PLoS One, 11*(12), e0167535. doi:10.1371/journal.pone.0167535

Thalhammer, A., Contestabile, A., Ermolyuk, Y. S., Ng, T., Volynski, K. E., Soong, T. W., . . . Cingolani, L. A. (2017). Alternative Splicing of P/Q-Type Ca(2+) Channels Shapes Presynaptic Plasticity. *Cell Rep, 20*(2), 333-343. doi:10.1016/j.celrep.2017.06.055

Thiagarajan, T. C., Lindskog, M., & Tsien, R. W. (2005). Adaptation to synaptic inactivity in hippocampal neurons. *Neuron, 47*(5), 725-737. doi:10.1016/j.neuron.2005.06.037

Tomizawa, K., Ohta, J., Matsushita, M., Moriwaki, A., Li, S. T., Takei, K., & Matsui, H. (2002). Cdk5/p35 regulates neurotransmitter release through phosphorylation and downregulation of P/Q-type voltage-dependent calcium channel activity. *Journal of Neuroscience*, *22*(7), 2590-2597.

Toonen, R. F., & Verhage, M. (2007). Munc18-1 in secretion: lonely Munc joins SNARE team and takes control. *Trends Neurosci, 30*(11), 564-572. doi:10.1016/j.tins.2007.08.008

Tsuriel, S., Geva, R., Zamorano, P., Dresbach, T., Boeckers, T., Gundelfinger, E. D., ... & Ziv, N. E. (2006). Local sharing as a predominant determinant of synaptic matrix molecular dynamics. *PLoS biology*, *4*(9), e271.

Tucker, W. C., Weber, T., & Chapman, E. R. (2004). Reconstitution of Ca2+-regulated membrane fusion by synaptotagmin and SNAREs. *Science*, *304*(5669), 435-438.

Turrigiano, G. G., & Nelson, S. B. (1998). Thinking globally, acting locally: AMPA receptor turnover and synaptic strength. *Neuron*, *21*(5), 933-935.

Verkhratsky, A. (2004). Endoplasmic reticulum calcium signaling in nerve cells. *Biological research*, *37*(4), 693-699.

Verkhratsky, A., & Shmigol, A. (1996). Calcium-induced calcium release in neurones. *Cell calcium*, *19*(1), 1-14.

Verstegen, A. M., Tagliatti, E., Lignani, G., Marte, A., Stolero, T., Atias, M., . . . Benfenati, F. (2014). Phosphorylation of synapsin I by cyclin-dependent kinase-5 sets the ratio between the resting and recycling pools of synaptic vesicles at hippocampal synapses. *J Neurosci, 34*(21), 7266-7280. doi:10.1523/JNEUROSCI.3973-13.2014

Waites, C. L., & Garner, C. C. (2011). Presynaptic function in health and disease. *Trends Neurosci, 34*(6), 326-337. doi:10.1016/j.tins.2011.03.004

Waites, C. L., Leal-Ortiz, S. A., Okerlund, N., Dalke, H., Fejtova, A., Altrock, W. D., . . . Garner, C. C. (2013). Bassoon and Piccolo maintain synapse integrity by regulating protein ubiquitination and degradation. *EMBO J, 32*(7), 954-969. doi:10.1038/emboj.2013.27

Wang, H., Xu, J., Lazarovici, P., & Zheng, W. (2017). Dysbindin-1 involvement in the etiology of schizophrenia. *International journal of molecular sciences*, *18*(10), 2044.

Wang, S. S. H., Held, R. G., Wong, M. Y., Liu, C., Karakhanyan, A., & Kaeser, P. S. (2016). Fusion competent synaptic vesicles persist upon active zone disruption and loss of vesicle docking. *Neuron*, *91*(4), 777-791.

Wang, X., Kibschull, M., Laue, M. M., Lichte, B., Petrasch-Parwez, E., & Kilimann, M. W. (1999). Aczonin, a 550-kD putative scaffolding protein of presynaptic active zones, shares homology regions with Rim and Bassoon and binds profilin. *J Cell Biol, 147*(1), 151-162. doi:10.1083/jcb.147.1.151

Wang, Y., Okamoto, M., Schmitz, F., Hofmann, K., & Südhof, T. C. (1997). Rim is a putative Rab3 effector in regulating synaptic-vesicle fusion. *Nature*, *388*(6642), 593.

Wang, Y., Sugita, S., & Sudhof, T. C. (2000). The RIM/NIM family of neuronal C2 domain proteins. Interactions with Rab3 and a new class of Src homology 3 domain proteins. *J Biol Chem, 275*(26), 20033-20044. doi:10.1074/jbc.M909008199

Watanabe, S., & Boucrot, E. (2017). Fast and ultrafast endocytosis. *Current opinion in cell biology*, *47*, 64-71.

Watanabe, S., Rost, B. R., Camacho-Perez, M., Davis, M. W., Sohl-Kielczynski, B., Rosenmund, C., & Jorgensen, E. M. (2013). Ultrafast endocytosis at mouse hippocampal synapses. *Nature, 504*(7479), 242-247. doi:10.1038/nature12809

Watanabe, S., Rost, B.R., Camacho-Perez, M., Davis, M.W., Sohl-Kielczynski, B., Rosenmund, C., and Jorgensen, E.M. (2013b). Ultrafast endocytosis at mouse hippocampal synapses. *Nature 504*, 242-247.

Watanabe, S., Liu, Q., Davis, M.W., Hollopeter, G., Thomas, N., Jorgensen, N.B., and Jorgensen, E.M. (2013a). Ultrafast endocytosis at Caenorhabditis elegans neuromuscular junctions. *eLife 2*, e00723.

Watanabe, S., & Boucrot, E. (2017). Fast and ultrafast endocytosis. *Current opinion in cell biology*, *47*, 64-71.

Waters, J., & Smith, S. J. (2002). Vesicle pool partitioning influences presynaptic diversity and weighting in rat hippocampal synapses. *The Journal of Physiology, 541*(3), 811-823. doi:10.1113/jphysiol.2001.013485

Watt, A. J., van Rossum, M. C., MacLeod, K. M., Nelson, S. B., & Turrigiano, G. G. (2000). Activity coregulates quantal AMPA and NMDA currents at neocortical synapses. *Neuron*, *26*(3), 659-670.

Werling, A. M., Bobrowski, E., Taurines, R., Gundelfinger, R., Romanos, M., Grunblatt, E., & Walitza, S. (2016). CNTNAP2 gene in high functioning autism: no association according to family and meta-analysis approaches. *J Neural Transm (Vienna), 123*(3), 353-363. doi:10.1007/s00702-015-1458-5

Wierenga, C. J., Walsh, M. F., & Turrigiano, G. G. (2006). Temporal regulation of the expression locus of homeostatic plasticity. *J Neurophysiol, 96*(4), 2127-2133. doi:10.1152/jn.00107.2006

Willeumier, Kristen, Stefan M. Pulst, and Felix E. Schweizer. Proteasome inhibition triggers activity-dependent increase in the size of the recycling vesicle pool in cultured hippocampal neurons. *Journal of Neuroscience* 26.44 (2006): 11333-11341.

Wiser, O., Bennett, M. K., & Atlas, D. (1996). Functional interaction of syntaxin and SNAP-25 with voltage-sensitive L-and N-type Ca2+ channels. *The EMBO journal*, *15*(16), 4100-4110.

Wong, F. K., Nath, A. R., Chen, R. H., Gardezi, S. R., Li, Q., & Stanley, E. F. (2014). Synaptic vesicle tethering and the CaV2.2 distal C-terminal. *Front Cell Neurosci, 8*, 71. doi:10.3389/fncel.2014.00071

Woudstra, S., van Tol, M. J., Bochdanovits, Z., van der Wee, N. J., Zitman, F. G., van Buchem, M. A., . Hoogendijk, W. J. (2013). Modulatory effects of the piccolo genotype on emotional memory in health and depression. PLoS One, 8(4), e61494. doi:10.1371/journal.pone.0061494.

Wu, X. S., & Wu, L. G. (2001). Protein kinase c increases the apparent affinity of the release machinery to Ca2+ by enhancing the release machinery downstream of the Ca2+ sensor. *Journal of Neuroscience*, *21*(20), 7928-7936.

Wu, X. S., Zhang, Z., Zhao, W. D., Wang, D., Luo, F., & Wu, L. G. (2014). Calcineurin is universally involved in vesicle endocytosis at neuronal and nonneuronal secretory cells. *Cell Rep, 7*(4), 982-988. doi:10.1016/j.celrep.2014.04.020

Wucherpfennig, T., Wilsch-Bräuninger, M., & González-Gaitán, M. (2003). Role of Drosophila Rab5 during endosomal trafficking at the synapse and evoked neurotransmitter release. *The Journal of cell biology*, *161*(3), 609-624.

Wucherpfennig, T., Wilsch-Bräuninger, M., & González-Gaitán, M. (2003). Role of Drosophila Rab5 during endosomal trafficking at the synapse and evoked neurotransmitter release. *The Journal of cell biology*, *161*(3), 609-624.

Xu, J., Luo, F., Zhang, Z., Xue, L., Wu, X. S., Chiang, H. C., . . . Wu, L. G. (2013). SNARE proteins synaptobrevin, SNAP-25, and syntaxin are involved in rapid and slow endocytosis at synapses. *Cell Rep, 3*(5), 1414-1421. doi:10.1016/j.celrep.2013.03.010

Yabe, I., Yaguchi, H., Kato, Y., Miki, Y., Takahashi, H., Tanikawa, S., ... & Matsushima, M. (2018). Mutations in bassoon in individuals with familial and sporadic progressive supranuclear palsy-like syndrome. *Scientific reports*, *8*(1), 819.

Yan, Z., Chi, P., A. Bibb, J., A. Ryan, T., & Greengard, P. (2002). Roscovitine: a novel regulator of P/Q-type calcium channels and transmitter release in central neurons. *The Journal of Physiology, 540*(3), 761-770. doi:10.1113/jphysiol.2001.013376

Yao, J., Kwon, S. E., Gaffaney, J. D., Dunning, F. M., & Chapman, E. R. (2012). Uncoupling the roles of synaptotagmin I during endo-and exocytosis of synaptic vesicles. *Nature neuroscience*, *15*(2), 243.

Yokoyama, C. T., Sheng, Z. H., & Catterall, W. A. (1997). Phosphorylation of the synaptic protein interaction site on N-type calcium channels inhibits interactions with SNARE proteins. *Journal of Neuroscience*, *17*(18), 6929-6938.

Zefirov, A. L., Abdrakhmanov, M. M., Mukhamedyarov, M. A., & Grigoryev, P. N. (2006). The role of extracellular calcium in exo- and endocytosis of synaptic vesicles at the frog motor nerve terminals. *Neuroscience, 143*(4), 905-910. doi:10.1016/j.neuroscience.2006.08.025

Zhai, R., Olias, G., Chung, W. J., Lester, R. A., tom Dieck, S., Langnaese, K., . . . Garner, C. C. (2000). Temporal appearance of the presynaptic cytomatrix protein bassoon during synaptogenesis. *Mol Cell Neurosci, 15*(5), 417-428. doi:10.1006/mcne.2000.0839

Zhao, C., Dreosti, E., & Lagnado, L. (2011). Homeostatic synaptic plasticity through changes in presynaptic calcium influx. *J Neurosci, 31*(20), 7492-7496. doi:10.1523/JNEUROSCI.6636-10.2011

Zhou, Y., Tanaka, T., Sugiyama, N., Yokoyama, S., Kawasaki, Y., Sakuma, T., ... & Sakurai, H. (2014). p38-Mediated phosphorylation of Eps15 endocytic adaptor protein. *FEBS letters*, *588*(1), 131-137.

Zhu, Y., Xu, J., & Heinemann, S. F. (2009). Two pathways of synaptic vesicle retrieval revealed by single-vesicle imaging. *Neuron, 61*(3), 397-411. doi:10.1016/j.neuron.2008.12.024

Ziv, N. E., & Garner, C. C. (2004). Cellular and molecular mechanisms of presynaptic assembly. *Nat Rev Neurosci, 5*(5), 385-399. doi:10.1038/nrn1370

Zucker, R. S., & Regehr, W. G. (2002). Short-term synaptic plasticity. *Annu Rev Physiol, 64*(1), 355-405. doi:10.1146/annurev.physiol.64.092501.114547

# List of publications

Altmüller F, Pothula S, Annamneedi A, Nakhaei-Rad S, Montenegro-Venegas C, Pina-Fernández E, Marini C, Santos M, Schanze D, Montag D, Ahmadian MR, Stork O, Zenker M, Fejtova A. Aberrant neuronal activity-induced signaling and gene expression in a mouse model of RASopathy. *PLoS Genet.* 2017 Mar 27;13(3): e1006684. doi: 10.1371/journal.pgen.1006684.

Montenegro-Venegas, C., Fienko, S., Anni, D., Pina-Fernández, E., Frischknecht, R., & Fejtova, A. Bassoon inhibits proteasome activity via interaction with PSMB4. *Cellular and Molecular Life Sciences*, 1-19. 2020

# Ehrenerklärung

Ich versichere hiermit, dass ich die vorliegende Arbeit ohne unzulässige Hilfe Dritter und ohne Benutzung anderer als der angegebenen Hilfsmittel angefertigt habe; verwendete fremde und eigene Quellen sind als solche kenntlich gemacht.

Ich habe insbesondere nicht wissentlich:

- Ergebnisse erfunden oder widersprüchliche Ergebnisse verschwiegen,
- statistische Verfahren absichtlich missbraucht, um Daten in ungerechtfertigter Weise zu interpretieren,
- fremde Ergebnisse oder Veröffentlichungen plagiiert,
- fremde Forschungsergebnisse verzerrt wiedergegeben.

Mir ist bekannt, dass Verstöße gegen das Urheberrecht Unterlassungs- und Schadensersatzansprüche des Urhebers sowie eine strafrechtliche Ahndung durch die Strafverfolgungsbehörden begründen kann.

Ich erkläre mich damit einverstanden, dass die Arbeit ggf. mit Mitteln der elektronischen Datenverarbeitung auf Plagiate überprüft werden kann.

Die Arbeit wurde bisher weder im Inland noch im Ausland in gleicher oder ähnlicher Form als Dissertation eingereicht und ist als Ganzes auch noch nicht veröffentlicht.

Magdeburg, den 28-Sep-2021

Eneko Pina Fernández